



UNIVERSITÀ  
DEGLI STUDI  
FIRENZE

DOTTORATO DI RICERCA IN  
Scienze Farmaceutiche

CICLO XXVII

COORDINATORE Prof. Teodori Elisabetta

**Application of the optical biosensor Biacore T100  
technology for the characterization of the interaction  
between autoantibodies and synthetic peptide antigens**

Settore Scientifico Disciplinare CHIM/08

**Dottorando**

Dott. Rossi Giada

---

**Tutore**

Prof. Rovero Paolo

---

**Coordinatore**

Prof. Teodori Elisabetta

---

Anni 2012/2014



## INDEX

1 INTRODUCTION .....	1
1.1 Autoimmune diseases .....	1
1.2 Biomarkers of autoimmune diseases .....	2
1.3 Synthetic probes to detect autoantibodies as biomarkers.....	2
1.4 Immunological assays: classical Enzyme-Linked Immunosorbent Assay and advanced Biosensors.....	3
1.4.1 SPR-based biosensor Biacore .....	4
1.4.1.1 Binding studies.....	10
1.4.1.2 Kinetic and affinity studies .....	11
1.5 References .....	12
2 AIM OF THE PROJECT.....	13
3: Biosensor characterization of Anti-Citrullinated Protein/Peptide Antibodies (ACPA) from Rheumatoid Arthritis patients' sera.....	15
3.1 Rheumatoid Arthritis .....	15
3.2 Anti-Citrullinated Peptides/Protein Antibodies: a diagnostic criteria for RA.....	17
3.3 Objective.....	19
3.4 Results and discussion .....	20
3.4.1 Sensor chips preparation for the characterization of IgG preparations .....	20
3.4.2 Affinity evaluation of ACPA from IgG preparations.....	22
3.4.3 Sensor chips preparation for purified ACPA detection.....	24
3.4.4 SPR characterization of purified ACPA .....	26
3.5 Conclusions .....	32
3.6 Matherials and methods.....	32
3.6.1 ACPA purification from patients' sera .....	33
3.6.2 PH scouting procedure.....	33
3.6.3 Citrullinated MAPs and tetanus peptide immobilization: amine coupling.....	33
3.6.4 Affinity studies with total IgG fractions .....	34
3.6.5 Citrullinated MAPs and control sequences immobilization: thiol coupling.....	34
3.6.6 SPR kinetic and affinity studies with anti-peptide antibodies.....	35
3.7 References .....	36
4: Autoantibodies from Multiple Sclerosis patients' sera: isolation, detection and characterization of their interaction with a <i>Haemophilus influenzae</i> N-glycosylated adhesion protein. ....	37
4.1 N-glycosylation, a widespread post-translational modification.....	37
4.2 N-glycosylated HMW1 adhesin from <i>Haemophilus influenzae</i> .....	39
4.3 Multiple Sclerosis: the state of the art.....	42
4.4 N-glycosylated peptide CSF114(Glc) for MS autoantibodies detection.....	46
4.5 Objective.....	47

4.6 Results and discussion .....	48
4.6.1 SP-ELISA optimization for protein antigens .....	49
4.6.2 Sera screening in SP-ELISA .....	51
4.6.3 Competitive ELISA assay .....	57
4.6.4 HMW1ct mutants for competitive ELISA .....	62
4.6.5 Competitive ELISA with adhesin derived peptides .....	65
4.6.6 Adhesin peptides immobilization on Biacore sensor chip.....	68
4.6.7 Antibody purification from one MS serum .....	72
4.6.7.1 Adhesin proteins conjugation to sepharose by thiol coupling .....	73
4.6.7.2 Adhesin proteins conjugation to sepharose by amine coupling.....	74
4.6.7.3 Sequential affinity chromatography .....	75
4.6.8 Purified antibodies titration .....	75
4.6.8.1 HMW1ct not retained fraction characterization .....	77
4.6.9 Surface Plasmon Resonance studies with purified antibodies.....	80
4.6.9.1 Biosensor surface preparation .....	80
4.6.9.2 Kinetic and affinity studies.....	82
4.6.9.3 Binding studies with sera.....	87
4.6.10 Immunohistochemistry assay .....	95
4.6.10.1 Validation of tissues .....	96
4.6.10.2 Immunohistochemistry with MS 1 serum.....	97
4.6.10.3 Immunohistochemistry with purified antibody fractions.....	99
4.7 Conclusions.....	103
4.8 Materials and methods .....	105
4.8.1 SP-ELISA.....	105
4.8.2 SP-ELISA denaturant conditions .....	106
4.8.3 Titration ELISA .....	106
4.8.4 Competitive ELISA.....	106
4.8.5 Proteins conjugation to sepharose: thiol coupling.....	107
4.8.6 Proteins and peptides conjugation to sepharose: amine coupling.....	107
4.8.7 Sequential affinity chromatography .....	107
4.8.8 Surface Plasmon Resonance studies.....	108
4.8.8.1 Antigen immobilization on CM5 sensor chip.....	108
4.8.8.2 Binding studies with sera.....	109
4.8.8.3 Kinetic and affinity studies with purified antibodies .....	109
4.8.9 Tissues fixation .....	109
4.8.10 Immunofluorescence test with paraformaldehyde-fixed tissues.....	109
4.9 References.....	111
5: Affinity determination of human recombinant domain antibodies specific for CSF114(Glc).....	114

5.1 Human single domain antibodies: origins and applications.....	114
5.2 Objective.....	115
5.3 Results and discussion .....	115
5.3.1 Peptides immobilization on Biacore chip .....	115
5.3.2 SPR binding studies with specific hV <sub>H</sub> -CSF114(Glc) phages .....	118
5.3.3 Kinetic and affinity characterization of hV <sub>H</sub> -CSF114(Glc)6xHis.....	118
5.4 Conclusions .....	121
5.5 Materials and methods .....	122
5.5.1 Production of hV <sub>H</sub> soluble antibodies .....	122
5.5.2 Peptides immobilization on Biacore CM5 chip .....	122
5.5.3 SPR binding studies with specific hV <sub>H</sub> -CSF114(Glc) phages .....	123
5.5.4 SPR characterization of hV <sub>H</sub> -CSF114(Glc)6xHis.....	123
5.6 References .....	124
6: SP-ELISA detection of anti N-glycosylation antibodies in Rett Syndrome patients' sera.....	125
6.1 Proposed correlation between Multiple Sclerosis and Rett syndrome.....	125
6.2 Objective.....	126
6.3 Results and discussion .....	126
6.3.1 Determination of specific anti N-glycosylated peptide antibodies by SP-ELISA.....	126
6.3.2 Determination of specific anti N-glycosylated adhesin antibodies by SP-ELISA .....	129
6.3.3 Competitive ELISA assay with Rett sera.....	132
6.4 Conclusions .....	133
6.5 Materials and methods.....	133
6.5.1 Patients.....	133
6.5.2 SP-ELISA assay.....	134
6.5.3 Competitive ELISA .....	134
6.6 References .....	135
7 LIST OF ABBREVIATIONS .....	136



# 1 INTRODUCTION

## 1.1 Autoimmune diseases

Autoimmune diseases affect at least 5% of the whole population and have a high social impact, because patients have a long expectation of life during which they are subordinated to the follow up of the disease by means of very invasive techniques, e.g. Magnetic Resonance Imaging (MRI) in Multiple Sclerosis diagnosis, that are not suitable for a routine use. Autoimmune diseases are characterized by the erroneous activation of the immune system that, because of the loss of the physiological tolerance, is no more able to distinguish foreign molecules from self ones; consequently self molecules are targeted and endogenous tissues expressing those molecules are damaged. Physiologically, after the induction of an unknown agent that is potentially pathogenic and antigenic, the organism can reply by two different reaction of the immune system: the cell mediated immune response that involves the production of specialized antigen presenting cells that react with foreign antigens and activate cytotoxic and helper T lymphocytes, and the humoral response that involves B lymphocytes producing antibodies able to specifically bind the antigen. Autoimmune disorders are up to now considered as triggered by T cells further inducing a B cell response; this last response is characterized by the production of serum antibodies which bind endogenous antigens and that are defined autoantibodies. Autoimmune diseases can be classified in local pathologies, if the antigen is confined to a particular organ system (e.g. type I diabetes), and systemic pathologies, which are characterized by a response to ubiquitous antigens present in more than one tissue (e.g. Systemic Lupus Erythematosus).

The etiology of these diseases is not yet fully understood and it is accepted that they have a multifactorial origin including genetic predisposition, female hormones, environmental factors and exogenous agents such as virus or bacteria. A pathogenic mechanism for autoimmune diseases has been proposed to be the so called molecular mimicry, a process by which exogenous agents can activate an immune response that cross-reacts with similar structures present in self molecules.

Autoimmune diseases are chronic conditions with no cure; treatment involves attempts to limit the progression of the disease and to decrease the symptoms and the inflammation processes. Actual therapies for autoimmune diseases include the administration of immunomodulators, glucocorticoids and non-steroidal anti-inflammatory drugs; however some patients may benefit from treatment with biotechnological drugs such as very specific and effective, but expensive

## INTRODUCTION

monoclonal antibodies that are approved for example in the treatment of psoriasis, Crohn's disease and Rheumatoid Arthritis.

### **1.2 Biomarkers of autoimmune diseases**

The main problem in autoimmune diseases diagnosis is due to their long period of latency and their initial sub-clinical manifestations; they are usually diagnosed when relevant clinical symptoms are present. Considering this in the last years several studies have been done with the aim of finding biomarkers for autoimmune diseases that could be used to set up diagnostic tests or to monitor the efficacy of therapeutic treatments. A biomarker can be defined as a physiological, anatomical or biochemical parameter which should be easily determined and used as indicator of normal physiological or pathogenic processes. Sera from patients suffering from autoimmune disorders often contain multiple types of autoantibodies; if these autoantibodies are present in high concentration in patients' sera and they are exclusive of a certain disease they can be used as biomarkers.<sup>1</sup> Evaluation of autoantibodies as disease biomarker is very important for an early diagnosis and in particular if autoantibodies concentration fluctuate with disease exacerbations or remissions, their quantitative and qualitative measurements can be very valuable in the follow-up of patients and in the evaluation of the efficacy of a certain therapeutic treatment<sup>2</sup>.

### **1.3 Synthetic probes to detect autoantibodies as biomarkers**

Protein antigens are fundamental in the pathological mechanism triggering autoimmune diseases, particularly if they contain aberrant post-translational modifications (e.g. acetylation, citrullination, glycosylation, etc.)<sup>3</sup>. The detection of autoantibodies by protein antigen isolated from biological material or obtained by recombinant technologies, presents several difficulties including mutations, lack of post-translational modifications, uncorrected folding and potential cross-reactivity between structurally homologous protein epitopes. To avoid these problems the "Chemical Reverse Approach" has been developed as a novel concept to design antigenic peptide probes for the detection of serum autoantibodies as biomarkers. This strategy is termed reverse since the research of antigenic peptides is based on antibodies circulating in patients' sera. The selection and the design of the chemical structure of the antigenic peptides is guided and optimized according to the specificity for autoantibodies. In this context it has been demonstrated that synthetic peptides, possibly but not necessarily deriving from the native proteins and



containing post-translationally modified amino acids, can be successfully used to set up diagnostic *in vitro* assays for the detection of biomarkers of diseases, such as Rheumatoid Arthritis<sup>4</sup> and Multiple Sclerosis<sup>5</sup>.

#### **1.4 Immunological assays: classical Enzyme-Linked Immunosorbent Assay and advanced Biosensors**

Up to now there are few technologies in clinical development capable of detecting these biomarkers in the blood, the most commonly used in clinic to screen a large number of sera is the Enzyme-Linked Immunosorbent Assay (ELISA). For the screening of big numbers of sera and the detection of antibodies, a Solid Phase ELISA (SP-ELISA) is often performed. In this case the antigenic probe is coated on the solid phase surface of a multi-well suitable plastic plate and allows to interact with the autoantibodies present in sera that will be quantified thanks to the colorimetric reaction generated after the incubation with a specific secondary antibody, conjugated to an enzyme able to produce a colored molecule, when treated with a suitable substrate in the final step of the assay.

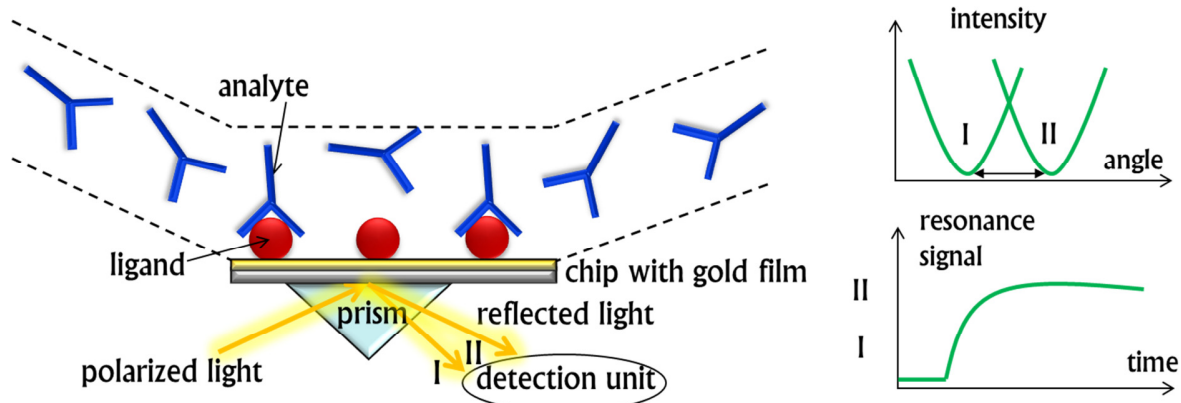
A competitive ELISA assay protocol has been developed and optimized to measure the average affinity of polyclonal antibodies in serum, a parameter of great interest in exploring B cell population dynamics *in vivo*<sup>6</sup>. This assay is based on a classical SP-ELISA, but in this case serum is applied with increasing concentration of an inhibitor molecule in solution; then thanks to the application of the appropriate secondary antibody, only antibodies that didn't bind to the inhibitor in solution will be detected through the colorimetric reaction.

A more detailed characterization of the antibody-antigen interaction, giving important information for the prognostic values of disease biomarkers, can be achieved thanks to the use of biosensors. A biosensor is a technological device composed of two elements: a biological recognition unit, able to specifically interact with a target or to form a complex with it, and a transducer system that converts into a recordable signal the change in property of the solution or surface due to the biological interaction. In contrast with conventional bioassays, biosensors allow the detection of molecular interactions as they take place, without requiring auxiliary procedures. In this project we have used an optical biosensor system (Biacore) to perform Biomolecular Interaction Analysis for different purposes, within the framework of the characterization of autoantibodies as biomarkers of autoimmune diseases.

## INTRODUCTION

### 1.4.1 SPR-based biosensor Biacore

Biacore is a label free system exploiting the phenomenon of the Surface Plasmon Resonance (SPR) to monitor the interaction between molecules in real time. The approach involves attaching one interacting partner called *ligand* to the surface of a sensor chip, and then flowing the samples containing the other interaction partner, defined *analyte*, over the surface. Binding of molecules to the sensor surface generates a response, which is directly proportional to the bound mass; this response is measured in Resonance Units (RU) and is graphically expressed by a sensorgram, showing the progress of the interaction during time. SPR is a phenomenon that occurs in thin conducting films at an interface between media of different Refractive Index (RI). In Biacore system, the two media are the glass of the sensor chip and the sample solution, and the conducting film is a thin layer of gold on the sensor chip surface; the wave length of the incident light and the reflective index of the inner surface are constant, so the SPR phenomenon is used to monitor the change of reflective index in the flowing solution close to the sensor chip surface. Under conditions of total internal reflection, light incident on the reflecting interface leaks an electric field intensity called evanescent wave field across the interface into the medium of lower refractive index, without losing net energy. The amplitude of the evanescent field wave decreases exponentially with distance from the surface, and the effective penetration depth in terms of sensitivity to refractive index is about 150 nm. At a certain combination of angle of incidence and wavelength, the incident light excites plasmons in the gold film. As a result, a characteristic absorption of energy via the evanescent wave field occurs and SPR is seen as a drop in the intensity of the reflected light (Figure 1). Changes in solute concentration at the surface of the sensor chip cause changes in the RI of the solution, which can be measured as an SPR response and expressed in RU, in particular a difference of  $0.1^\circ$  in the angle of reflection generates a response of 1000 RU that correspond to a variation in mass over the chip surface of about  $1 \text{ ng/mm}^2$ .



**Figure 1:** Schematic representation of the Surface Plasmon Resonance occurring in the inner core of a Biacore instrument.

SPR arises in any thin conducting film under the conditions above described, although the wavelength at which resonance occurs and the shape of the energy absorption profile differ with different conducting materials. Gold is used in Biacore sensor chips because it combines favorable SPR characteristics with stability and a high level of inertness in biomolecular interaction contexts.

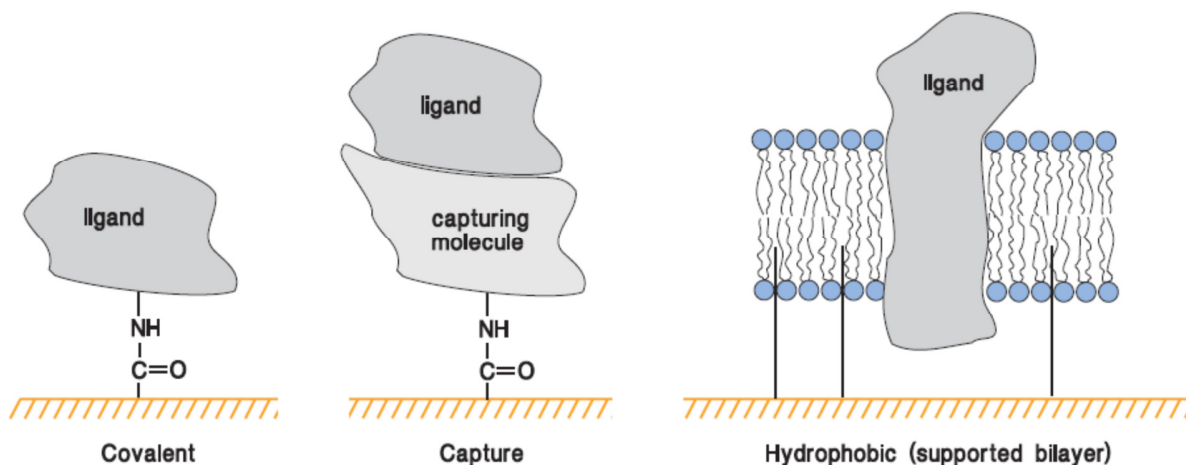
This advanced technology can be used to investigate the specificity of an interaction, by testing the extent of binding between different pairs of molecules, or to describe the kinetics and affinity of an interaction, by analyzing the binding behavior in terms of mathematical interaction models, or to quantify the concentration of specific molecules present in the sample by measuring the response obtained from the sample itself.

Biacore studies can be applied to a wide range of biomolecules including proteins, lipids, nucleic acids, carbohydrates and small molecules such as synthetic drugs. Analytes to be detected should have a molecular weight above 100 Da in order to produce a sufficient change in the reflective index; considering that the evanescent wave penetration depth is 300-400 nm, molecules longer than 400 nm can be detected but not accurately characterized because they produce a non-linear signal.

The heart of Biacore systems is the sensor chip, which provides the physical conditions necessary to generate the SPR signal and to monitor the interactions occurring on its surface. A sensor chip is composed by two fundamental parts; the first is a glass surface covered by a thin gold layer (50 nm) that is required to generate the SPR signal and the second is an inert matrix covering the gold layer containing the reactive groups necessary to anchor the ligand.

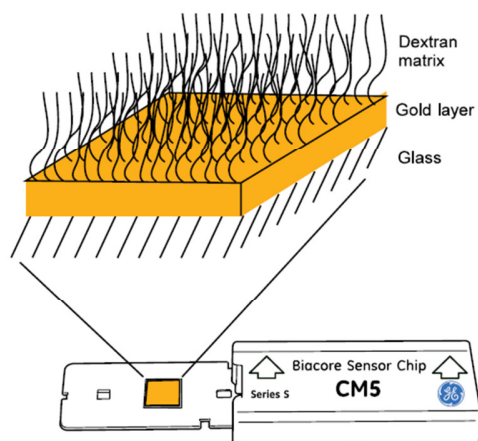
## INTRODUCTION

Different biological compatible matrices are commercially available offering the opportunity to immobilize the ligand through several approaches such as a covalent immobilization, where it is linked to the surface through a covalent chemical link or a high affinity capture, where it is attached by noncovalent but high specific interaction with another molecule and a hydrophobic adsorption, which exploits more or less specific hydrophobic interactions to attach either the molecule of interest or a hydrophobic carrier, such as a lipid monolayer or bilayer, to the sensor chip surface (Figure 2).



**Figure 2:** Three most commonly used approaches for attaching biomolecules to the sensor chip surface.

The most commonly used sensor chip is the CM5 type, carrying a matrix of carboxymethylated dextran covalently attached to the gold surface (Figure 3), the dextran matrix is flexible, allowing relatively free movement of attached ligands within the surface layer and it provides a high surface capacity for immobilizing a wide range of ligands with every chemical strategies.

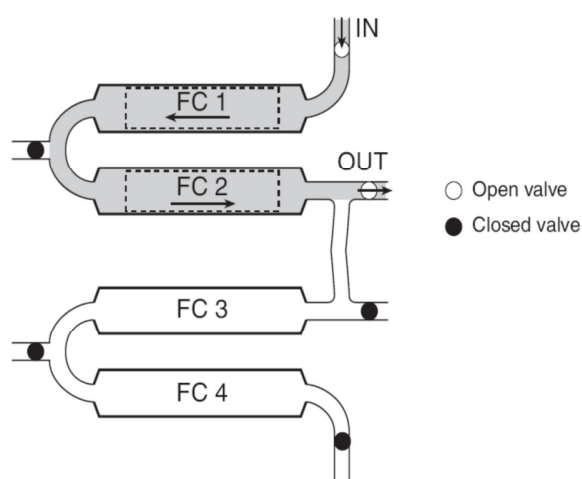


**Figure 3:** Schematic illustration of the structure of a CM5 sensor chip.

Other sensor chips frequently used include the CM4, with a lower degree of carboxymethylation resulting in reduced immobilization capacity; the CM3, containing a carboxymethylation consisting of shorter dextran chains helpful to reduce steric effects when working with large molecules; the sensor chips SA, on the dextran matrix of which, streptavidin has been covalently pre-attached to allow the high affinity capture of biotinylated ligands; sensor chip NTA with immobilized nitrilotriacetic acid, providing a means for capturing polyhistidine-tagged ligands through metal chelation.

Sample containing analyte can be injected over the immobilized ligands thanks to a sophisticated microfluidic system. The sensor surface itself forms one wall of a flow cell, which is an integral part of the microfluidic system that consists of a series of channels and valves in a plastic block, the Integrated Microfluidic Cartridge (IFC). The flow cells are formed by pressing the sensor chip against a set of open channels on the surface of the IFC, so that the chip can easily be exchanged. Delivery of sample and buffer to the flow cells is precisely controlled by the pump system and by the valves in the IFC, in this way a continuous flow of liquid is maintained over the sensor surface throughout the analysis.

Thanks to the valves, the operator can regulate the flow and chose in how many channels the sample has to be injected (Figure 4). For each cycle of analysis a maximum of 4 channels (flow cells) can be simultaneously used, the flow cells are optimized to be used in pairs (2-1 and 4-3) and the flow cell 1 could also be used as reference for all the other three channels (2-1, 3-1, 4-1).



**Figure 4:** Schematic representation of the 4 flow cells and of the valves involved in the control of the flow; in this case sample flows in channel 1 and channel 2.

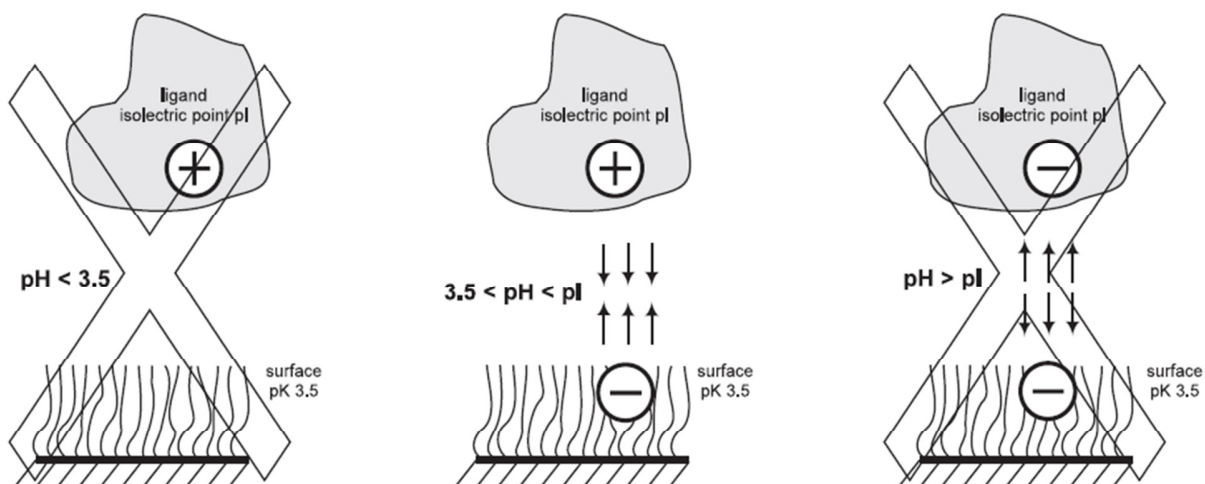
The signal registered in the reference channel will be subtracted from the one obtained in the active channels. This subtraction has the advantage of removing the aspecific interactions that

## INTRODUCTION

can be registered on a gold surface when injecting a complex matrix. The other advantage is the removal of the so call bulk effect that can mask interactions involving low molecular weight analytes and that is due to a high difference in the reflective indices of the sample solution and of the running buffer.

Covalent immobilization to the dextran matrix is the most commonly used approach for attaching the ligand to the surface, and it is also the method of choice for immobilizing capturing molecules. Covalent immobilization generally results in stable attachment of the ligand to the surface under the buffer conditions normally used for surface regeneration that removes bound analyte at the end of each analysis cycle but leaves the ligand attached to the surface.

To obtain a good immobilization level, the electrostatic pre-concentration of ligands in the dextran matrix must be achieved. It's important to consider that at pH values above 3.5 the carboxymethylated dextran on the sensor chip surface is negatively charged, so the primary requirement for the electrostatic pre-concentration on the surface is that the pH of the ligand solution should lie between 3.5 and the isoelectric point of the ligand, so that the surface and the ligand carry opposite net charges (Figure 5).



**Figure 5:** Schematic representation of ligand pre-concentration on chip surface; ligand is concentrated electrostatic attraction between ligand and chip is possible only when the pH lies between the isoelectric point of the ligand and the  $pK_a$  of the surface.

In addition, the electrostatic interactions involved in pre-concentration are favored by low ionic strength in the coupling buffer. The optimum values of pH and ionic strength can be determined experimentally for every ligand with the *pH scouting* procedure; this procedure consists in injecting the ligand in different buffers over the non-activated surface of the chip and evaluating the instrumental response at the end of the injection which depends only on the electrostatic

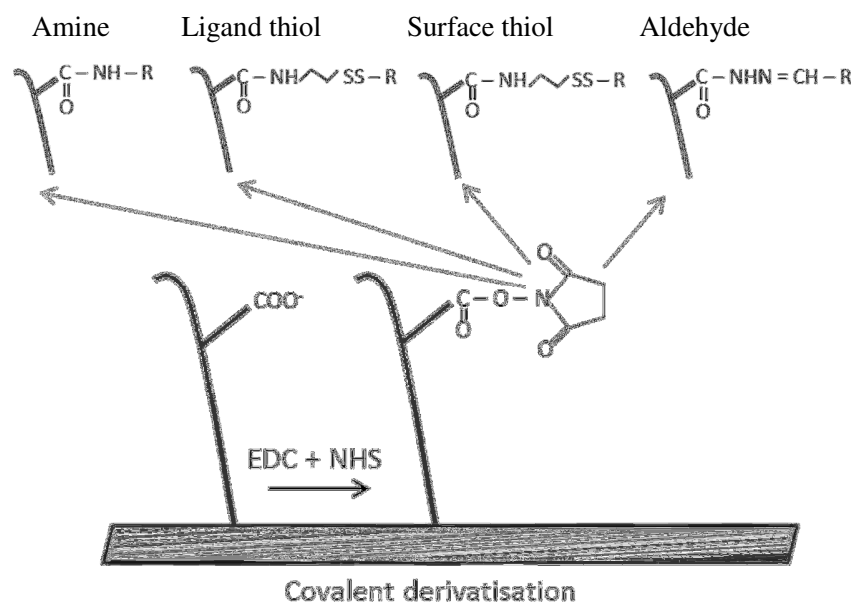
interactions between the chip surface and the ligand and that consequently will give an indication of whether the conditions are suitable.

The general pattern for essentially all covalent immobilization methods consists in the following steps:

- chip surface activation by the injection of appropriate reagents;
- ligand injections in the previously identified best immobilization buffer up to reaching a satisfactory immobilization level;
- injection of a reagent to deactivate remaining active groups on the surface and to remove non-covalently bound ligand.

The most common immobilization chemistries (Figure 6) are:

- amine coupling, exploiting primary amine groups of the ligand after activation of the surface;
- thiol coupling, exploiting thiol-disulfide exchange between thiol groups and active disulfides introduced on either the ligand (surface thiol coupling) or the surface matrix (ligand thiol coupling);
- aldehyde coupling, using the reaction between hydrazine or carbohydrazide groups introduced on the surface and aldehyde groups obtained by oxidation of carbohydrates in the ligand.



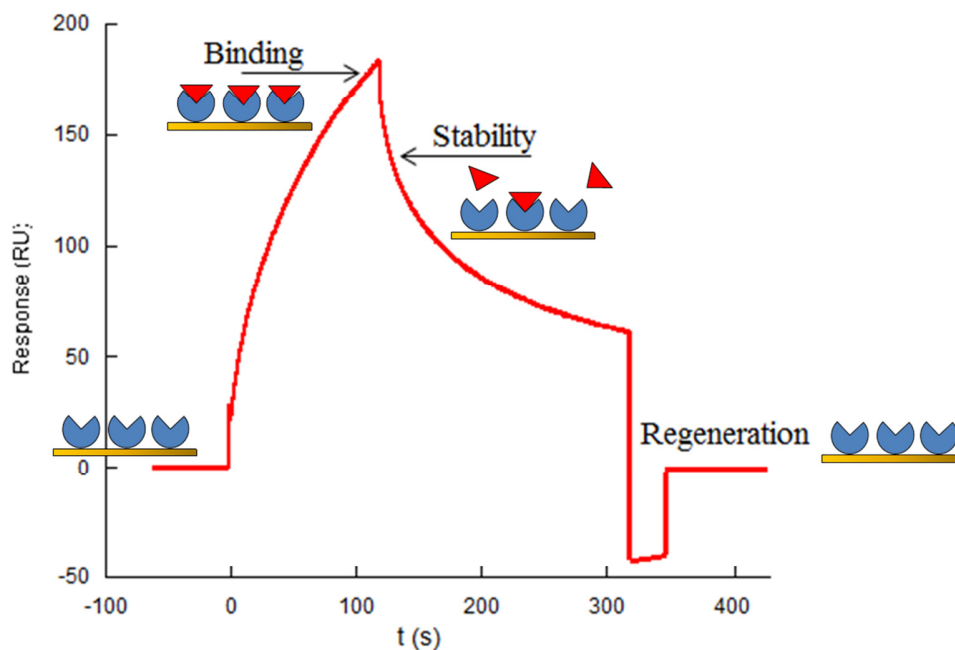
**Figure 6:** Covalent immobilization approaches for attaching the ligand to the surface.

## INTRODUCTION

### 1.4.1.1 Binding studies

Once the ligand has been immobilized on the surface of the chip, binding measurement can be done to quantify the interaction between the ligand and the samples containing the analyte we want to reveal.

A binding experiment is performed for each sample to be tested, by repeating the same cycle of analyses consisting in the following steps: sample injection under a continuous flow of running buffer to allow the formation of the complex, running buffer flow to obtain a partial dissociation, chip surface regeneration to completely remove the analyte that interacted with the ligand without altering the ligand itself. During the injection time the interaction between ligand and analyte generates a change in the reflective index and is converted into an instrumental signal that is directly related to the change in mass concentration on the surface, so that molar responses are proportional to the size of the molecule involved. A given response will represent a higher molar concentration of a small molecule than a large one: conversely, a given number of molecules binding to the surface will give a lower response if the molecule is small. This response is graphically expressed by a sensorgram (Figure 7) showing the progress of the interaction during time.



**Figure 7:** Typical sensorgram resulting from a binding experiment; the signal in Resonance Units is directly related to the quantity of the analyte that binds to the ligand.

To compare the results obtained injecting different samples, two kinds of reference points illustrated in Figure 7 can be considered: the *binding* values that indicate the maximum



interaction signal that is revealed at the end of the injection or the *stability* values that indicate the signal registered 20 seconds after the end of the injection and that only depends on very high specific interactions.

#### 1.4.1.2 Kinetic and affinity studies

The biosensor Biacore T100 allows the characterization of the kinetic and the affinity of the interaction between the biomolecules of interest. Kinetic and affinity are normally determined from the binding characteristics of a series of analyte concentrations. These concentrations may be injected in separate cycles with surface regeneration between the cycles (*multi-cycle analysis*) or sequentially in a single cycle with no regeneration between injections (*single-cycle analysis*).

The minimal requirements to perform a kinetic and affinity evaluation are the knowledge of the molecular weight of the analyte, the application of a concentration series of analyte with at least four non-zero concentrations and one blank cycle consisting of zero concentration sample.

Results from these two approaches are evaluated in the same way, experimental data obtained with every sample are fitted to a series of mathematical models describing the interaction. The association phase during sample injection contains information on both association and dissociation processes and allows the calculation of the association rate  $k_a$  ( $M^{-1}s^{-1}$ ), from the dissociation phase when buffer flow removes dissociated analyte molecules, the dissociation rate  $k_d$  ( $s^{-1}$ ) can be obtained. For the simple 1:1 binding model, the affinity constant  $K_D$  (M) is equal to the ratio of the rate constants ( $k_d/k_a$ ) and can therefore be derived from kinetic measurements.

The fitting procedure used to determine rate constants from experimental data uses numerical integration methods with an iterative approximation algorithm to find the best mathematical model describing the interaction. The standard kinetic interaction models provided with Biacore systems are: a) the 1:1 binding that describes one molecule of analyte binding to one molecule of ligand; b) the bivalent analyte that indicates the interaction of a monovalent ligand with analyte molecules that carry two identical and independent binding sites; c) the heterogeneous ligand describing the interaction of one analyte with two independent ligands on the surface; in this case, the observed binding is the sum of the interaction with the two ligands.

The closeness of the fit is judged in terms of the chi-square value, which describes the deviation between the experimental and the fitted curves. The fitting algorithm seeks to minimize chi-square, and is judged to be complete when the difference in chi-square values between successive iterations is sufficiently small. The significance of the parameter values returned by the fitting

## INTRODUCTION

procedure is indicated by the standard error, which represents the degree to which the value can be varied without significantly affecting the closeness of fit; one parameter is considered significant if its standard error is no more than 1/10 of the parameter value. Other indicators of the closeness of the fitted model are the residuals, which indicate the difference between experimental and fitted value for each data point in the sensorgrams. The residuals should lie within reasonable limits and for a perfect fit they scatter around zero (typically  $\pm 1-2$  RU).

In order to obtain a high quality of kinetic and affinity data, it is necessary that the sensorgrams have a sufficient curvature during the association and the dissociation phase; consequently interactions characterized by a very slow kinetic have to be monitored for a longer time and for interactions characterized by a fast kinetic, the flow should be decreased. The optimal concentration range of the analyte has to be chosen in order to achieve the saturation of the signal at the highest concentration used.

## 1.5 References

---

<sup>1</sup> M.C. Alcaro, F. Lolli, P. Migliorini, M. Chelli, P. Rovero, A.M. Papini; Peptides as autoimmune diseases antigenic probes: a peptide-based reverse approach to detect biomarkers of autoimmune diseases; *Chemistry Today*; 2007 (25): -16.

<sup>2</sup> M. Baker ; *Nature Biotech.* ; 2005 (23): 297-304.

<sup>3</sup> H.A. Doyle, M.J. Mamula, *Trends Immunol.* 2001 (22): 443-449.

<sup>4</sup> E.R. Vossenaar, W.J. van Venrooij; *Clin. Appl. Immunol. Rev.*; 2004 (4): 239-262.

<sup>5</sup> F.Lolli, B.Mulinacci et all; An N-glucosylated peptide detecting disease-specific autoantibodies, biomarkers of multiple sclerosis; *Proc. Natl. Acad. Sci.* 2005 (102): 10273-10278.

<sup>6</sup> S.Rath, C.M. Stanley, M.W. Steward; An inhibition enzyme immunoassay for estimating relative antibody affinity and affinity heterogeneity; *J. Immunol. Method* 1988 (106): 245-249.

## 2 AIM OF THE PROJECT

This PhD work deals with different projects grouped together at first by the aim of selecting the best synthetic peptide bearing aberrant post-translational modifications that could be used as probe in non invasive *in vitro* assays (SP-ELISA or biosensor analysis), to allow a rapid and relatively low expensive detection of specific autoantibodies as diagnostic or prognostic biomarkers of autoimmune diseases.

The second aim is to deeply characterize the kinetic and the affinity of the interactions between antibodies from patients' sera and previously selected antigens thanks to an advanced Surface Plasmon Resonance based biosensor Biacore, in order to obtain information that could have a prognostic value for the follow-up of the disease or that could clarify which is the minimal epitope of a high molecular weight antigen, required for antibody recognition.

In particular, the following four projects have been pursued in the framework of this PhD thesis:

- The first topic deals with specific autoantibodies recognizing citrullinated antigens and currently used as diagnostic biomarkers of rheumatoid arthritis. We used SPR to thoroughly characterize the kinetic and the binding affinity of immunoglobulins from RA patients or normal health subjects to different synthetic citrullinated peptides of previously proved diagnostic power, using both patients' sera and affinity purified antibody fractions.
- The other three projects are based on the knowledge of the ability of the N-glycosyl moiety chemically introduced on CSF114(Glc) peptide to detect specific autoantibodies in MS patients' sera, when the peptide is employed in *in vitro* assays. Considering the recent discovery that the same N-glycosylation present in CSF114(Glc) can be introduced by a bacterial enzyme on the adhesin protein of *Haemophilus influenzae*, the second topic investigates the ability of recombinant glycosylated protein to interact with antibodies in MS patient's sera. The final aim is to investigate if the MS immune deregulation can be triggered by a bacterial infection through a mechanism of molecular mimicry.
- The third topic deals with the SPR characterization of the interaction of CSF114(Glc) with some phage clones and with one selected soluble human antibody domain, in order to understand if this kind of engineered antibodies can be relevant for the development of antigen detection strategies to be used in MS diagnosis.

## AIM OF THE PROJECT

- A recent study suggested a clinical correlation between Rett syndrome and MS, so the last part of this thesis we studied the ability of both CSF114(Glc) and the recombinant glucosylated adhesin protein mentioned above, to reveal antibodies in Rett patients', using immunoenzymatic assays on a large number of patients and control sera.

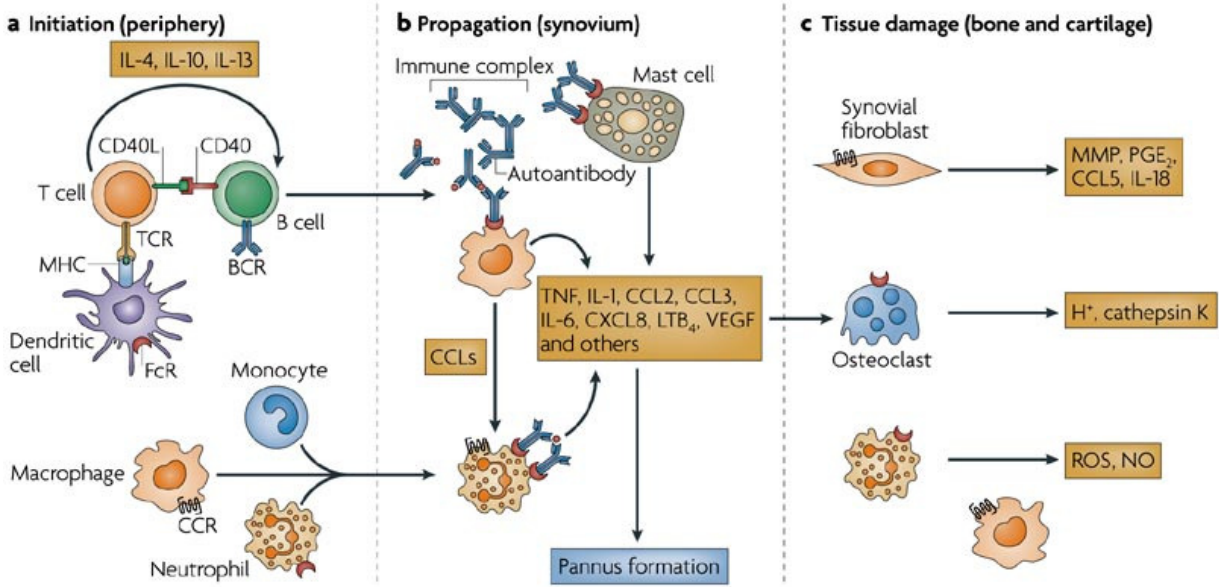
All together these studies could help to solve a very common problem in the field of autoimmune diseases, regarding the knowledge of the real in vivo antigen that triggers the pathological autoimmune response and contribute to develop better diagnostic and prognostic assay.

### **3: Biosensor characterization of Anti-Citrullinated Protein/Peptide Antibodies (ACPA) from Rheumatoid Arthritis patients' sera.**

#### **3.1 Rheumatoid Arthritis**

Rheumatoid Arthritis (RA) is a systemic autoimmune disease occurring in 1% of the adult population worldwide, it is characterized by chronic synovial inflammation that may lead to the destruction of joints, of tissue around joints and of other organs in the whole body.

As shown in Figure 8, three different phases can be identified in RA<sup>1</sup>: the *initiation* of the disease that takes place in peripheral lymphoid organs and whose symptoms are similar to common arthritis, is characterized by synovitis causing swelling of small joints and pain upon motion. Disease is probably initiated by dendritic cells that present self-antigens to autoreactive T cells, which in turn activate autoreactive B cells through cytokines and co-stimulatory molecules, resulting in the production of autoantibody and the deposition of immune complexes in the joint. After the migration of immune cells into the joint, antigen presentation can also occur at the synovium, but direct T-cell contact can also activate other cells in an antigen-independent manner. The *propagation* stage is mediated by immune complexes binding to Fc receptors on macrophages, neutrophils and mast cells; this leads to the release of pro-inflammatory cytokines such as the Tumor Necrosis Factor- $\alpha$  (TNF- $\alpha$ ) and chemokines by these activated cells, as well as to marked leukocyte infiltration and consequent synovial pannus formation. The *terminal* phase is characterized by joint and bone damage and by the possible involvement of other organs such as kidney, blood vessels and lungs; during this last step high levels of cytokines and chemokines activate and recruit synovial fibroblasts, macrophages, osteoclasts and neutrophils, which release proteases, Reactive Oxygen Species (ROS), nitric oxide and prostaglandin E2.



**Figure 8:** Stepwise progression of the immune response involved in the development of RA; three different phases can be identified and all steps collectively contribute to irreversible bone and cartilage destruction.

Although the etiology of RA is poorly understood, genetic factors, humoral and cellular autoimmune mechanisms and environmental factors are all involved in the pathogenesis of the disease<sup>2</sup>. It has been demonstrated that some common factors of risk for the development of the disease include oral contraceptives, female hormones, smoke and infectious agents such as the Epstein-Barr Virus (EBV).

In patients with early disease, the joint manifestations are often difficult to distinguish from other forms of inflammatory polyarthritis and the sub-clinical manifestation of the disease could be very long, so the diagnosis of RA is extremely complicated.

Up to now there is no cure for RA, the therapy is based on the administration of classical drugs (nonsteroidal anti-inflammatory drugs, corticosteroids and immunosuppressants) used to reduce inflammation in order to relieve pain and prevent or slow joint damages; some patients can also benefit of the treatment with innovative biological drugs such as very expensive monoclonal antibodies targeting TNF- $\alpha$ .

In this background the detection of specific biomarkers that allow an early diagnosis and treatment of the pathology is fundamental in order to control inflammation and to prevent the irreversible damages typical of the disease.

### **3.2 Anti-Citrullinated Peptides/Protein Antibodies: a diagnostic criteria for RA.**

The best known RA biomarker is the Rheumatoid Factor (RF), a class of IgM antibodies directed against the Fc-region of the IgG isotype of immunoglobulins. However, RF is not a specific RA marker as it can be found also in other pathological conditions and in healthy individuals. The discovery of the involvement of citrullinated epitopes in RA using anti-perinuclear factor and anti-keratin antibodies boosted the identification of novel highly specific biomarkers of RA<sup>3</sup>.

A family of specific autoantibodies recognizing different citrullinated peptides and proteins and so named Anti-Citrullinated Peptide/Protein Antibodies (ACPA) has been extensively studied in the last decades. ACPA represent a family of heterogeneous antibodies with overlapping specificity, they have been detected in up to 80% RA patients<sup>4</sup> and correlate with disease severity; moreover they are present in the early stage of RA when the differential diagnosis from other chronic arthritis may not be easy and they can also be found in healthy subjects who later developed RA. In 2010 new diagnostic criteria for RA have been defined<sup>5</sup>, attributing a score to the different clinical evidences observed in the patient (Table 1), such as the presence of synovitis in at least one joint, the absence of an alternative diagnosis that better explains the synovitis and the presence of autoantibodies as serological markers; the diagnosis is confirmed if the patient reaches a total score of 6 or more. Because ACPA represent an important biomarker of the disease they have been included in the serological criteria for the classification of RA.

Clinical manifestations	Score
Joints involved: <ul style="list-style-type: none"> <li>• 1 big joint</li> <li>• 2 – 10 big joints</li> <li>• 1 – 3 small joints (with or without big joint involvement)</li> <li>• 4 – 10 small joints (with or without big joint involvement)</li> <li>• &gt; 10 joints (at least 1 small joint)</li> </ul>	0 1 2 3 5
Serology (at least one positive parameter) <ul style="list-style-type: none"> <li>• RF and ACPA negative</li> <li>• RF or ACPA slightly positive</li> <li>• RF or ACPA very positive</li> </ul>	0 2 3
Acute-phase indicators: <ul style="list-style-type: none"> <li>• Normal protein C and erythrocyte sedimentation coefficient levels</li> <li>• Abnormal protein C or erythrocyte sedimentation coefficient levels</li> </ul>	0 1
Clinical symptoms duration: <ul style="list-style-type: none"> <li>• &lt; 6 weeks</li> <li>• &gt; 6 weeks</li> </ul>	0 1

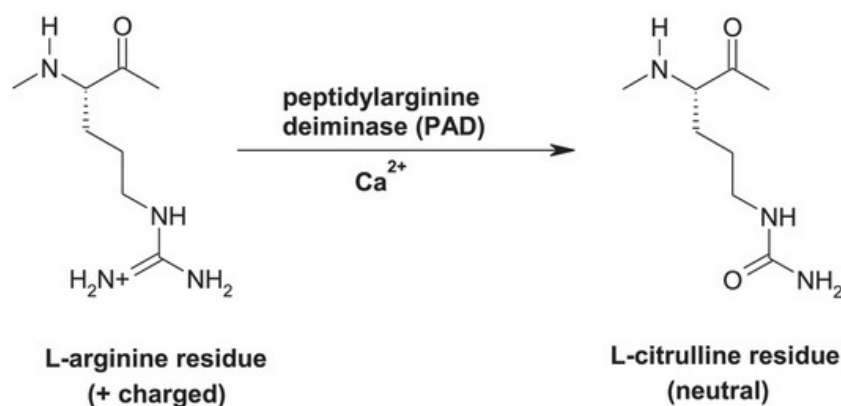
**Table 1:** Rheumatoid Arthritis classification criteria.

It has been demonstrated that ACPA recognize different self proteins<sup>6</sup>, such as filaggrin, fibrinogen, vimentin, collagen II, enolase and histone H4<sup>7</sup>, but also viral citrullinated sequences derived from EBV-encoded proteins<sup>8</sup>, the arginyl residues of which have been post-translationally transformed into citrullyl ones.

Citrulline is a non standard amino acid deriving from a post translational modification catalyzed by the enzyme Peptidyl-Arginine Deiminase (PAD). This modification results in the deimination of arginine residues of proteins into citrulline via the hydrolysis of the guanido group of arginine giving an ureido group and free ammonia; consequently for each deiminated residue, the modified protein acquired one neutral charge instead of one net positive charge (Figure 9).

Five PAD isotypes have been described, among them only PAD4 has a nucleic localization<sup>9</sup> compared with the cytosolic distribution of the other isotypes and together with PAD2 its presence has been demonstrated in synovial fluid cells and extracellular synovial fluid.





**Figure 9:** Deimination of arginine into citrulline catalyzed by the PAD.

Deimination is a physiological process that regulates genes expression, the normal development of tissues and organs such as skin and brain, and also the response to infections because it is a fundamental step in the unfolding of the chromatin followed by Neutrophil Extracellular Traps (NET) formation<sup>10</sup>.

PAD is a  $\text{Ca}^{2+}$  dependent enzyme that is inactive at normal intracellular calcium concentration, but events such as cell death or oxidative stress can increase the  $\text{Ca}^{2+}$  concentration up to the threshold level, activating the enzyme and inducing proteins deimination.

Several in vitro assays have been developed to specifically reveal ACPAs from RA patients' sera using synthetic citrullinated peptides as probes as, for example, the anti-Viral Citrullinated Peptides (VCP1 and VCP2)<sup>11</sup> test or the anti-Modified Citrullinated Vimentin (MVC) one. Up to now the more frequently used assay for ACPA detection is based on a mixture of filaggrin derived Cyclic Citrullinated Peptides (CCPs)<sup>12</sup>. Interestingly, the comparison of the performance of the tests based on CCPs, and VCPs suggested that different citrullinated sequences can detect different subgroups of ACPA in the same set of patients.

### 3.3 Objective

The association of ACPAs, measured using any of the above-mentioned antigens, with erosive arthritis has suggested a role of the antibodies in inducing inflammation and joint damage. One of the possible pathogenic activities of ACPAs is the formation of immune complexes, with consequent release of pro-inflammatory cytokines such as  $\text{TNF-}\alpha$  from monocytes and macrophages<sup>13</sup>.

Considering that the affinity of autoantibodies for their target is considered a relevant parameter in determining their pathogenicity, the aim of the current project was to employ the SPR-

## CHAPTER 3

biosensor Biacore to characterize the affinity and the kinetic of ACPAs, analyzing at first the binding of immunoglobulins from RA patients or normal health subjects and then of affinity purified antibodies from RA patients, to different synthetic citrullinated peptides of previously proved diagnostic power.

### **3.4 Results and discussion**

In the first part of this project the affinity of ACPAs was measured by SPR, analyzing the interaction of IgG fractions from RA sera containing ACPA (9 patients, RA1-RA9) and normal health sera (2 donors, NHS1 and NHS2) with 4 different citrullinated Multiple Antigen Peptides (MAPs) and a tetanus toxoid peptide. Then three diagnostic citrullinated peptides and two non-citrullinated arginine containing control peptides were selected and their interaction with anti-peptide antibody fractions isolated from five RA patients' sera were characterized.

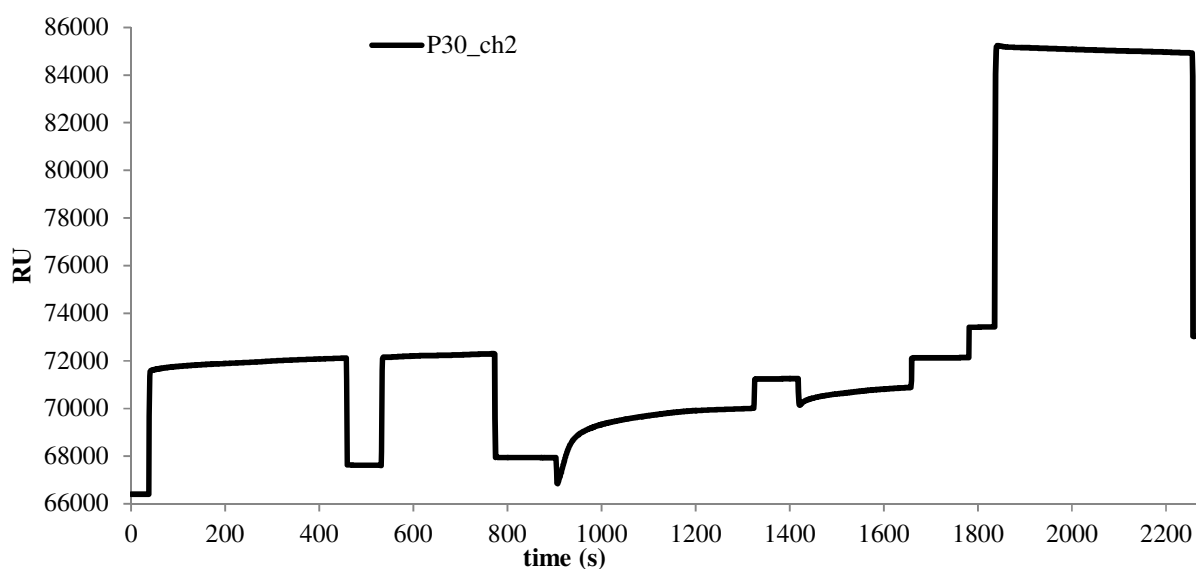
#### **3.4.1 Sensor chips preparation for the characterization of IgG preparations**

Two viral citrullinated peptides (VCP1 and VCP2) and two histone citrullinated peptide (HCP1 and HCP2)<sup>14</sup> were synthesized as tetrameric MAPs by the company Toscana Biomarkers srl and P30 peptide of Tetan Toxoid (947–967)<sup>15</sup> was received from the Institute of Biochemistry, University of Lausanne. For each peptide the best immobilization buffer maximizing the electrostatic interaction with chip surface was selected with the pH scouting procedure and peptides were covalently immobilized onto gold sensor chips to reach immobilization levels reported in Table 2.

Name	Sequence	Immobilization buffer	Immobilized Peptide (RU)
VCP1	(Gly Gly Asp Asn His Gly <b>Cit</b> Gly <b>Cit</b> Gly <b>Cit</b> Gly <b>Cit</b> Gly <b>Cit</b> Gly <b>Cit</b> Gly Gly Gly Gly <b>Cit</b> Pro Gly Ala Pro Gly) <sub>4</sub> Lys <sub>2</sub> Lys βAla	CH <sub>3</sub> COO-Na+ 0.1 mM pH 4.5	885
VCP2	(Gly Gln Ser <b>Cit</b> Gly Gln Ser <b>Cit</b> Gly <b>Cit</b> Gly <b>Cit</b> Gly <b>Cit</b> Gly <b>Cit</b> Gly <b>Cit</b> Gly <b>Cit</b> Gly <b>Cit</b> Gly Lys Gly) <sub>4</sub> Lys <sub>2</sub> Lys βAla	CH <sub>3</sub> COO-Na+ 0.1 mM pH 4.5	2080
HCP1	(Ala Lys <b>Cit</b> His <b>Cit</b> Lys Val Leu <b>Cit</b> Asp Asn Ile Gln Gly Ile Thr Lys Pro Ala Ile) <sub>4</sub> Lys <sub>2</sub> Lys βAla	CH <sub>3</sub> COO-Na+ 5 mM pH 6.0	4100
HCP2	(Lys Pro Ala Ile <b>Cit</b> <b>Cit</b> Leu Ala <b>Cit</b> <b>Cit</b> Gly G ly Val Lys <b>Cit</b> Ile Ser Gly Leu Ile) <sub>4</sub> Lys <sub>2</sub> Lys βAla	CH <sub>3</sub> COO-Na+ 5 mM pH 5.0	3300
P30	(Phe Asn Asn Phe Tyr Val Ser Phe Trp Leu Arg Val Pro Lys Val Ser Ser Ala His Leu Glu) <sub>4</sub> Lys <sub>2</sub> Lys βAla	CH <sub>3</sub> COO-Na+ 10mM pH 5	6025

**Table 2:** MAPs used for the SPR characterization of IgG fractions, optimal immobilization buffer and quantity of peptide immobilized on chip surface expressed in Resonance Unit (RU).

Peptides were linked according to the amine coupling strategy: an amine bond was formed between a primary amine group of each peptide and the previously activated carboxylic group on chip surface, then free reactive sites on chip were blocked with the appropriate reagent. The instrumental signal generated with the immobilization of P30 peptide is given in Figure 10.



**Figure 10:** Sensorgram for amine coupling immobilization of tetanus P30 peptide on channel 2 of a CM5 chip type.

Since sensor chips contain four independent channels, two sensor chips were employed for the immobilization of five ligands. One channel of each sensor chip was used as reference to subtract unspecific interaction between samples and gold surface, this channel was activated and directly blocked.

### 3.4.2 Affinity evaluation of ACPA from IgG preparations

IgG antibodies from patients or control sera, obtained by protein G-affinity chromatography were flowed over each immobilized peptides in individual cycle of analysis based on the following steps: sample injection (association), washing with running buffer (dissociation), and finally chip surface regeneration. Results were elaborated separately for each sample with Biacore Evaluation Software 2.0, fitting the experimental values to theoretical kinetic models and obtaining a high quality fitting with both the 1:1 binding model and the bivalent analyte one. According to this latter model, after analyte–ligand interaction at the first site, engagement of the second site does not contribute to SPR response because there is no change in RI or mass over the chip; there is only a sort of rearrangement of the bound analyte. However, a low amount of peptide was immobilized on the sensor chip, thereby limiting the rebinding effect, and in fact the “check data components” option of the software indicated that the interaction with the first binding site was greater than the interaction with the second one. Thus the 1:1 binding model, considering the interaction between a monovalent analyte molecule and a monovalent immobilized ligand was selected and validated by three statistical parameters: the residual values between the experimental points and the theoretical ones that were closely distributed along the zero, the minimal chi-square value, and the standard errors that were less than 10% of the referred parameter value.

The 9 RA samples resulted to be ACPA positive according to the biosensor assay because antibodies interacting at least with two different citrullinated peptides were detected in each patient serum. As reported in Table 3, the vast majority of interactions between RA IgG and histone derived peptides were characterized by higher affinity ( $10^{-6} \text{ M} > K_D > 10^{-8} \text{ M}$ ) compared to the interactions between RA IgG and peptides VCP1 and VCP2 that were characterized by lower affinity ( $10^{-5} \text{ M} > K_D > 10^{-6} \text{ M}$ ).

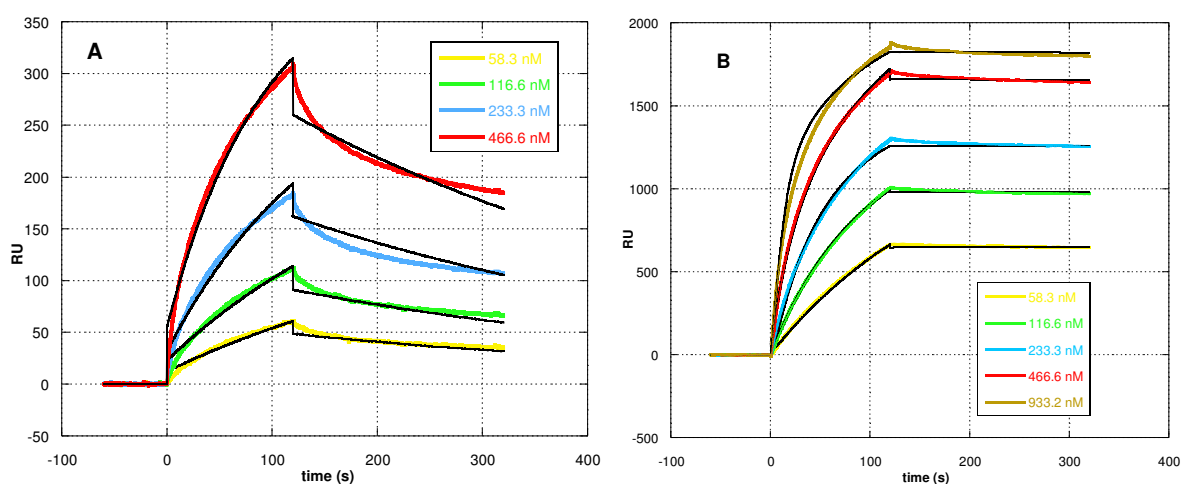
IgG from healthy subject (NHS1 and NHS2) recognized HCP2 citrullinated peptide, and in particular NHS1 IgGs interacted with HCP2 with higher affinity ( $K_D = 10^{-9} \text{ M}$ ) than NHS2 IgGs ( $K_D = 10^{-7} \text{ M}$ ) (Figure 11 A).

IgG from RA patients or controls interacted with peptide P 30 with high affinity ( $10^{-7} \text{ M} > K_D > 10^{-9} \text{ M}$ ) as expected with antibodies induced by repeated cycles of immunization. The sensorgrams resulting from the kinetic study of NHS2 IgG and tetanus peptide is reported in Figure 11 B. Results obtained with P30 peptide were important because they could be considered

as an internal control, confirming the ability of the biosensor assay to reveal high affinity antibodies and consequently giving significant results.

$K_D$ (M)											
	RA1	RA2	RA3	RA4	RA5	RA6	RA7	RA8	RA9	NHS1	NHS2
VCP1	$1.1 \times 10^{-6}$	$3.8 \times 10^{-6}$	No binding	$5.8 \times 10^{-6}$	No binding	$1.2 \times 10^{-4}$	$2.0 \times 10^{-6}$	$1.0 \times 10^{-6}$	No binding	No binding	No binding
VCP2	$1.4 \times 10^{-6}$	$1.5 \times 10^{-6}$	$1.5 \times 10^{-7}$	$4.8 \times 10^{-7}$	No binding	$1.3 \times 10^{-6}$	$8.7 \times 10^{-7}$	$5.5 \times 10^{-7}$	$6.1 \times 10^{-5}$	No binding	No binding
HCP1	$5.9 \times 10^{-8}$	$1.9 \times 10^{-7}$	$1.4 \times 10^{-7}$	$6.9 \times 10^{-8}$	$1.8 \times 10^{-6}$	$1.0 \times 10^{-4}$	No binding	$7.0 \times 10^{-8}$	No binding	No binding	No binding
HCP2	$3.2 \times 10^{-8}$	$2.6 \times 10^{-8}$	$1.9 \times 10^{-7}$	$1.8 \times 10^{-7}$	$4.4 \times 10^{-8}$	$8.5 \times 10^{-8}$	$5.7 \times 10^{-8}$	$9.2 \times 10^{-8}$	$3.6 \times 10^{-8}$	$3.0 \times 10^{-9}$	$2.3 \times 10^{-7}$
P30	$1.7 \times 10^{-8}$	$2.7 \times 10^{-8}$	$7.5 \times 10^{-8}$	$4.7 \times 10^{-8}$	$7.6 \times 10^{-8}$	$9.5 \times 10^{-8}$	$7.2 \times 10^{-8}$	$7.1 \times 10^{-8}$	$3.8 \times 10^{-8}$	$2.5 \times 10^{-9}$	$7.7 \times 10^{-7}$

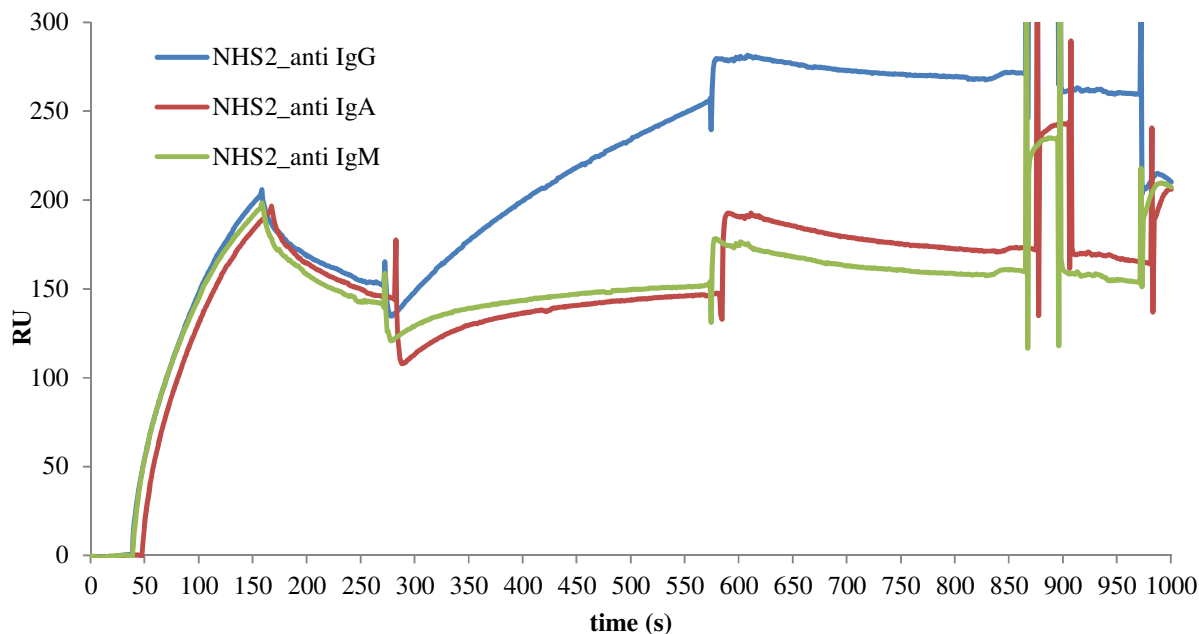
**Table 3:** Affinity constants  $K_D$  calculated with the 1:1 binding model for interactions between IgG samples (9 RA patients and 2 Normal Health Subjects) and four citrullinated peptides and tetanus peptide.



**Figure 11:** Sensorgrams showing the kinetic of the interaction between peptide HCP2 and IgG fraction from NHS2 (A) or between peptide P30 and NHS2 IgG. Experimental curves are reported in different colors according to the sample concentration, black lines represent the 1:1 binding mathematical model fitted to the experimental values.

To confirm the presence of IgG antibodies in NHS samples as well as in RA sera, interacting with peptide HCP2, we performed binding studies with NHS1, NHS2 and RA1 IgG preparations. For each sample three cycles of analysis were performed, characterized by the following steps: sample injection, secondary anti-human antibody application, sensor surface regeneration. All the samples were tested at the same concentration and in each cycle a different secondary antibody was applied (anti-IgG, anti-IgA or anti-IgM). Figure 12 shows the result of the binding study performed with NHS2 sample: a similar binding level was registered at the end on sample injection indicating the reproducibility of the assay and the efficacy of surface regeneration; once

the secondary antibodies were injected, a significant enhancement in the response was registered only in the case of the anti-IgG.



**Figure 12:** Result of the binding study performed with NHS2 sample applying three different secondary anti-human antibodies; an increase in the SPR signal was obtained with the anti-IgG antibody.

The same results were obtained with the other two tested samples confirming the presence of IgG isotype antibodies not specific for RA disease that, in the experimental conditions of this SPR assay, interacted with immobilized HCP2.

### 3.4.3 Sensor chips preparation for purified ACPA detection

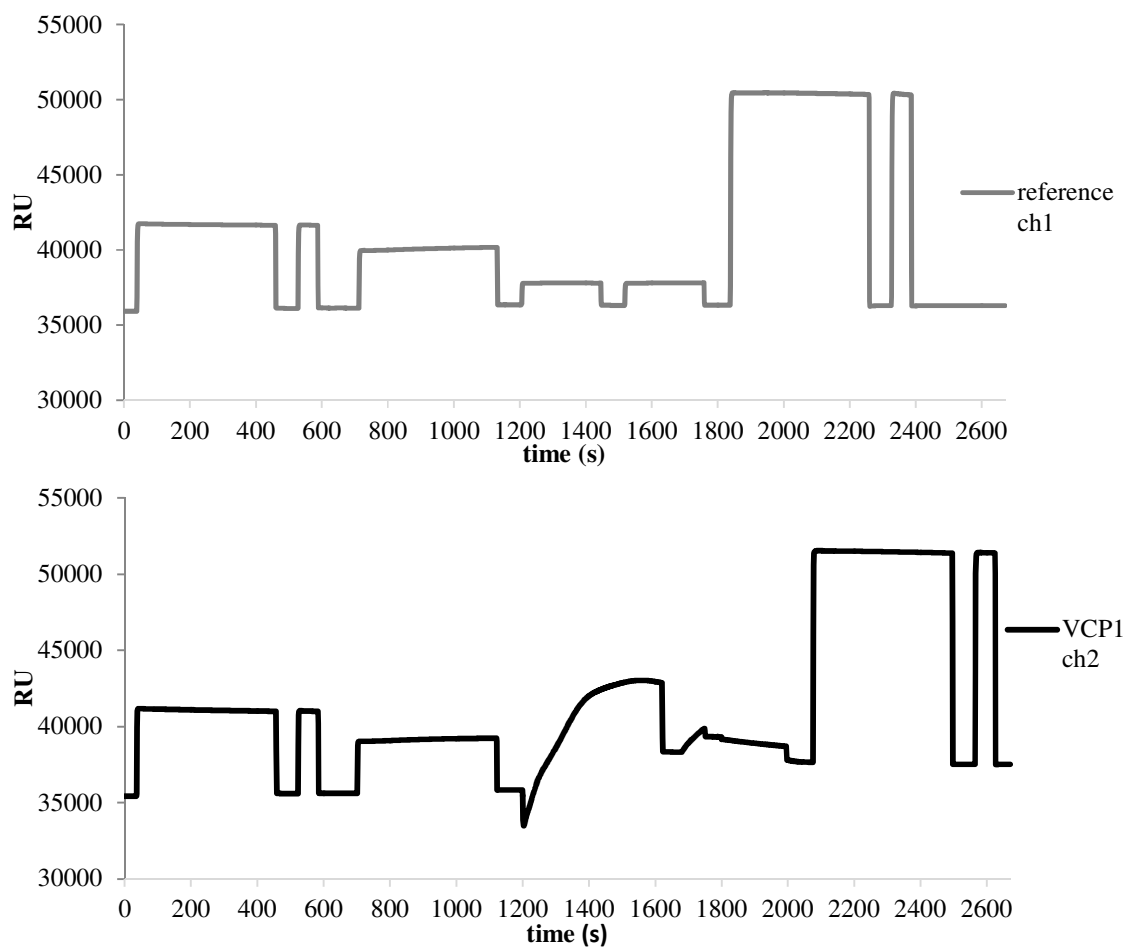
Considering the results obtained from the above reported biosensor analysis, we decided to deeply characterize the affinity and the kinetic of ACPA interaction with different antigens, by testing anti-peptide antibodies purified by affinity chromatography with three citrullinated peptides, from five ACPA positive RA patients.

For this purpose a new sensor surface was prepared by immobilizing the two viral citrullinated peptides VCP1 and VCP2, the histone citrullinated peptide HCP1 and two control sequences (VArgP2 and HArgP1); because of its aspecificity problems HCP2 was not used. The five selected peptides listed in Table 4, were synthesized as tetrameric MAP by the company Toscana Biomarkers srl. For each peptide the best immobilization buffer maximizing the electrostatic interaction with chip surface was selected with the pH scouting procedure and they were covalently immobilized onto gold sensor chips to reach immobilization levels listed in Table 4.

Name	Sequence	Immobilization buffer	Immobilized Peptide (RU)
<b>VCP1</b>	(Gly Gly Asp Asn His Gly <b>Cit</b> Gly <b>Cit</b> Gly <b>Cit</b> Gly <b>Cit</b> Gly <b>Cit</b> Gly <b>Cit</b> Gly Gly Gly Gly <b>Cit</b> Pro Gly Ala Pro Gly) <sub>4</sub> Lys <sub>2</sub> Lys βAla Cys	CH <sub>3</sub> COO-Na <sup>+</sup> 0.5 mM pH 4.5	4080
<b>VCP2</b>	(Gly Gln Ser <b>Cit</b> Gly Gln Ser <b>Cit</b> Gly <b>Cit</b> Gly <b>Cit</b> Gly <b>Cit</b> Gly <b>Cit</b> Gly <b>Cit</b> Gly <b>Cit</b> Gly <b>Cit</b> Gly Lys Gly) <sub>4</sub> Lys <sub>2</sub> Lys βAla Cys	CH <sub>3</sub> COO-Na <sup>+</sup> 0.1 mM pH 4.5	4234
<b>HCP1</b>	(Ala Lys <b>Cit</b> His <b>Cit</b> Lys Val Leu <b>Cit</b> Asp Asn Ile Gln Gly Ile Thr Lys Pro Ala Ile) <sub>4</sub> Lys <sub>2</sub> Lys βAla Cys	CH <sub>3</sub> COO-Na <sup>+</sup> 0.1 mM pH 4.5	4750
<b>VArgP2</b>	(Gly Gln Ser <b>Arg</b> Gly Gln Ser <b>Arg</b> Gly <b>Arg</b> Gly <b>Arg</b> Gly <b>Arg</b> Gly <b>Arg</b> Gly <b>Arg</b> Gly <b>Arg</b> Gly Lys Gly) <sub>4</sub> Lys <sub>2</sub> Lys βAla Cys	Running Buffer pH 7.4	3336
<b>HArgP1</b>	(Ala Lys <b>Arg</b> His <b>Arg</b> Lys Val Leu <b>Arg</b> Asp Asn Ile Gln Gly Ile Thr Lys Pro Ala Ile) <sub>4</sub> Lys <sub>2</sub> Lys βAla Cys	CH <sub>3</sub> COO-Na <sup>+</sup> 0.1 mM pH 5.0	4282

**Table 4:** MAPs used for the SPR characterization of purified ACPAs, optimal immobilization buffer and quantity of peptide immobilized on chip surface expressed in Resonance Unit (RU).

Thanks to the C-terminal cysteine residue that was introduced in each of the five peptides, the thiol coupling strategy was employed for their immobilization on Biacore sensor chips. By this approach, each peptide was covalently immobilized in a well defined orientation on the chip surface, obtaining a better exposition of its antigenic branches. This coupling approach consisted in the activation of carboxylic groups on chip surface, in the introduction of active disulfide groups and in the injection of the peptide containing the free thiol in order to allow the exchange reaction between thiols and active disulfide groups introduced in the dextran matrix. Free reactive sites on chip surface were blocked with appropriate reagents. Figure 13 shows the resonance signal generated by the immobilization of VCP1 peptide on channel 2. The channel 1 of each sensor chip was used as reference to subtract unspecific interaction between samples and gold surface, this channel was activated and directly blocked obtaining the sensorgram shown in Figure 13.



**Figure 13:** Sensorgrams registered from channel 1 during the blank immobilization and from channel 2 during the immobilization of VCP1 according to the ligand thiol coupling strategy.

#### 3.4.4 SPR characterization of purified ACPA

Each anti-peptide antibody fraction was diluted up to a suitable final concentrations and flowed over each immobilized peptide in an individual cycle of analysis based on the same steps described for IgG fractions characterization. Results were elaborated separately for each sample fitting the experimental values to the theoretical 1:1 binding model that was validated by the statistical parameters of the residual values, the chi-square value, and the standard errors. The affinity constants  $K_D$ , and the kinetic parameters of the association rate  $k_a$  and dissociation rate  $k_d$ , describing the interactions between each purified antibody fraction and the three citrullinated peptides were calculate and reported in Table 5.



	$k_a$ (L/mol·s)	$k_d$ (1/s)	$K_D$ (mol/L)	$k_a$ (L/mol·s)	$k_d$ (1/s)	$K_D$ (mol/L)	$k_a$ (L/mol·s)	$k_d$ (1/s)	$K_D$ (mol/L)
	VCP1			VCP2			HCP1		
RA1 anti VCP1	$51.7 \pm 1.0.8 \times 10^2$	$64.0 \pm 0.4 \times 10^{-4}$	$1.24 \pm 0.03 \times 10^{-6}$	$67.9 \pm 0.8 \times 10^2$	$93.0 \pm 1.0 \times 10^{-4}$	$1.37 \pm 0.03 \times 10^{-6}$	$64.8 \pm 2.6 \times 10^3$	$33.1 \pm 0.4 \times 10^{-4}$	$5.10 \pm 0.27 \times 10^{-8}$
RA2 anti VCP1	$87.3 \pm 1.8 \times 10^2$	$10.0 \pm 0.2 \times 10^{-3}$	$1.15 \pm 0.04 \times 10^{-6}$	$10.6 \pm 0.2 \times 10^3$	$96.1 \pm 1.3 \times 10^{-4}$	$9.09 \pm 0.29 \times 10^{-7}$	$14.9 \pm 0.1 \times 10^3$	$21.0 \pm 0.7 \times 10^{-5}$	$1.41 \pm 0.06 \times 10^{-8}$
RA3 anti VCP1	$54.0 \pm 0.7 \times 10^2$	$63.7 \pm 0.4 \times 10^{-4}$	$1.18 \pm 0.02 \times 10^{-6}$	$68.1 \pm 1.0 \times 10^2$	$62.9 \pm 0.8 \times 10^{-4}$	$9.24 \pm 0.25 \times 10^{-7}$	$10.1 \pm 1.2 \times 10^3$	$19.5 \pm 2.6 \times 10^{-4}$	$1.93 \pm 0.49 \times 10^{-7}$
RA4 anti VCP1	$11.4 \pm 0.2 \times 10^3$	$12.5 \pm 0.2 \times 10^{-3}$	$1.10 \pm 0.04 \times 10^{-6}$	$10.9 \pm 0.2 \times 10^3$	$48.3 \pm 0.6 \times 10^{-4}$	$4.44 \pm 0.14 \times 10^{-7}$	$59.0 \pm 0.2 \times 10^3$	$28.1 \pm 0.2 \times 10^{-4}$	$4.76 \pm 0.05 \times 10^{-8}$
RA5 anti VCP1	$15.8 \pm 0.5 \times 10^3$	$34.4 \pm 0.6 \times 10^{-4}$	$2.18 \pm 0.11 \times 10^{-7}$	$11.8 \pm 3.5 \times 10^3$	$59.1 \pm 3.4 \times 10^{-4}$	$4.99 \pm 1.77 \times 10^{-7}$	$28.3 \pm 1.0 \times 10^3$	$22.2 \pm 0.3 \times 10^{-4}$	$7.82 \pm 0.38 \times 10^{-8}$
RA1 anti VCP1	$33.9 \pm 1.3 \times 10^3$	$35.5 \pm 1.3 \times 10^{-3}$	$1.05 \pm 0.08 \times 10^{-6}$	$10.7 \pm 0.1 \times 10^3$	$71.3 \pm 0.6 \times 10^{-4}$	$6.68 \pm 0.12 \times 10^{-7}$	$66.0 \pm 0.4 \times 10^3$	$16.4 \pm 1.0 \times 10^{-4}$	$2.48 \pm 0.17 \times 10^{-8}$
RA2 anti VCP1	$60.5 \pm 1.1 \times 10^2$	$10.9 \pm 0.2 \times 10^{-3}$	$1.81 \pm 0.07 \times 10^{-6}$	$85.0 \pm 0.2 \times 10^2$	$12.3 \pm 0.3 \times 10^{-3}$	$1.45 \pm 0.04 \times 10^{-6}$	$36.9 \pm 0.3 \times 10^3$	$15.1 \pm 0.1 \times 10^{-4}$	$4.10 \pm 0.06 \times 10^{-8}$
RA3 anti VCP1	$63.1 \pm 1.0 \times 10^2$	$92.6 \pm 0.7 \times 10^{-4}$	$1.47 \pm 0.03 \times 10^{-6}$	$52.7 \pm 0.9 \times 10^2$	$50.5 \pm 0.6 \times 10^{-4}$	$9.58 \pm 0.28 \times 10^{-7}$	$14.0 \pm 0.9 \times 10^3$	$29.5 \pm 0.6 \times 10^{-4}$	$2.11 \pm 0.18 \times 10^{-7}$
RA4 anti VCP1	$51.3 \pm 0.4 \times 10^3$	$49.4 \pm 3.4 \times 10^{-3}$	$9.62 \pm 0.74 \times 10^{-7}$	$17.8 \pm 0.5 \times 10^3$	$91.7 \pm 2.1 \times 10^{-4}$	$5.15 \pm 0.26 \times 10^{-7}$	$27.2 \pm 1.6 \times 10^3$	$34.4 \pm 0.4 \times 10^{-4}$	$1.27 \pm 0.09 \times 10^{-7}$
RA5 anti VCP1	$83.8 \pm 1.6 \times 10^2$	$61.6 \pm 0.6 \times 10^{-4}$	$7.36 \pm 0.21 \times 10^{-7}$	$46.9 \pm 0.8 \times 10^2$	$46.5 \pm 0.4 \times 10^{-4}$	$9.92 \pm 0.25 \times 10^{-7}$	$34.3 \pm 0.8 \times 10^4$	$14.9 \pm 0.3 \times 10^{-3}$	$4.33 \pm 0.19 \times 10^{-8}$
RA1 anti VCP1	$17.7 \pm 0.2 \times 10^3$	$20.3 \pm 0.1 \times 10^{-3}$	$1.15 \pm 0.02 \times 10^{-6}$	$38.6 \pm 0.7 \times 10^3$	$97.1 \pm 1.2 \times 10^{-4}$	$2.52 \pm 0.08 \times 10^{-7}$	$56.1 \pm 0.2 \times 10^3$	$14.1 \pm 0.1 \times 10^{-4}$	$2.51 \pm 0.03 \times 10^{-8}$
RA2 anti VCP1	$86.5 \pm 0.7 \times 10^2$	$53.2 \pm 0.2 \times 10^{-4}$	$6.15 \pm 0.07 \times 10^{-7}$	$12.0 \pm 0.1 \times 10^3$	$21.8 \pm 0.1 \times 10^{-4}$	$1.82 \pm 0.02 \times 10^{-7}$	$40.8 \pm 0.1 \times 10^3$	$65.8 \pm 1.5 \times 10^{-5}$	$1.61 \pm 0.04 \times 10^{-8}$
RA3 anti VCP1	$12.1 \pm 0.1 \times 10^3$	$55.1 \pm 0.2 \times 10^{-4}$	$4.54 \pm 0.05 \times 10^{-7}$	$96.9 \pm 1.7 \times 10^2$	$41.5 \pm 0.4 \times 10^{-4}$	$4.29 \pm 0.12 \times 10^{-7}$	$52.2 \pm 1.0 \times 10^3$	$223.4 \pm 2.2 \times 10^{-5}$	$4.28 \pm 0.12 \times 10^{-8}$
RA4 anti VCP1	$22.9 \pm 0.2 \times 10^3$	$56.4 \pm 0.3 \times 10^{-4}$	$2.46 \pm 0.03 \times 10^{-7}$	$21.0 \pm 0.3 \times 10^3$	$59.6 \pm 0.7 \times 10^{-4}$	$2.84 \pm 0.07 \times 10^{-7}$	$43.8 \pm 1.1 \times 10^3$	$21.6 \pm 0.2 \times 10^{-4}$	$4.94 \pm 0.17 \times 10^{-8}$
RA5 anti VCP1	$26.6 \pm 0.6 \times 10^3$	$38.7 \pm 0.8 \times 10^{-4}$	$1.45 \pm 0.04 \times 10^{-7}$	$84.5 \pm 1.1 \times 10^3$	$14.0 \pm 0.2 \times 10^{-4}$	$1.66 \pm 0.05 \times 10^{-8}$	$90.9 \pm 0.4 \times 10^3$	$13.6 \pm 0.1 \times 10^{-4}$	$1.49 \pm 0.02 \times 10^{-8}$

**Table 5:** Kinetic parameters  $k_a$  and  $k_d$  and affinity constant  $K_D$  calculated with the 1:1 binding model for interactions between purified antibodies fractions and citrullinated peptides.

CHAPTER 3

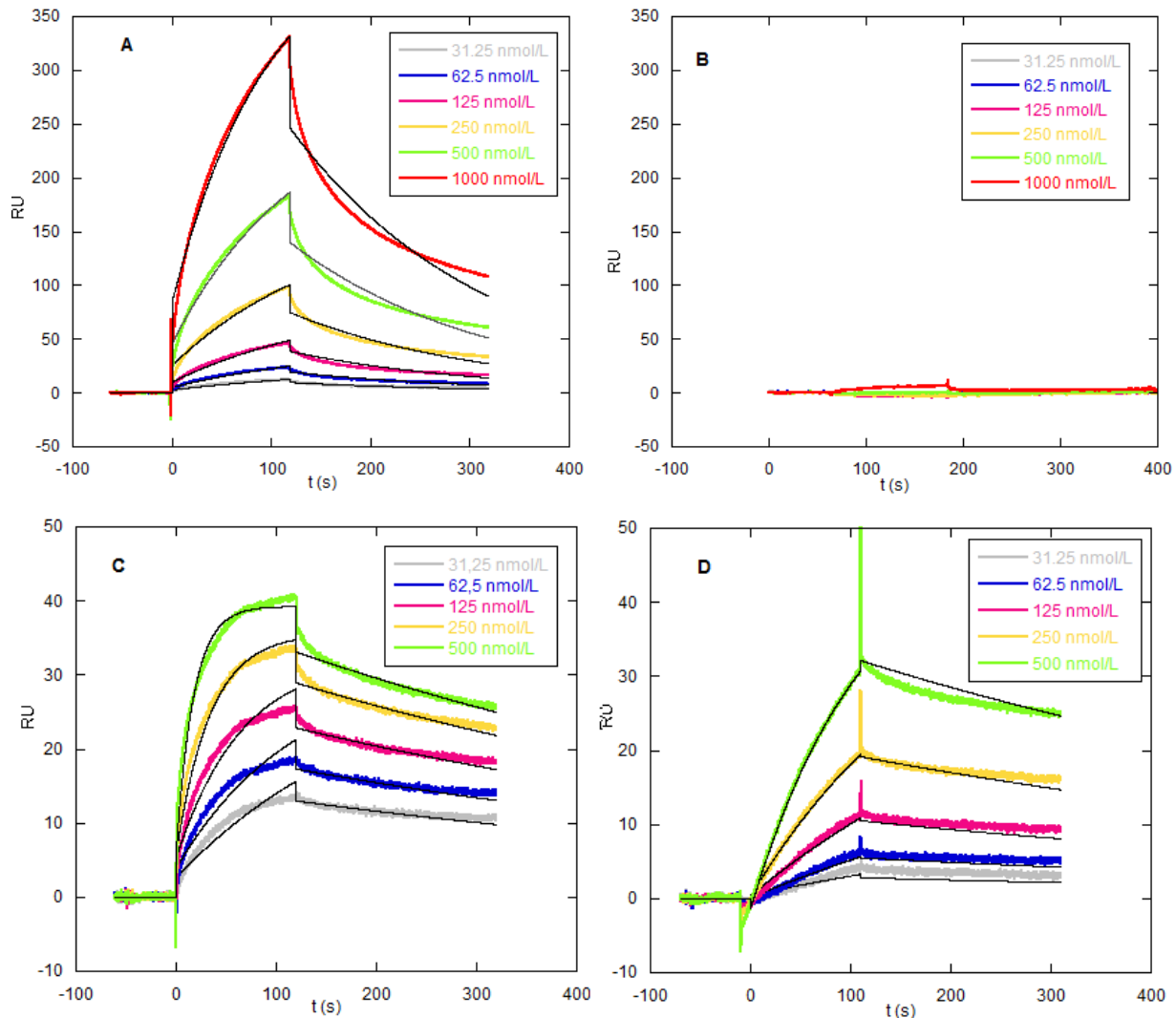
As a negative control demonstrating the requirement of citrulline residues for antibodies recognition, we then tested the binding of anti-VCP2 antibodies to non-citrullinated arginine-containing peptide VArgP2, and the binding of anti-HCP1 antibodies to non-citrullinated arginine-containing peptide HArgP1. In four cases out of five, no binding signals were detected to VArgP2, while RA3 and RA5 showed respectively no and low binding to HArgP1. In the case in which the interaction signal was proportional to the injected concentration, the experimental data were fitted to the 1:1 binding model and the affinity constants  $K_D$  were calculated (Table 6).

	$K_D$ (mol/L)				
	RA1 anti VCP2	RA2 anti VCP2	RA3 anti VCP2	RA4 anti VCP2	RA5 anti VCP2
<b>VArgP2</b>	No binding	No binding	No binding	$3.39 \pm 0.02 \times 10^{-7}$	No binding
	RA1 anti HCP1	RA2 anti HCP1	RA3 anti HCP1	RA4 anti HCP1	RA5 anti HCP1
<b>HArgP1</b>	$1.80 \pm 0.04 \times 10^{-7}$	$6.95 \pm 0.21 \times 10^{-9}$	Low binding	$1.76 \pm 0.12 \times 10^{-5}$	No binding

**Table 6:** Affinity constant  $K_D$  calculated with the 1:1 binding model for interactions between the non-citrullinated sequences and antibodies purified with the corresponding citrullinated peptide.

In order to summarize all the kinetic and affinity results, we used the Biacore T100 Kinetic Summary application and we obtained the  $k_a/k_d$  plot. This graph provides an overview of kinetic and affinity properties for the different interactions studied, by plotting the association rate parameter ( $k_a$ ) against the dissociation rate parameter ( $k_d$ ), both on logarithmic scale. Affinity constants  $K_D$  (calculated as  $k_d/k_a$  ratio) are displayed on diagonal lines. Thus, interactions having the same affinity but different kinetic are indicated by points lying on the same diagonal line. In Figure 14 we reported the  $k_a/k_d$  plot for the 15 interactions between each purified antibody fraction and the peptide used for its purification and for the 4 characterized interactions with the two arginine containing control peptides.





**Figure 15:** Sensorgrams showing: A) a low affinity interaction between RA3 anti-VCP2 antibodies and VCP2; B) the lack of an interaction signal with control peptide VArgP2; C) a high affinity interaction between RA1 anti-HCP1 antibodies and HCP1; D) the interaction between RA1 anti-HCP1 antibodies and the control peptide HArgP1. Experimental curves are reported in different colors according to the sample concentration, black lines represent the 1:1 binding mathematical model fitted to the experimental values.

On the whole, the data reported in Table 5 indicated a high cross-reactivity of anti-peptide antibodies. In fact, each antibody fraction, obtained by affinity chromatography on a given peptide, reacted also with the other two citrullinated peptides. Under this aspect, it is of interest that purified anti-VCP1 and anti-VCP2 antibodies had a higher affinity for HCP1 than for VCP1 and VCP2.

These results confirmed and extended previous data on the binding specificity, the cross-reactivity and the affinity of ACPA. It has been demonstrated that ACPA represent a family of antibodies with overlapping specificities and variable cross-reactivity. The analysis of RA sera on

panels of citrullinated peptides from filaggrin or fibrin has demonstrated that, despite the existence of major epitopes, recognized by many sera, RA patients displayed many different reactivity profiles<sup>16</sup>. Comparing the results obtained testing a panel of sera on VCP2, VCP1 and CCP, a general overall correlation was found, but some sera reacted with only one or two antigens, thus suggesting that different non overlapping epitopes may be targeted by ACPA<sup>17</sup>.

Analyzing the binding to non citrullinated sequences, we found that in most cases the antibodies were specific for citrullinated peptides because no interaction signal was registered with the non citrullinated sequences. When a specific signal was detected, the calculated affinity constants indicated that RA1 and RA4 bound with a much lower affinity the arginine containing peptides with respect to HCP1, while RA2 bound the arginine-containing peptide with a higher affinity than HCP1. RA4 displayed the same affinity for both VCP2 and VArgP2 peptides. This result represented an additional evidence for the exquisite specificity of antibodies from RA patients for citrullinated sequences. The only exception was represented by the antibodies specific for the citrullinated histone peptide obtained from RA2 patient that bound with a higher affinity the arginine containing sequence. It was likely that these antibodies were specific for the C-terminal portion of the peptide that did not contain citrullines, and thus represent an example of anti-histone antibodies detectable in RA sera<sup>18</sup>.

According to the results of the present study, ACPA resulted to be heterogeneous not only in terms of specificity, but also of affinity. ACPA specific for the EBNA-derived peptides VCP1 and VCP2 were in fact characterized by a lower affinity than those binding the histone peptide. VCP1 and VCP2 contain a glycine-citrulline stretch, that represents an epitope shared by the two sequences and targeted by antibodies present in RA sera; a second non overlapping epitope is located in the N-terminal portion of VCP2<sup>17</sup>. Thus, the structural similarity of VCP1 and VCP2 may explain a similar affinity of antibodies that bind the two peptides. HCP1, on the contrary, is structurally different: it does not contain stretches of citrullines flanked by small/neutral aminoacids and, despite the substitution of arginine with citrulline, it has a strong positive charge due to several lysine residues.

Citrullinated proteins as well as CCP, which is a mixture of synthetic peptides, bear multiple epitopes recognized by RA sera and thus allow an average evaluation of affinity without detecting a difference in affinity among antibodies binding to the different antigens. On the contrary, using synthetic peptides that bear a limited number of epitopes and allow analyzing an oligoclonal population of antibodies, a spectrum of affinity was detected. Thanks to the present

## CHAPTER 3

biosensor assay we characterized the interaction of ACPA with citrullinated peptides derived from exogenous antigens (VCP1, VCP2) or autoantigens (HCP1) and we found that the affinity for HCP1 was higher, also when antibodies affinity purified on VCP1 and VCP2 were tested. These results may suggest that antibodies initially elicited by an infectious antigen (such as EBV) could be then selected and expanded by autoantigens (such as histones).

### 3.5 Conclusions

The Surface Plasmon Resonance biosensor Biacore was employed to evaluate the affinity of the total IgG fraction of nine RA patients' sera and two NHS sera for four citrullinated peptides and for one tetanus toxoid peptide. The presence of ACPA was confirmed in every RA sera, because they recognized at least two citrullinated peptides. Histone peptide HCP2 was recognized by both NHS samples highlighting some specificity problems. Tetanus peptide interacted with high affinity antibodies in every tested sample, confirming the ability of the chosen approach to detect high affinity antibodies. The kinetic and the affinity of the interaction between purified antibodies from RA patients' sera, and citrullinated peptides VCP1, VCP2, and HCP1 were performed observing high cross-reactivity and heterogeneity. Calculated affinity constants for ACPA-peptide interactions presented sensible differences (1-fold in  $K_D$  values) between viral peptides VCP1-VCP2 and histone peptide HCP1 and as we recently reported in our publication, this result suggested that two different ACPA subfamilies were identified<sup>19</sup>. These findings have a potential clinical relevance since the peptides here analyzed are employed in solid phase assays for the diagnosis of RA and from this point of view it will be very interesting to test ACPAs purified from patients in different phase of the disease in order to understand if there is a change in the affinity of ACPAs interaction with a certain peptide during the progression of the disease or if a subfamily of autoantibodies is exclusive and so detectable in one phase of the disease and not in the others.

### 3.6 Materials and methods

All experiments were conducted using a Biacore T100 instrument from GE Healthcare. All solutions and buffers were prepared with milliQ water obtained by the Sartorius system (arium 611 VF). Sensor chips CM5, amine coupling kit, thiol coupling kit and Running Buffer HBS-EP+ 10x (0.1 mol/L HEPES, 1.5 mol/L NaCl, 30 mmol/L EDTA, 0.5% v/v p20) were purchased by GE Healthcare. Running Buffer was diluted ten times with milliQ water at pH 7.4 and filtered

daily with a Millipore Express™ PLUS 0.22µm system. Sodium acetate and Sodium hydroxide were purchased by Carlo Erba (Milano). The four citrullinated peptides VCP1, VCP2, HCP1 and HCP2 and the two non-citrullinated control sequences VArgP2 and HArgP1 were synthesized as tetrameric Multiple Antigen Peptides, by the Company Toscana Biomarkers srl; peptide P30 was a gift of Prof. Corradin from the Institute of Biochemistry, University of Lausanne.

### **3.6.1 ACPA purification from patients' sera**

Five ACPA positive RA patients (RA1-RA5) were enrolled in this project. IgG fractions containing ACPAs were obtained, from the laboratory of Clinical and Experimental Medicine of the University of Pisa (Prof. Migliorini), by precipitation with 50% saturated ammonium sulfate and purified by Protein-G affinity chromatography. In order to isolate anti-peptide antibodies, citrullinated MAPs were conjugated to CNBr activated Sepharose (Sigma-Aldrich) according to the standard manufacturer instructions. Antibodies bound to the column were eluted by 100 mM glycine buffer (pH 2.8), and dialyzed overnight against PBS. The anti-peptide antibody concentration was determined by UV absorbance at 280<sub>nm</sub>. A total of fifteen purified anti-peptide antibody fractions were obtained by affinity chromatography from five different RA sera using each of the three citrullinated MAP.

### **3.6.2 PH scouting procedure**

Immobilization buffers were selected separately for each peptide using the pH scouting procedure, using the following buffers: PBSbuffer pH 7.2, sodium acetate buffer 0.1 mM pH 4.5 and 6.0, sodium acetate buffer 0.5 mM pH 4.5 and 5.0, sodium acetate buffer 5 mM pH 4.5, 5.0 and 6.0, sodium acetate buffer 10 mM pH 6.0. Peptides were solubilized in each buffer at a final concentration of 10 µg/mL and injected over the non-activated sensor chip surface for 120s at a flow rate of 10µL/min; after each injection chip surface was regenerated with a pulse of 0,1M NaOH for 30s at a flow rate of 10µL/min. The selected buffer and the immobilized peptide quantities are reported in Table 4.

### **3.6.3 Citrullinated MAPs and tetanus peptide immobilization: amine coupling**

The five peptides listed in Table 2 were individually immobilized on a different channel of sensor chips CM5-type according to the amine coupling strategy. For immobilization, sensor chip surface was activated with two injections of N-hydroxysuccinimide (NHS 0.1 M) and 1-ethyl-3-

## CHAPTER 3

(3-dimethylaminopropyl)-carbodiimide (EDC 0.4 M) 50:50 for 420 and 240 seconds respectively at a flow rate of 10  $\mu\text{L}/\text{min}$ . After surface activation each peptide, solubilized in the previously selected immobilization buffer (10  $\mu\text{g}/\text{mL}$ ), was injected for 420 seconds at a flow rate of 10  $\mu\text{L}/\text{min}$ . Immobilization was continued in manual mode by injecting peptide solution up to reaching a satisfactory immobilization level. Non-reacted sites on sensor chip surface were blocked injecting ethanolamine-HCl 1 M pH 8.5 for 420 and 60 seconds at a flow rate of 30  $\mu\text{L}/\text{min}$ . Reference channels were activated injecting NHS/EDC 50:50 and directly blocked with ethanolamine-HCl.

### 3.6.4 Affinity studies with total IgG fractions

RA and NHS IgG samples (at different initial concentrations tested by UV absorbance at 280<sub>nm</sub>) were diluted in running buffer to final concentration of 3732.8, 1866.4, 933.2, 466.6, 233.3, 116.6 and 58.3 nM. Each diluted sample was injected over each immobilized peptide for 120 seconds at a flow rate of 30  $\mu\text{L}/\text{min}$ . Running buffer was then flushed for 200 seconds at a flow rate of 30  $\mu\text{L}/\text{min}$  and finally the chip surface was regenerated by injecting a glycine solution 10 mM pH 2.5 for 30 seconds and a sodium hydroxide solution 0.1 M for 60 seconds both at a flow rate of 30  $\mu\text{L}/\text{min}$ .

Binding studies on HCP2 were performed injecting selected samples [466.6 nM] for 120 seconds at a flow rate of 30  $\mu\text{L}/\text{min}$ , followed by the injection of anti-human IgG or IgA or IgM –alkaline Phosphatase antibody (Sigma) 1:4000 for 240 seconds at a flow rate of 5  $\mu\text{L}/\text{min}$ , running buffer was then flushed for 200 seconds and chip surface was regenerated as above described for affinity studies.

### 3.6.5 Citrullinated MAPs and control sequences immobilization: thiol coupling

The five MAP reported in Table 4 were individually immobilized on a different channel of sensor chips CM5-type according to the ligand thiol coupling strategy consisting in the following steps:

- chip surface activation with two injections of N-hydroxysuccinimide (NHS 0.1 M) and 1-ethyl-3-(3-dimethylaminopropyl)-carbodiimide (EDC 0.4 M) 50:50 for 420 s at a flow rate of 10  $\mu\text{L}/\text{min}$ ;
- active disulfide groups introduction by injecting twice a solution of 67% 120mM 2-(2-pyridinyldithio)ethaneamine (PDEA) and 33% sodium borate 0.1 M pH 8.5 for 420 s at a flow rate of 10  $\mu\text{L}/\text{min}$ ;



- peptide injection in the selected immobilization buffer [10 $\mu$ g/mL] for 420 s and 60 s at a flow rate of 10  $\mu$ L/min;
- non-reacted disulfide groups on sensor chip surface blocking by injecting 50mM cysteine and 1M NaCl in 0.1M sodium acetate pH 4.3 for 240 s at a flow rate of 10  $\mu$ L/min;
- free reactive sites formed by NHS/EDC activation blocking with 1M ethanolamine-HCl pH 8.5 for 420 s at a flow rate of 10  $\mu$ L/min.

Reference channel was activated injecting NHS/EDC 50:50 and PDEA and directly blocked with cysteine buffer and ethanolamine-HCl.

### **3.6.6 SPR kinetic and affinity studies with anti-peptide antibodies**

Anti-citrullinated peptide antibody fractions (at different initial concentrations tested by UV absorbance at 280<sub>nm</sub>) were diluted in running buffer to final concentration of 2000, 1000, 500, 250, 125, 62.5, and 31.25 nM. Diluted samples were injected over each ligand for 120 s at a flow rate of 30  $\mu$ L/min. Running buffer was then flushed for 200 s at a flow rate of 30  $\mu$ L/min and finally the chip surface was regenerated by injecting a 10mM glycine solution pH 2.5 for 30 s and a 0.1M NaOH solution for 60 s both at a flow rate of 30  $\mu$ L/min.

Each sample was applied in a different cycle of analysis and instrumental results were elaborated with the Biacore Evaluation Software 2.0 and summarized with the Biacore T100 Kinetic Summary application.

## 3.7 References

- <sup>1</sup> S.A. Paget, M.D. Lockshin, S. Loeb; Rheumatoid Arthritis Handbook. New York, NY: John Wiley and Sons, Inc; 2002.
- <sup>2</sup> Y. Alamanos, A.A. Drosos; Epidemiology of adult Rheumatoid Arthritis; *Autoimmun. Rev.* 2005 (4):130-136.
- <sup>3</sup> M. Simon, E. Girbal, M. Sebbag, C. Vincent, C. Masson-Bessiere, J.J. Durieux; The antiperinuclear factor and the so called antikeratin antibodies are the same rheumatoid arthritis specific autoantibodies; *J.Clin. Invest.* 1995 (95): 2672-2679.
- <sup>4</sup> G.J. Pruijn, A. Wiik, W.J. van Venrooij; The use of citrullinated peptides and proteins for the diagnosis of rheumatoid arthritis; *Arthritis Res. Ther.* 2010 (12): 203.
- <sup>5</sup> D. Aletaha, T. Neogi, A.J. Silman, J. Funovits; Rheumatoid arthritis classification criteria: an American College of Rheumatology/European League Against Rheumatism collaborative initiative; *Ann. Rheum. Dis.* 2010 (69): 1580-1588.
- <sup>6</sup> H. Uysal, K.S. Nandakumar, C. Kessel, S. Haag, S. Carlsen, H. Burkhardt, R. Holmdahl, Antibodies to citrullinated proteins: molecular interactions and arthritogenicity; *Immunol. Rev.* 2010 (233): 9-33.
- <sup>7</sup> F. Pratesi, I. Dioni, C. Tommasi, M.C. Alcaro, I. Paolini, F. Barbetti, F. Boscaro, F. Panza, I. Puxeddu, P. Rovero, P. Migliorini; Antibodies from patients with rheumatoid arthritis target citrullinated histone 4 contained in neutrophils extracellular traps; *Ann. Rheum. Dis.* 2014 (73): 1414-1422.
- <sup>8</sup> F. Pratesi, C. Tommasi, C. Anzilotti, I. Puxeddu, E. Sardano, G. Di Colo, P. Migliorini; Antibodies to a new viral citrullinated peptide, VCP2: fine specificity and correlation with anti-cyclic citrullinated peptide (CCP) and anti-VCP1 antibodies; *Clin. Exp. Immunol.* 2011 (164): 337-345.
- <sup>9</sup> K. Nakashima, T. Hagiwara, M. Yamada; Nuclear localization of peptidylarginine deiminase VI and histone deamination in granulocytes; *J. Biol. Chem.* 2002 (277): 49562-49568.
- <sup>10</sup> Y. Wang, M. Li, S. Stadler et al; histone hypercitrullination mediates chromatin decondensation and neutrophils extracellular trap formation; *J. Cell. Biol.* 2009 (184): 205-213.
- <sup>11</sup> P. Migliorini; Viral citrullinated peptides and uses thereof; WO2004087747A2.
- <sup>12</sup> M.A. van Boekel, E.R. Vossenaar, F.H. van den Hoogen, W.J. van Venrooij, Autoantibody systems in rheumatoid arthritis: specificity, sensitivity and diagnostic value; *Arthritis Res.* 2002 (4): 87-93.
- <sup>13</sup> C. Clavel, L. Nogueira, L. Laurent, C. Iobagiu, C. Vincent, M. Sebbag, G. Serre, Induction of macrophage secretion of tumor necrosis factor alpha through Fc gamma receptor IIa engagement by rheumatoid arthritis-specific autoantibodies to citrullinated proteins complexed with fibrinogen; *Arthritis Rheum.* 2008 (58): 678-688.
- <sup>14</sup> F. Pratesi, M.C. Alcaro, M. Chelli, F. Lolli, I. Paolini, A.M. Papini, P. Rovero, P. Migliorini; Histone citrullinated peptides and uses thereof; WO2012001103.
- <sup>15</sup> C. Barbey, J.M. Tiercy, N. Fairweather; Processing and presentation of tetanus toxin by antigen-presenting cells from patients with chronic granulomatous disease (CGD) to human specific T cell clones are not impaired; *Clin. Exp. Immunol.* 1994 (95): 227-231.
- <sup>16</sup> J.J. van Beers, A. Willemze, J.J. Jansen, G.H. Engbers, M. Salden, J. Raats, J.W. Drijfhout, A.H. van der Helm-van Mil, R.E. Toes, G.J. Pruijn; ACPA fine-specificity profiles in early rheumatoid arthritis patients do not correlate with clinical features at baseline or with disease progression; *Arthritis Res. Ther.* 2013 (15): R140.
- <sup>17</sup> F. Pratesi, C. Tommasi, C. Anzilotti, I. Puxeddu, E. Sardano, G. Di Colo, P. Migliorini; Antibodies to a new viral citrullinated peptide, VCP2: fine specificity and correlation with anti-cyclic citrullinated peptide (CCP) and anti-VCP1 antibodies; *Clin. Exp. Immunol.* 2011 (164): 337-345.
- <sup>18</sup> Y. Allano, J. Sellam, F. Batteux, C. Job Deslandre, B. Weill, A. Kahan; Induction of autoantibodies in refractory rheumatoid arthritis treated by infliximab; *Clin. Exp. Rheumatol.* 2004 (22): 756-758.
- <sup>19</sup> **G. Rossi, F. Real-Fernández, F. Panza, F. Barbetti, F. Pratesi, P. Rovero, P. Migliorini; Biosensor analysis of anti citrullinated protein/peptide antibodies affinity; *Anal. Biochem.* 2014 (465): 96-101.**

## **4: Autoantibodies from Multiple Sclerosis patients' sera: isolation, detection and characterization of their interaction with a *Haemophilus influenzae* N-glycosylated adhesion protein.**

### **4.1 N-glycosylation, a widespread post-translational modification**

In the field of the research of the native antigen triggering the autoimmune response characterizing multiple sclerosis (MS) disease, different hypothesis have been done, but at now a proved and overall accepted explanation is not present. Nevertheless, in the pathogenesis of MS the production of autoantibodies targeting myelin proteins is believed to be a key point. Growing evidences indicated that antibodies can bind aberrant glycosylated self-proteins, or that they can recognize non modified self-antigens that, because of molecular mimicry reasons, are homologous to glycosylated infectious agents proteins. In this background, the present research will be conducted with the aim of understanding the importance, for MS antibodies interaction, of the N-glycosylation enzymatically introduced on a bacterial protein, in comparison to the results obtained with a synthetic peptide bearing the same N-glycosylation and currently used as probe to detect autoantibodies biomarker of MS. This work will be helpful in the complex context of the study of the initial event involved in MS pathogenesis.

Protein synthesis is a well-known process whose last steps include post-translational modifications (PTM) such as glycosylation, acetylation, phosphorylation, etc., leading to changes in the protein structure and affecting its biological function. In particular protein glycosylation plays important roles in major biological events such as cell-cell and cell-matrix interactions, intracellular localization, stabilization of the three-dimensional structure, thermal and chemical stability, receptor binding, cellular signaling or protein clearance.

Glycosylation is the most abundant protein PTM occurring in eukaryotic and prokaryotic cells<sup>1</sup>. In the past decade, the first evidence of a system of N-glycosylation in bacteria was discovered by studying the human mucosal pathogen *C. jejuni*<sup>2</sup>. Glycoproteins are now being recognized increasingly in prokaryotes; some examples of bacterial glycoproteins include the flagellins of *Pseudomonas aeruginosa*<sup>3</sup> and the non-pilus adhesins of *Chlamydia trachomatis*<sup>4</sup>.

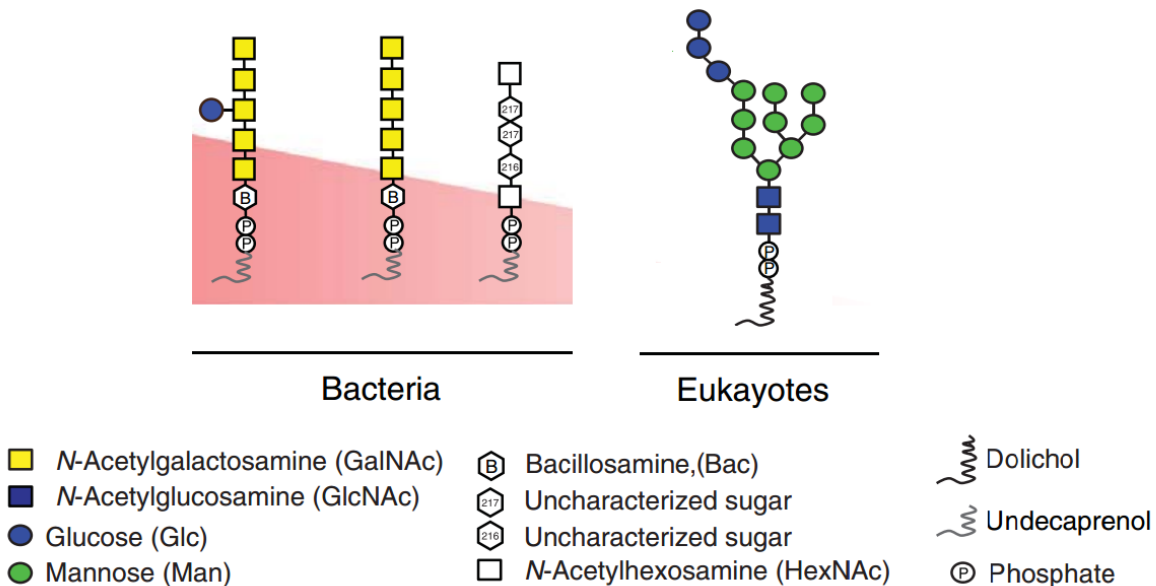
In eukaryotes cell membranes proteins and secreted proteins are highly glycosylated and nearly 50% of the plasma protein are so modified. There are three major types of protein glycosylation: N-linked is the most common, it involves the transfer of an oligosaccharide onto the side chain

CHAPTER 4

amide nitrogen of asparagine residues of acceptor proteins; O-linked, in which monosaccharides are sequentially added onto the side chain hydroxyl oxygen atom of serine or threonine residues; GPI-anchored, requiring a complex glycosylphosphatidylinositol moiety that is transferred to the C-terminus of a target protein with the function of anchoring it to the cell membrane.

Although a number of variations occur, studies in model organisms revealed that two homologous processes represent the core of N-glycosylation both in eukaryotes and prokaryotes.

In eukaryotes the biosynthesis of N-glycans begins on the cytosolic face of the Endoplasmic Reticulum (ER) where the conserved tetradecasaccharide (Glc<sub>3</sub>Man<sub>9</sub>GlcNAc<sub>2</sub>) is assembled onto a dolichyl pyrophosphate carrier and then *en-bloc* transferred, by the multimeric Oligosaccharyl Transferase (OT) complex, to the asparagine side chain of the acceptor polypeptides; phosphorylated lipids function as good leaving groups in the OT reaction and remain bound to the membrane, where they can be recycled for further rounds of biosynthesis. In prokaryotes the assembly process begins at the plasma membrane where unique monosaccharide building blocks are assembled together and transferred by a simple monomeric OT enzyme to the acceptor proteins; in addition the first sugar Asn-linked in prokaryote glycoproteins is an N,N'-diacetylbacillosamine (Bac) instead of the initial N-acetylglucosamine (GlcNAc) present on eukaryote glycoproteins. A schematic illustration of the lipid-linked glycans that is conserved in eukaryotes and variable in bacteria is shown in Figure 16.



**Figure 16:** Representative glycan structures, in eukaryotes and bacteria, indicated with colored geometric symbols

The final heterogeneity of N-glycans found among eukaryotes is a consequence of a successive elaboration, taking place in the Golgi apparatus that is introduced thanks to a series of glycosidases and glycosyltransferases that trim and add carbohydrates such as sialic acid, fucose or galactose; this step is absent in prokaryotes. The acceptor substrate of N-glycosylation is the side chain amide of asparagine residue in receptive Asn-X-Ser/Thr consensus sequences; OT does not glycosylate proteins that contain a proline in position X<sup>5</sup> and prefers Asn-X-Thr sites compared with Asn-X-Ser ones<sup>6</sup>. A specific conformation of the acceptor peptide is required to increase the nucleophilicity of the amide group of asparagine<sup>7</sup>, and from recent experimental data appeared that the sequence requirements of the acceptor substrate are less strict than previously reported.<sup>8</sup>

Mutations in almost every step of glycan biosynthesis and processing lead to a group of debilitating and often fatal diseases termed Congenital Disorders of Glycosylation, underscoring the importance of this PTM for human health<sup>9</sup>. Some glycomic analyses have noticed an altered protein glycosylation during HIV infection<sup>10</sup> or allergy<sup>11</sup> and abnormal glycosylation of target antigen has also been involved in the pathophysiology of autoimmune diseases. Hence high levels of antibodies directed to glycosylated antigen were found in antiphospholipid syndrome patients' sera<sup>12</sup>; in systemic sclerosis antibodies directed to 4-sulfated N-acetyl-lactosamine were associated with higher prevalence of pulmonary hypertension<sup>13</sup>; in multiple sclerosis polymorphism in the gene coding for the glycosylation enzyme MGAT5 correlated to disease severity<sup>14</sup>.

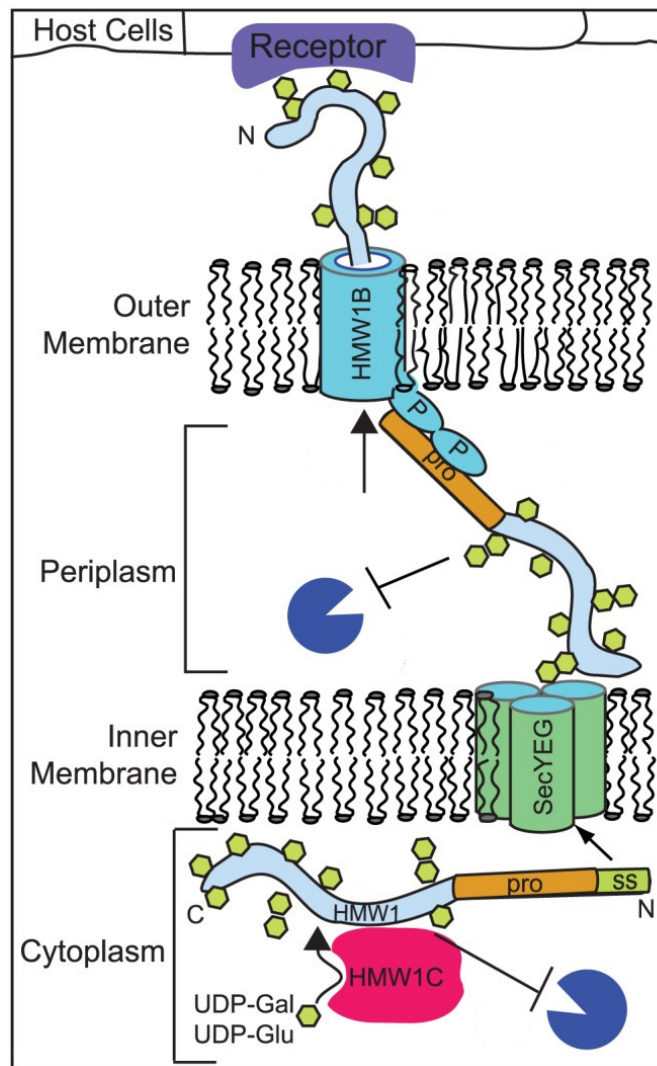
#### **4.2 N-glycosylated HMW1 adhesin from *Haemophilus influenzae***

The nontypeable Gram-negative bacterium *Haemophilus influenzae* is a common cause of human respiratory tract disease including otitis media, sinusitis, conjunctivitis, bronchitis and pneumonia and it initiates infection by colonizing the upper respiratory tract<sup>15</sup>. *H. influenzae* expresses a related High Molecular Weight protein called HMW1, that promotes efficient adherence to respiratory epithelial cells and facilitate the process of colonization<sup>16</sup>. It was demonstrated that HMW1 adhesin interacts with a glycoprotein receptor expressed by epithelial cells and containing N-linked oligosaccharide chains with a sialic acid in an  $\alpha$ 2-3 configuration<sup>17</sup>.

HMW1 is synthesized as preproprotein and is secreted by the Two Partner Secretion (TPS) system<sup>18</sup>. TPS pathway consists of a large extracellular protein, TpsA, and a cognate outer membrane pore-forming translocator protein called HMW1B (Figure 17).

CHAPTER 4

Amino acids 1–68 of HMW1 direct the preprotein to the Sec apparatus, where they are cleaved by signal peptidase I. Subsequently, amino acids 69–441 target the proprotein to the outer membrane and interact with the outer membrane translocator protein, undergoing removal by an unknown process. Following translocation across the outer membrane, the mature 160 kDa HMW1 protein remains associated with the bacterial surface via a non-covalent interaction that requires the C-terminal 20 amino acids of the protein and that is dependent upon disulfide bond formation between two conserved cysteine residues in this region<sup>19</sup>.

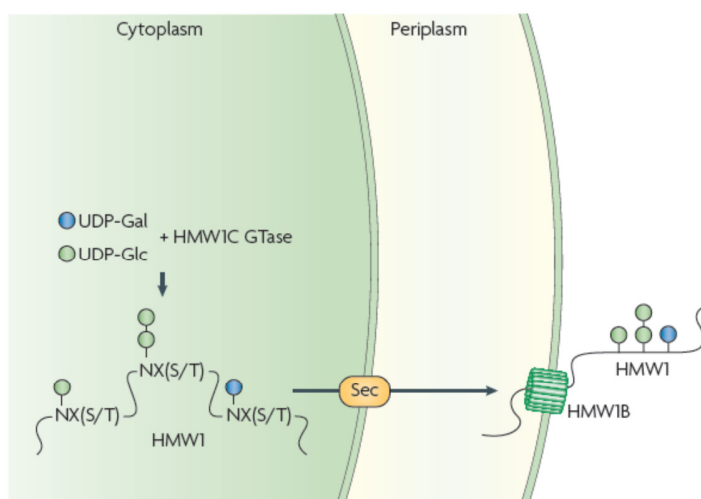


**Figure 17:** Schematic representation of proteolytic cleavage of HMW1 and two partner secretion system, resulting in mature HMW1exposition on the outer membrane of the cell.

Recent studies demonstrated that HMW1 is a glycoprotein and its glycosylation appears to increase its stability, to protect against premature degradation and to be fundamental for protein adherence to target structures. In addition, glycosylation appears to influence HMW1 tethering to

the bacterial surface, as indicated by the fact that the little amount of HMW1 that is secreted is not glycosylated<sup>20</sup>.

Analysis of mature HMW1 proteolytic fragments by mass spectrometry identified 31 sites of modification carrying 47 hexose units, corresponding to a molecular mass of about 7.6 kDa. All of the modified sites were asparagine residues, in all except one case within the conventional sequence motif for eukaryotic N-linked glycosylation, *Asn-X-Ser/Thr*<sup>21</sup>. Interestingly, the modifying carbohydrates at these sites are hexose (glucose or galactose) or dihexose sugars (glucose-glucose or glucose-galactose) rather than N-acetylated sugars, revealing an unusual carbohydrate modification and suggesting a glycosyltransferase with a novel enzymatic activity capable of both transferring nucleotide activated monosaccharides to asparagine side chains without the requirement for a lipid donor, and to generate O-glycosidic bonds between hexose sugar<sup>21</sup> (Figure 18). The enzyme responsible for the glycosylation of HMW1 is the cytoplasmic N-glycosyltransferase (GTase) HMW1C.



**Figure 18:** Overview of the sequential transfer of hexoses from UDP-activated donors to the eukaryotic-like *Asn-X-Ser/Thr* sequons of HMW1 by the glycosyltransferase HMW1C in the cytoplasm.

HMW1C has the potential to contribute to several different processes that occur during HMW1 synthesis: glycosylation may increase the stability of HMW1 in the cytoplasm and in the periplasm, alternatively the HMW1C protein may improve the stability of HMW1 by acting as a chaperone. It is still unclear whether glycosylation influences interaction of HMW1 with the periplasmic domain of the translocator protein HMW1B prior to transit, or with its pore during transit or with the docking region of HMW1B upon surface tethering. At now it is not understood how HMW1C recognizes its target and chooses specific glycosylation sites, as only a subset of *Asn-X-Ser/Thr* motifs in HMW1 are modified, based on mass spectrometry analysis; it is clear

that HMW1C interacts directly with HMW1, but the number of enzyme molecules that bind to HMW1 and the duration of this interaction in the cytoplasm is still unknown<sup>20</sup>.

The HMW1C protein is encoded by the *hmw1* gene cluster and shares homology with a group of bacterial proteins that are generally associated with the TPS systems and that are expressed in a number of other Gram-negative bacterial pathogens (e.g. the enterotoxigenic *Escherichia coli*, *Yersinia pseudotuberculosis*, *Yersinia pestis* and *Actinobacillus pleuropneumoniae*).

The *Actinobacillus pleuropneumoniae* HMW1C (ApHMW1C) is 65% identical to *Haemophilus influenzae* HMW1C and it has been demonstrated that ApHMW1C is able to transfer glucose and galactose to known asparagine glycosylation sites on HMW1, analogous to HMW1C. In addition it has been proved that ApHMW1C can complement a deficiency of HMW1C and mediate HMW1 glycosylation and adhesive activity in whole bacteria<sup>22</sup>.

Currently HMW1C is classified into the GT41 family which includes both eukaryotic and bacterial O-linked GlcNAc (OGT) transferases<sup>23</sup>; the OGT enzymes contain a long N-terminal domain responsible for the recognition of a broad range of target proteins and a C-terminal glycosyltransferase domain responsible for transferring GlcNAc to target proteins. Given that HMW1C and ApHMW1C lack the N-terminal domain and that they catalyze N-glycosylation and in particular that they transfer simply hexose sugars to asparagine sites on HMW1 adhesin, HMW1C-like proteins clearly differ from enzymes of the GT41 family suggesting the existence of a new family of bacterial HMW1C-like proteins with similar glycosyltransferase activity<sup>24</sup>.

### **4.3 Multiple Sclerosis: the state of the art.**

Multiple Sclerosis is the most frequent chronic inflammatory demyelinating disease involving different areas of the Central Nervous System (CNS). MS affects 0.05% to 0.15% of white populations, leading over time to severe disability in half of them. MS occurs twice as often in women as in men and usually starts between the ages of 20 and 40 years. Multiple sclerosis is a disease that predominantly affects CNS white matter and leads to demyelinating lesions that are mainly characterized by disturbance of the blood brain barrier, local edema and global atrophy. Demyelination of axons, activation of microglia, and infiltration of immune cells, such as T cells, macrophages and B cells, are key features of these lesions<sup>25</sup>. Two lesion patterns have been noted most frequently, one characterized by significant antibody deposits and remyelination, the other by oligodendrocyte loss without remyelination. Although in particular the extent of the humoral immune response appears to be stable over time in MS patients, it varies significantly inter-



individually<sup>26</sup>. Together with the high variability of the clinical phenotype and in disease progression, it is possible to speculate whether different pathogenetic pathways and even etiologies underlie those histologically defined subtypes.

In the absence of specific biomarkers, the diagnosis and the prognosis of the disease continues to rely on clinical history, neurological examination and clinical evidences of temporal and spatial dissemination of CNS lesions. MRI is up to now the most reliable and sensitive technique in detecting MS lesions for the diagnosis of the disease<sup>27</sup>, but it cannot be considered a routine technique when the clinical symptoms are not still visible to guide a targeted MRI check-up.

Because plaques may form in any part of the CNS, the symptoms of MS vary widely from person to person and from stage to stage of the disease. The most common symptoms include muscle weakness, loss of balance, visual disturbances, tremors, vertigo, muscle spasticity and cognitive disturbances. The symptoms of MS may occur in one of three patterns: the most common is the *relapsing remitting* one, in which there are clearly defined symptomatic attacks lasting one day or more, followed by complete or almost complete improvement and the period between attacks may be a year or more at the beginning of the disease, but may shrink to several months later on. In the *primary progressive* pattern, the disease progresses without remission or with slight improvements. The *secondary progressive* is the pattern in which people with MS begin with relapses and remissions followed by more steady progression of symptoms.

To date there are three major drugs approved for the treatment of MS, but none of them are cure, they can only slow disease progression in many patients. Novantrone is a cytotoxic drug with immunosuppressive properties that seems to reduce relapse rates and progression; Glatiramer acetate, a randomly synthesized polypeptide mixture based on four amino acids that are contained at high levels in myelin proteins, seems to decrease relapse rates too and to have neuroprotective properties; Interferon beta (IFN- $\beta$ ), is the most active molecule in decreasing relapse rates, it also seems to affect disease progression, it is known that IFN- $\beta$  has both antiviral and immunomodulatory effects, although the mechanism of action in MS is still not entirely understood.

Both genetic and environmental factors influence the susceptibility and the course of MS. Prevalence is high in white people, but MS is rare in Asians and Africans; family members of MS patients are at greater risk. Multiple genome screens and family studies recently completed, indicate that MS follows a polygenetic trait which involves a large number of genes with each contributing little to the overall risk, but between them only the human leukocyte antigen (HLA)

## CHAPTER 4

class II alleles DRB1\*1501 and HLA-DQB1\*0601 have consistently been associated with MS in white people<sup>28</sup>. Evidence from clinical and epidemiological studies suggests that environmental factors, such as viral infections, may play an important role in the etiology of MS<sup>29,30</sup>.

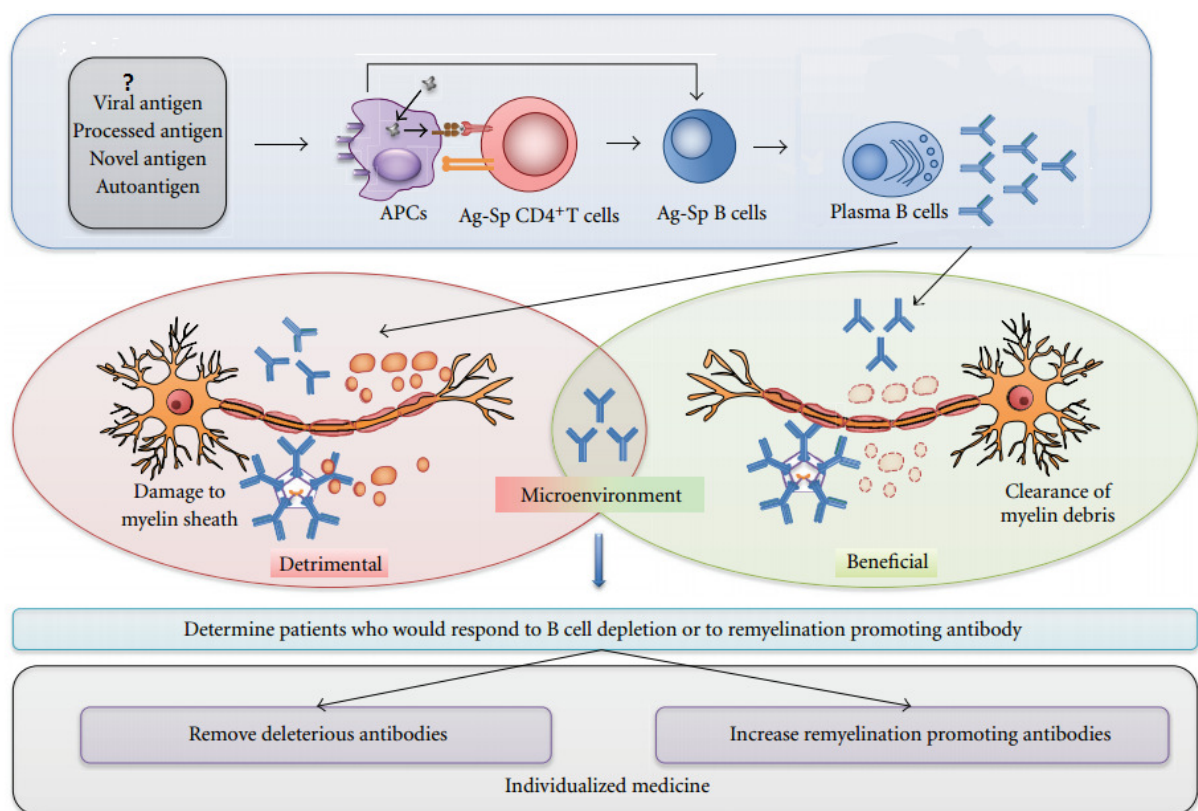
A role of the immune system in the pathogenesis of MS was first suggested by observations of acute demyelinating episodes induced by an anti-myelin immune response in animal models of Experimental Autoimmune Encephalomyelitis (EAE). In conclusion from all the studies it was established that a Th-1 CD4+ T cell response to myelin antigens was destructive, whereas a Th-2 CD4+ T cell response was protective<sup>31</sup>, but this hypothesis has not been confirmed in humans.

Recent studies demonstrated that CD4+ T cells can recognize a large number of different antigens, among them a variety of self and foreign antigens including peptides derived from microbes<sup>32</sup>. Nevertheless, the high degeneracy in T cell recognition observed provides a possible explanation of how autoreactive T cells may be activated by epitopes from exogenous infectious agents that for molecular mimicry reasons share structural or sequence homology to self-antigens<sup>33</sup> and consequently can initiate the first demyelinating episode. This hypothesis is supported by a recent study that demonstrated molecular mimicry between a portion of myelin basic protein, a candidate autoantigen for MS, and the protein U24 of human herpesvirus-6, a viral agent that could be associated with MS<sup>34</sup>. Another study performed in mice using a proteolipid protein mimic peptide from protease IV of *Haemophilus influenzae* demonstrated that the infection of the target organ with a mimic-expressing pathogen during childhood may activate a population of autoreactive T cells that cross-reacted with myelin epitopes and that could be later reactivated and expanded by different stimuli (e.g. stress, trauma, vaccination or reinfection with the same mimic expressing virus) and that consequently could be involved in inducing the autoimmune disease<sup>35</sup>. Many microbes have been associated with the disease because many features of MS are compatible with a chronic CNS infection, but up to now evidence is lacking that any of them play a definitive role in the pathogenesis of MS.

In this background the primary event that drives the immune response in CNS is still unknown, but it is accepted that antigens released from the CNS compartment are processed and presented by antigen-presenting cells to T cells in the lymphoid tissue. Similarly B cell response initiates when soluble antigens enter lymph nodes. After that, the polyreactive autoimmune process defined as epitope spreading<sup>36</sup> takes place and clonal expanded B and T cell enter the CNS where they encountered their target antigens. CD8+ T plays a central role in the inflammation process, they can lyse neurons and oligodendrocytes<sup>37</sup>; CD4+ T cells synthesize proinflammatory

cytokines and chemokines recruiting other inflammatory cells but they have also the capacity of releasing neurotropic factors as Brain-Derived Neurotrophic Factor, suggesting that some of them are important for neuroregeneration and protection<sup>38</sup>.

Concerning the humoral response, antibodies binding to CNS cells may have a detrimental effect by activating the complement cascade or directly damaging the myelin sheaths of axons<sup>39</sup>; however antibodies may also promote regeneration depending on the microenvironment<sup>40</sup>. The oligoclonal immune response observed in patients with MS thus represents an ambivalent role (Figure 19).



**Figure 19:** The possible role of B cells in MS pathogenesis; unknown antigens are presented by the antigen presenting cells to T and B cells; activated B cells undergo clonal expansion and secrete antigen-specific antibodies that may have a destructive or a protective role.

Consequently it is of priority to determine clinical assays, supporting the concept of the individualized medicine, to delineate patients who would respond to B cell depletion therapies, where deleterious antibodies would be removed from circulation, or to promote antibody therapy in the case in which remyelination is stimulated by circulating antibodies.

The autoimmune hypothesis generated in the EAE model involving both molecular mimicry and epitope spreading can explain many aspects of MS but experimental support for this hypothesis is

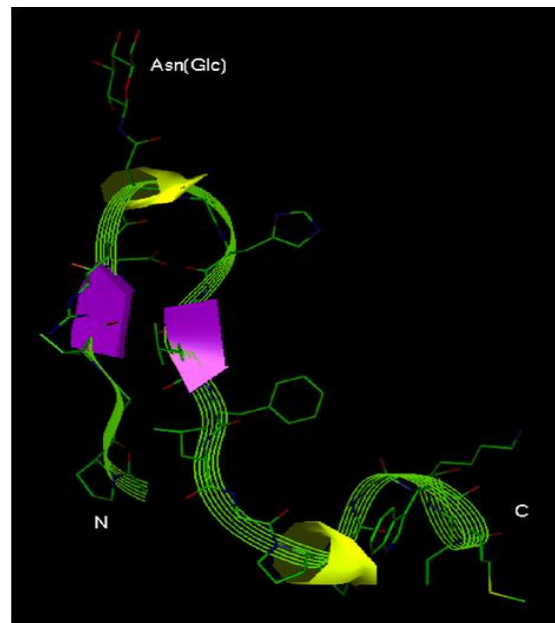
still limited. The first problem is that CD4+ T cells specific for myelin antigens were also found in healthy donors, indicating that autoreactive T cells are part of the normal T-cell repertoire and not necessarily harmful<sup>41</sup>. Similarly, myelin-specific antibodies are not confined to MS, but can be detected in different neurologic diseases and even in healthy control subjects<sup>42</sup> and moreover the exact target antigens of myelin proteins remain elusive.

#### **4.4 N-glycosylated peptide CSF114(Glc) for MS autoantibodies detection**

Although the immune system play a fundamental role in the pathogenesis of MS, target antigens are still uncertain and pathways leading to tissue destruction have not been fully elucidated. The most studied putative self-antigens of CNS myelin are the myelin basic protein, the proteolipid lipoprotein and the myelin oligodendrocyte glycoprotein, and they are mostly post-translationally modified<sup>43</sup>.

Growing evidences indicate that post-translational modifications, in particular aberrant glycosylation<sup>44</sup>, can mask self-antigens, creating new ones no longer recognized by the immune system, and so can play a fundamental role for specific autoantibodies recognition in MS.

It was demonstrated that the synthetic N-glycosylated peptide CSF114(Glc), selected from a library of peptides through the chemical reverse approach, was able to detect autoantibodies in a subpopulation of MS patients' sera by Enzyme-Linked Immunosorbent Assay (ELISA)<sup>45</sup> and using a surface plasmon resonance biosensor approach<sup>46</sup>; in addition this glucopeptide mimetic was successfully used to identify novel autoantigens in MS<sup>47</sup>. The ability of the glycosylated sequence to detect autoantibodies in MS patients' sera was correlated to the N-linked  $\beta$ -D-glucopyranosyl moiety<sup>48</sup> characterized by a type I'  $\beta$ -turn structure that optimally exposes the minimal epitope Asn(Glc) to autoantibodies as shown in Figure 20 and that possibly reproduces an aberrant N-glycosylation of myelin proteins<sup>49</sup>.



**Figure 20:** Ribbon diagram of the calculated lower energy conformer of CSF114(Glc) derived from NMR data.

#### 4.5 Objective

The initial mechanism responsible for the triggering of the autoimmune response in MS is still unknown, but two main accepted theories are present. It could be possible that aberrant N-glycosylation of myelin proteins, by a still unknown mechanism, could transform self-antigens in non-self ones and trigger an autoimmune response; conversely the molecular mimicry between exogenous structures (e.g. glycosylated bacterial proteins) and self-proteins could be responsible for the induction of the autoreactive immune response.

In the last years, CSF114(Glc) peptide was successfully employed to detect autoantibodies in MS patients' sera and this ability was related to the presence of one N-glycosylation chemically introduced on the side chain amide of an asparagine residue. Following the hypothesis that MS immune deregulation could be triggered by a viral or a bacterial infection that because of molecular mimicry reasons stimulates autoreactive immune cells and considering that recent studies demonstrated that the same N-glycosylation introduced in CSF114(Glc) is generated in vivo by the HMW1C glycosyltransferase on HMW1 adhesin from *Haemophilus influenzae*, we investigated if a portion of this N-glycosylated bacterial protein was able to interact with autoantibodies in MS patients' sera and if there was a correlation between antibodies detected by both N-glycosylated molecules.

To answer those questions the following experiments have been performed:

## CHAPTER 4

- SP-ELISA assay to investigate the ability of glycosylated and non glycosylated proteins to detect antibodies in MS sera as compared to control sera;
- competitive ELISA assay to calculate the relative mean affinity and to understand the cross-reactivity of anti-CSF114(Glc) antibodies, present in MS sera, for protein and peptide inhibitors applied in solution;
- SPR binding study on one selected glycosylated adhesin derived peptide, to investigate its ability to interact with specific antibodies when MS sera are injected under a continuous flow;
- antibody purification from one MS serum by two sequential affinity chromatographies to elute antibodies highly specific for the glycosyl moieties of glycosylated adhesin or of CSF114(Glc);
- SP-ELISA titration assay with purified antibody fractions, to confirm the ability of the sequential affinity chromatography process to deplete serum from antibodies recognizing the non glycosylated antigens;
- SPR kinetic and affinity studies to characterize the kinetic and the affinity of the interaction between each purified antibody fraction and each glycosylated and non glycosylated antigen and to understand the cross-reactivity of purified antibodies for the different antigens;
- SPR binding study with MS and control sera on immobilized adhesin proteins with and without glycosylation, to realize at first if they are able to interact with antibodies flowing in solution and then to compare results obtained when the same molecules are employed in SP-ELISA assay;
- immunohistochemistry assay to investigate if one selected MS serum and if purified antibody fractions can bind to some mimetic structures present on rat nervous tissues.

### 4.6 Results and discussion

This study was conducted using the protein HMW1ct, corresponding to the C-terminal fragment of HMW1 adhesin of *H. influenzae*. We received HMW1ct in the framework of a collaboration with Prof. Barbara Imperiali of the Department of Biology of the Massachusetts Institute of Technology (MIT, Cambridge, USA); this protein fragment was produced by recombinant technologies and *in vitro* N-glycosylated by the HMW1C glycosyltransferase using as substrate UDP activated glucose. HMW1ct structure is represented in Figure 21: it corresponds to the

residues 1205 – 1536 listed in Table 7 and contains 12 potential Asn-X-Ser/Thr N-glycosylation sites; 8 of them were in fact in vitro glucosylated using the HMW1C enzyme. We received both the N-glycosylated (HMW1ct-Glc) and the unmodified protein (HMW1ct).

HMW1ct sequence
ANSGALTTLAGSTIKGTESVTTSSQSGDIGGTISGGTVEVKATESLTTQSNSKIKATTGEA <b>N(1)VT</b> SATGTIGGTISGNTV <b>N(2)VT</b> ANAGDLTVGNGAEIN <b>(3)ATE</b> GAAATLTTSSGKLTTE ASSHITSAKGQVN <b>(4)LS</b> AQDGSVAGSINAAN <b>(5)VT</b> LN <b>(6)TT</b> GTLTTVKGSN <b>(7)AT</b> SGT LVINAKDAELNGAALGN <b>(8)HT</b> VVN <b>(9)AT</b> NAN <b>(10)G</b> SGSVIATTSSRVN <b>(11)IT</b> GDLITING LNIISKNGINTVLLKGVKIDVKYIQPGIASVDEVIEAKRILEKVKDLSDEEREALAKLGVS AVRFIEPN <b>(12)NT</b> ITVDTQNEFATRPLSRIVISEGRACFSNSDGATVCVNIADNGR

**Table 7:** HMW1ct sequence in one letter aa code; the 8 N-glycosylated sites are reported in red.



**Figure 21:** Ribbon diagram of HMW1ct fragment calculated structure, potential Asn-X-Ser/Thr glucosilation sites are shown in yellow and red.

#### 4.6.1 SP-ELISA optimization for protein antigens

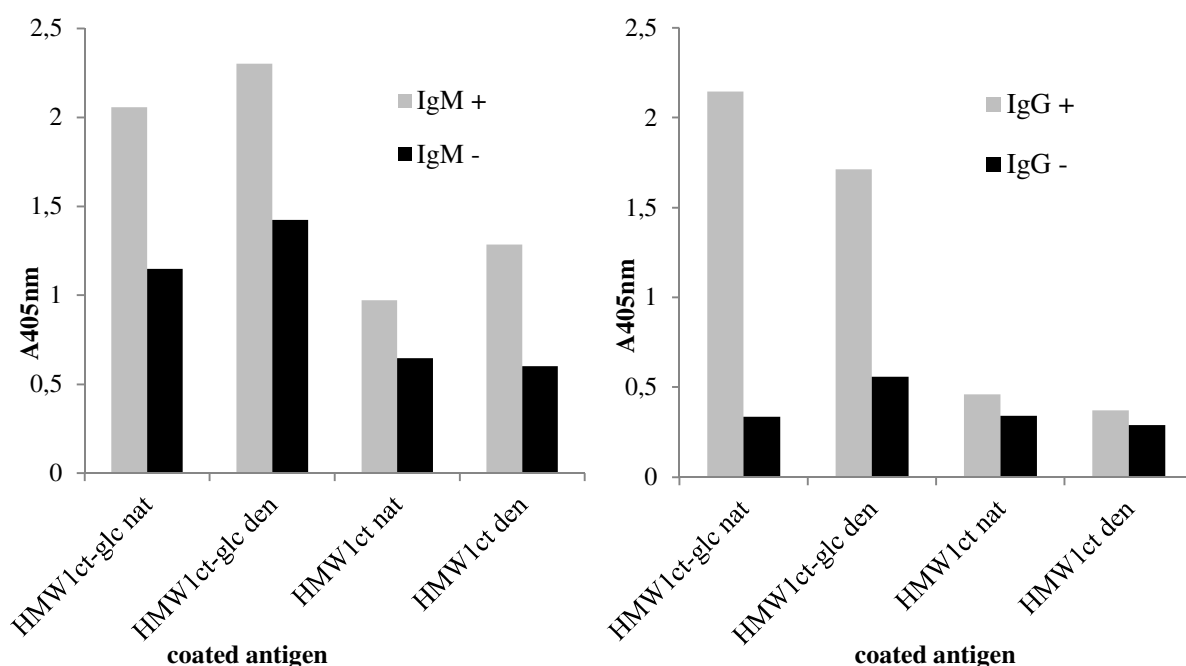
The first part of this project was devoted to the optimization of an ELISA procedure using HMW1ct and HMW1ct-Glc proteins as antigens. In order to study the coating efficiency of these antigens to maxisorp plates, proteins were diluted in different buffers to find the best conditions

## CHAPTER 4

of pH and ionic strength maximizing their adsorption on the solid support. Three coating buffers were used: carbonate buffer at pH 9.6, PBS at pH 7.2 and PBS at pH 5.0. Three sera were applied at 1:100 dilution: one IgG positive, one IgM positive and one IgG and IgM negative to CSF114(Glc). After the addition of the appropriate enzyme labeled secondary antibody and the application of its substrate, the resulting colorimetric reaction was read at 405nm; registered absorbance directly quantify serum antibodies bound to the coated antigens. No significant difference in absorbance values was registered when using in the coating step the three buffers mentioned above. However, the best buffer for the following SP-ELISA assays was identified as PBS at pH 7.2, being the one minimizing unspecific interactions with the plate surface, as indicated by the lower *blank* value, and maximizing the difference between positive and negative IgG sera.

Protein stability and the importance of protein folding for antibody recognition were then investigated to understand if conformational epitopes were present on HMW1ct-Glc and on HMW1ct. To do this an SP-ELISA assay in denaturant condition was set up. Adhesin proteins were coated in PBS buffer at pH 7.2 and after overnight incubation at +4 °C, the denaturant solution was applied. This solution contained urea to reversibly denature proteins and  $\beta$ -mercaptoethanol to reduce the disulfide bridge involving the two cysteine residues that were present in the C-terminal part of the proteins. A iodoacetamide solution was then applied in order to covalently modify the SH group of cysteine residues, making impossible the disulfide bridge regeneration. The assay was then performed applying the same sera used in the coating optimization step. Absorbance values obtained for IgG and for IgM in the previous ELISA assay in native condition and in the ELISA assay in denaturant one are shown in Figure 22.





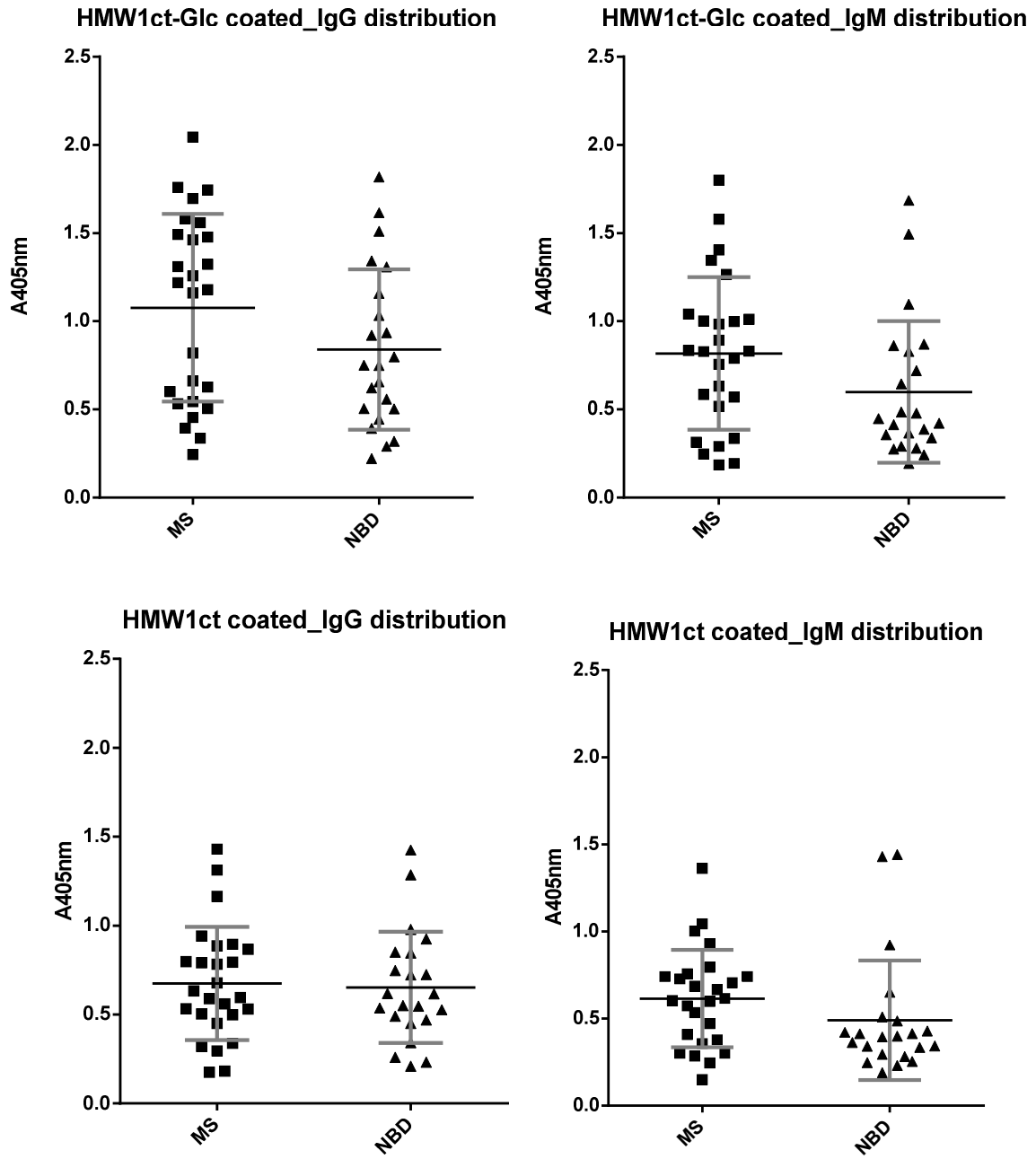
**Figure 22:** Comparison between results obtained from the classical SP-ELISA in native conditions and the SP-ELISA in denaturant conditions

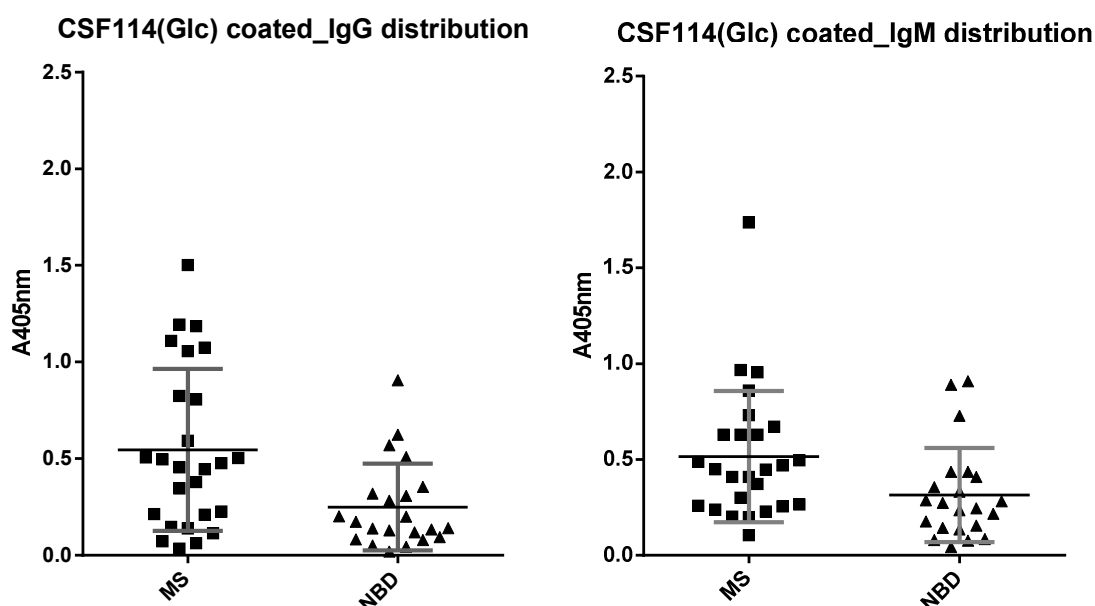
Very similar results were obtained and they could indicate that the denaturing process was not adequate for HMW1ct proteins or that the disulfide in the C-terminal part was not important for protein conformation or that antibodies didn't recognize conformational epitopes, maybe because they were not present when the proteins were adsorbed on the solid support.

#### 4.6.2 Sera screening in SP-ELISA

A total of 26 MS sera and 22 Normal Blood Donor (NBD) sera were screened in SP-ELISA assay coating glycosylated HMW1ct and non glycosylated HMW1ct proteins. Results were compared with previously obtained data coating CSF114(Glc) peptide.

The graphs summarizing the distribution of antibody levels detected in MS and in NBD sera are reported in Figure 23 for each of the 3 antigens for both IgG and IgM. The mean of the absorbance values and the relative Standard Deviation (SD) for IgG and IgM revealed in MS and in NBD sera with the present SP-ELISA are listed in Table 8.





**Figure 23:** Distribution graphs indicating serum IgG and IgM in MS patients and in healthy subjects; coated antigens are HMW1ct-Glc, HMW1ct and CSF114(Glc). Mean and SD are shown inside the graphs.

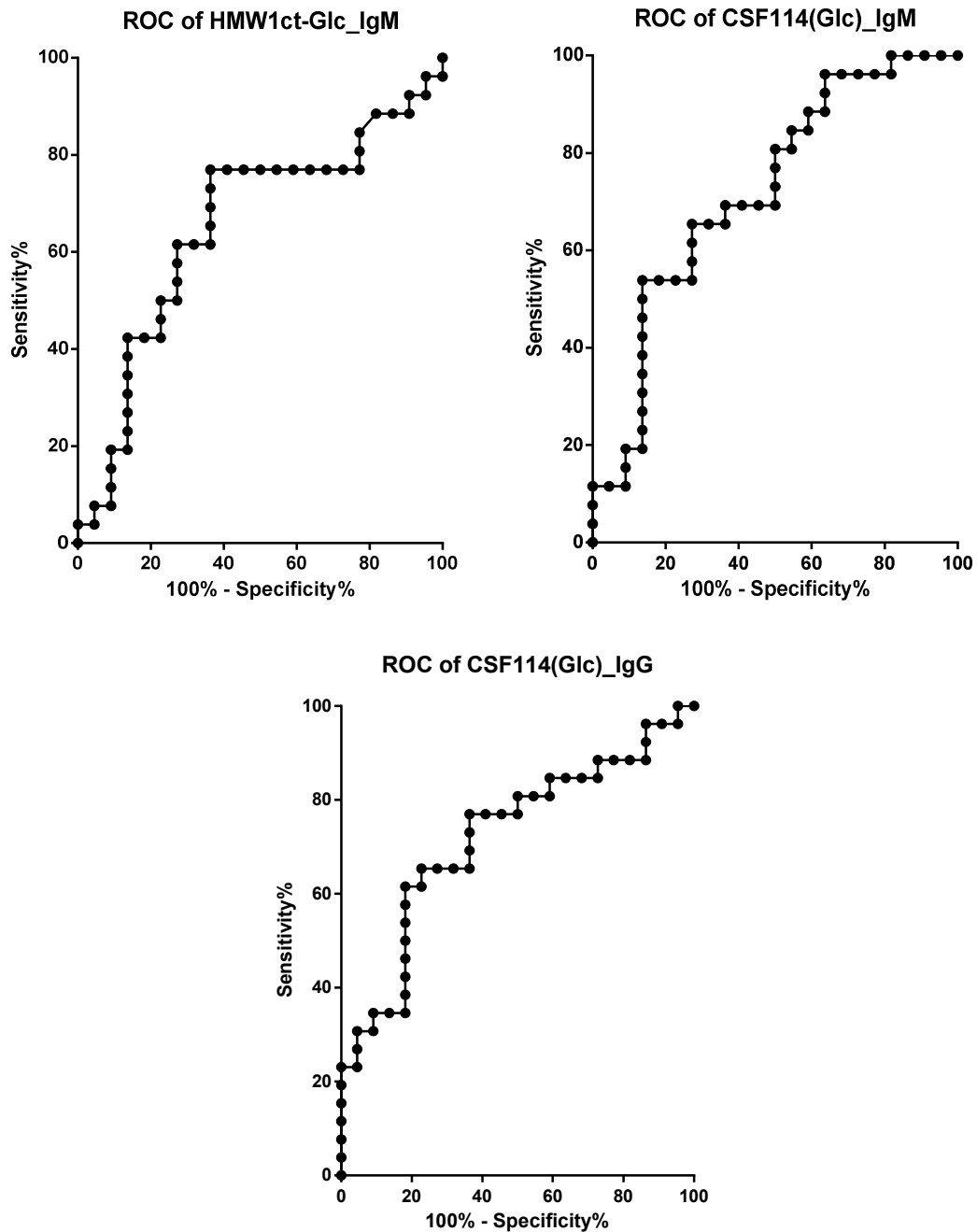
Coated antigen	IgM				IgG			
	MS		NBD		MS		NBD	
	Mean	SD	Mean	SD	Mean	SD	Mean	SD
HMW1ct-Glc	0.82	0.43	0.60	0.40	1.07	0.52	0.84	0.45
HMW1ct	0.62	0.28	0.49	0.34	0.68	0.31	0.65	0.31
CSF114(Glc)	0.52	0.35	0.32	0.25	0.55	0.41	0.25	0.22

**Table 8:** Mean and SD calculated for the screening of 26 MS and 22 NBD sera, in SP-ELISA.

HMW1ct coated on plates was able to detect the same level of serum IgG and a similar level of IgM in both NBD and MS groups; HMW1ct was not able to detect specific antibodies in MS sera as compared to healthy subjects, anti-HMW1ct antibodies seemed to be physiologically present in human serum. The glucosylated protein was able to discriminate between MS and NBD in the case of IgM, but the difference was lower in the case of IgG. A significant difference between the two groups emerged in the case of both IgG and IgM when coating peptide CSF114(Glc), confirming its ability to be used as probe to detect specific autoantibodies in MS patients' sera.

To quantify the ability of N-glycosylated protein and N-glycosylated peptide to detect specific antibodies in MS sera in comparison to NBD control sera, the Receiver Operating Characteristic (ROC)-based analysis was employed comparing different combinations of cut-off values, specificities and sensitivities. Three ROC curves shown in Figure 24 for anti-HMW1ct-Glc IgM

and for anti-CSF114(Glc) IgM and IgG activities were constructed based on 26 cases of MS versus 22 controls.



**Figure 24:** ROC curves analysis of IgMs interacting with HMW1ct-Glc and CSF114(Glc), and of IgG interacting with CSF114(Glc) in MS versus NBD sera.

A discriminative power for anti-HMW1ct-Glc IgM was found with an area under the curve of 0.65 and a p-value of 0.07; the optimal diagnostic cut-off value for the method was 1.18 with a

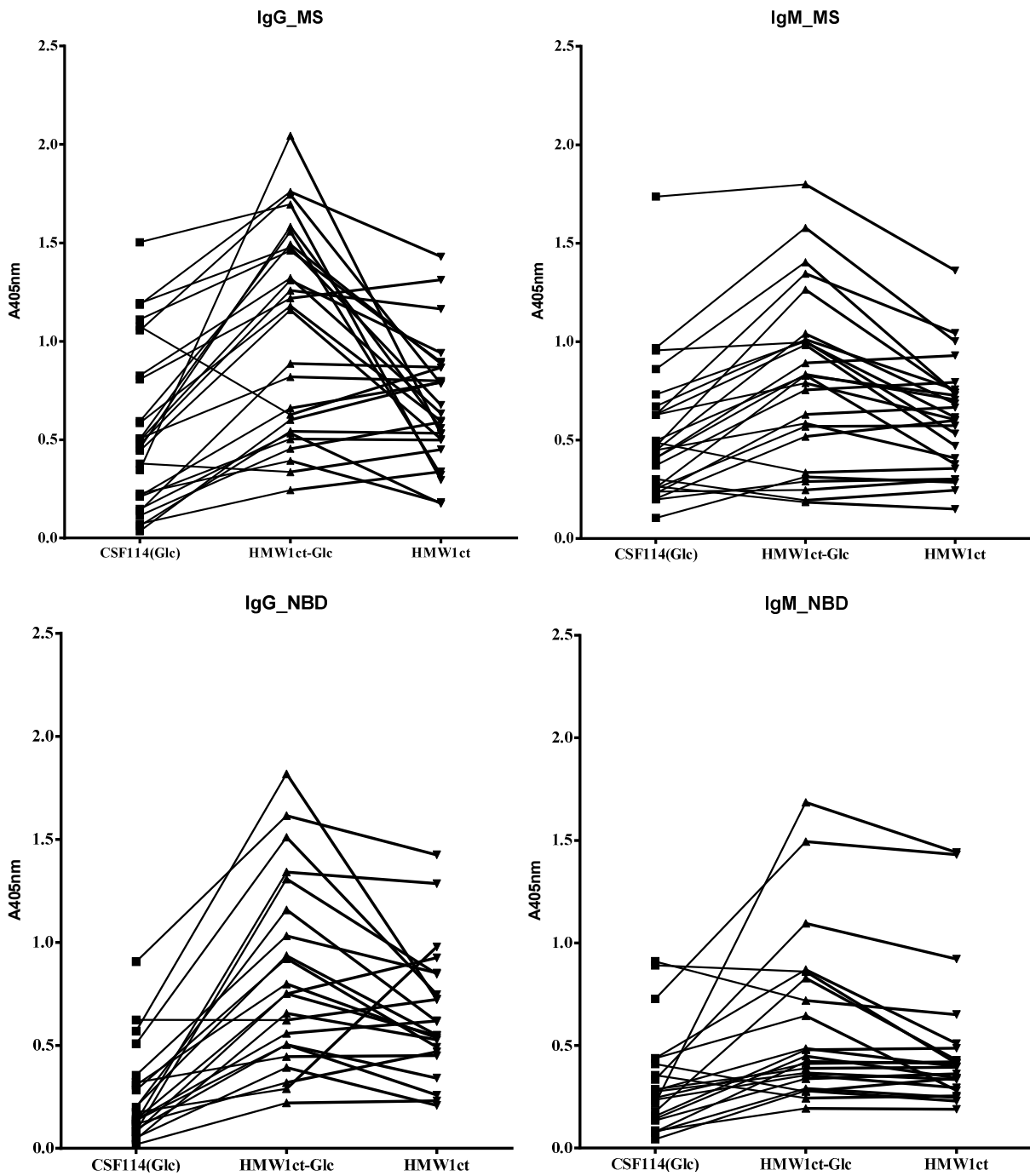
sensitivity of 19.2% and a specificity of 90.9%. According to this cut-off value, an increased antibody level was detected in 5/26 MS sera and in 2/22 NBD sera.

Analyzing the data obtained with immobilized CSF114(Glc), we obtained a discriminative power indicated by an area under the curve of 0.72 and a p-value of 0.009; the diagnostic cut-off for the method was set at 0.73 with a sensitivity of 19.2% and a specificity of 90.9%. We registered an increased antibody level in 5/26 MS sera and in 2/22 NBD sera.

From this ROC based analysis the same sensitivity and specificity was found for the two assays with a different cut-off value, but the higher area under the curve and the lower p-value indicated that the CSF114(Glc) based SP-ELISA assay had a higher statistical significance in detecting specific antibodies in MS patients' sera.

In the case of IgG a discriminative power was found only for anti-CSF114(Glc) antibodies with an area under the curve of 0.72 and a p-value of 0.009; from the ROC analysis the optimal diagnostic cut-off for the method was 1.1 with a sensitivity of 19.2% and a specificity of 100%, meaning that an increased antibody level was revealed in 5/26 MS sera and that no false positive serum was detected among the applied NBD samples.

Figure 25 reports a graphical comparison of the antibody levels detected in MS and in NDB group with the three coated antigens. A complete different trend in registered absorbances can be seen among the different sera for IgGs revealed by the three molecules and an overall different trend was observed also in the case of IgMs, suggesting that different antibody families were revealed through the SP-ELISA assay when HMW1ct, HMW1ct-Glc or CSF114(Glc) were used as probes on the solid support.



**Figure 25:** Comparison between absorbance values obtained with each MS serum and each NBD serum on the three coated molecules.

Concerning MS sera and according to the above established cut-off values, 3/5 patients were IgM positive to both HMW1ct-Glc and CSF114(Glc) and 2 of them exhibited the highest absorbance levels on HMW1ct too.

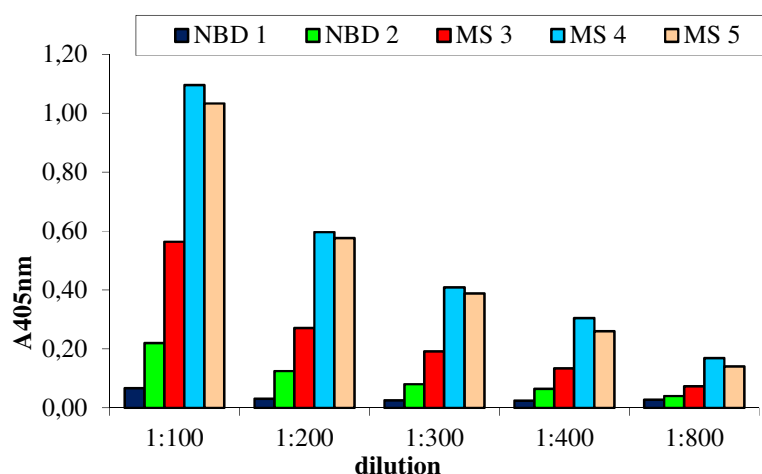
In the case of IgG in MS group and according to the cut-off value of 1.1, 5 sera were positive to CSF114(Glc) and 4 of them displayed a high absorbance level on coated HMW1ct-Glc and among this 4 MS patients, 2 had a low IgG titer against the coated HMW1ct.

In conclusion in the experimental conditions of this SP-ELISA we were able to identify one MS serum containing high levels of IgM and 2 MS sera containing high levels of IgG antibodies that specifically recognized the two N-glycosylated molecules CSF114(Glc) and HMW1ct-Glc, without interacting with the non glycosylated HMW1ct.

#### 4.6.3 Competitive ELISA assay

Considering the previously described results of the screening of the small cohort of sera, we decided to continue the project by coating on the solid support the peptide CSF114(Glc) and by testing the two proteins as inhibitors in solution. For this purpose we selected 5 MS sera and 2 NBD sera IgG positive to HMW1ct-Glc and/or to CSF114(Glc) to be used in competitive ELISA assays according to the method of Wrath, Stanley and Steward<sup>50</sup>.

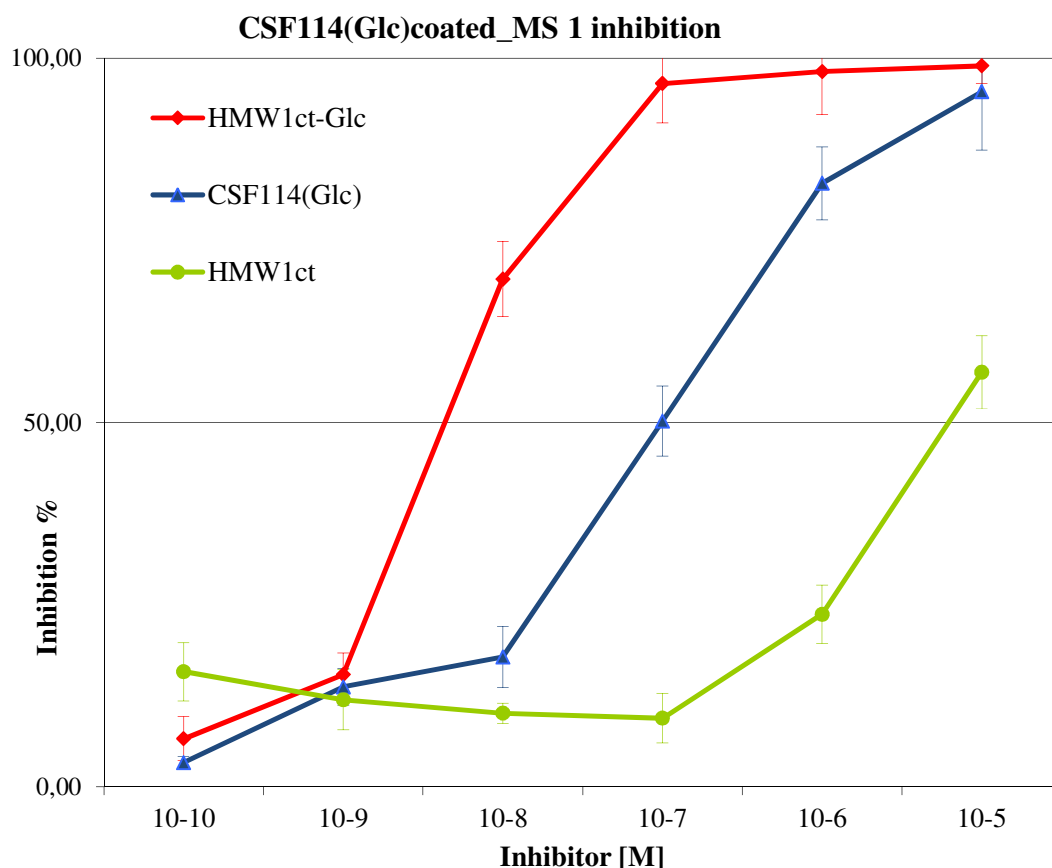
Sera were at first titrated by testing them at 5 different dilutions in the same experimental conditions of the competitive assay; from the titration curve (one example is given in Figure 26) the semi-saturating dilution giving an absorbance of around 0.5, to be used in competitive ELISA, was found for each MS serum. No positive NBD serum was found in the experimental conditions of the competitive ELISA.



**Figure 26:** IgG titration curve obtained with 3 MS and 2 NBD sera coating CSF114(Glc). The optimal dilution resulted to be 1:100 for MS 3 and 1:250 for MS 4 and MS 5.

The competitive ELISA was performed coating CSF114(Glc) and incubating each MS serum in triplicate at the previously selected dilution with increasing concentration of inhibitors in solution. HMW1ct-Glc, HMW1ct and CSF114(Glc) were used as inhibitors in the concentration

range from  $10^{-5}$  to  $10^{-10}$  M. Then the anti-human IgG secondary antibody was added and absorbance was read at 405 nm. From registered absorbance we calculated the inhibition curve reporting the absorbance values (%) for each inhibitor concentrations used; as a representative example the inhibition curves obtained for MS 1 serum are shown in Figure 27.



**Figure 27:** Inhibition curves obtained from the competitive ELISA performed with MS 1 serum.

Experiments were repeated twice and the average relative mean affinity of serum anti CSF114(Glc) antibodies for the three inhibitors was calculated in terms of  $IC_{50}$  and is reported in Table 9. This value indicates the molar concentration of each inhibitor that is necessary to inhibit half of the maximum binding (corresponding to the absorbance of serum without inhibitors). Consequently  $IC_{50}$  is inversely related to antibodies affinity for the inhibitor: lower  $IC_{50}$  value indicates stronger inhibitors.



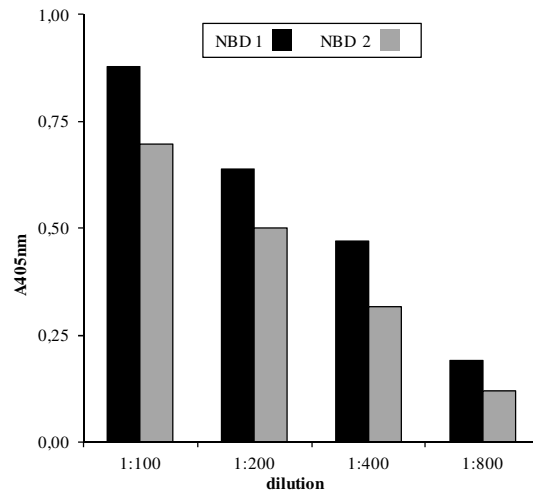
CSF114(Glc) coated_IC <sub>50</sub> value (M)			
Serum	HMW1ct-Glc	HMW1ct	CSF114(Glc)
MS 1	10 <sup>-8.5</sup>	10 <sup>-5</sup>	10 <sup>-7</sup>
MS 2	10 <sup>-9</sup>	10 <sup>-5.5</sup>	10 <sup>-7.5</sup>
MS 3	10 <sup>-9</sup>	no inhibition	10 <sup>-7.5</sup>
MS 4	10 <sup>-9</sup>	no inhibition	10 <sup>-7</sup>
MS 5	10 <sup>-9</sup>	no inhibition	10 <sup>-8</sup>

**Table 9:** IC<sub>50</sub> quantifying the relative mean affinity of anti CSF114(Glc) antibodies in MS sera for 3 inhibitors applied in solution.

The data reported in table 9 indicated that the N-glycosylated protein was able to inhibit antibodies binding in MS sera with a higher affinity than peptide CSF114(Glc), the difference was between 1.5 and 2 log unit. The other observation was that the N-glycosylated moieties on HMW1ct-Glc seemed to be fundamental for antibody recognition because non glycosylated HMW1ct inhibited antibodies binding in MS 1 and MS 2 sera only, with 3.5 log lower affinity.

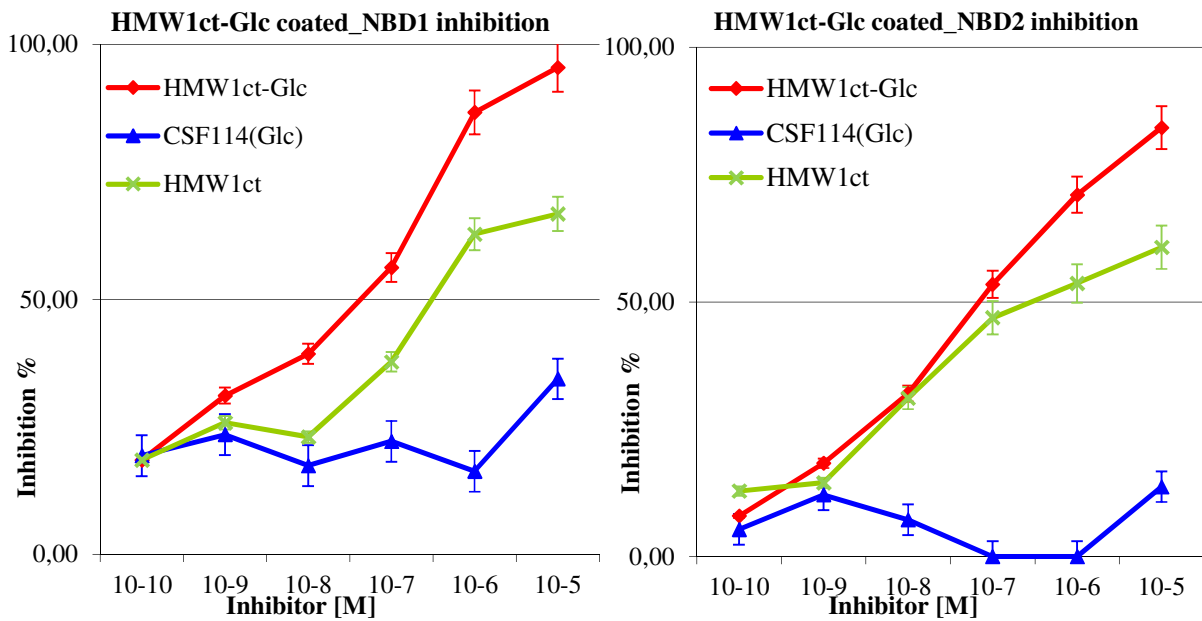
For a statistical validation of the results, we repeated six times MS 1 inhibition experiment coating CSF114(Glc) and using as inhibitors in solution CSF114(Glc) and HMW1ct-Glc. We obtained an average IC<sub>50</sub> of 10<sup>-7.5</sup> M with a standard deviation of 0.35 for the peptide, and an average IC<sub>50</sub> of 10<sup>-9.0</sup> M with a standard deviation of 0.38 for the protein. We also repeated three times MS 2 inhibition experiments coating CSF114(Glc) and using the same two inhibitors in solution; the average IC<sub>50</sub> of CSF114(Glc) was 10<sup>-7.3</sup> M with a standard deviation 0.25, concerning HMW1ct-Glc the average IC<sub>50</sub> was 10<sup>-9.3</sup> M with a standard deviation 0.34. Considering that the IC<sub>50</sub> standard deviation was always below 1.0, we could assess that competitive assay results were significant.

Because no positive NBD serum to CSF114(Glc) was found in the experimental conditions of the competitive ELISA, we decided to titrate NBD sera coating HMW1ct-Glc. By doing this, two NBD sera, whose titration is shown in Figure 28, were selected for the next assays.



**Figure 28:** IgG titration curve obtained with 2 NBD sera coating HMW1ct-Glc. The optimal dilution resulted to be 1:400 for NBD 1 and 1:200 for NBD 2.

The competitive ELISA was performed coating HMW1ct-Glc and the binding of NBD sera was inhibited adding increasing concentrations of HMW1ct-Glc, HMW1ct and CSF114(Glc). Inhibition curves and IC<sub>50</sub> values are reported in Figure 29 and in Table 10 respectively.



**Figure 29:** Inhibition curves resulting from the competitive ELISA performed with 2 NBD sera.

HMW1ct-Glc coated_IC <sub>50</sub> value [M]			
Serum	HMW1ct-Glc	HMW1ct	CSF114(Glc)
NBD 1	10 <sup>-7.5</sup>	10 <sup>-6.5</sup>	no inhibition
NBD 2	10 <sup>-7.5</sup>	10 <sup>-7</sup>	no inhibition

**Table 10:** IC<sub>50</sub> quantifying the relative mean affinity of anti HMW1ct-Glc antibodies in NBD sera for 3 inhibitors applied in solution.

Obtained results indicated that anti HMW1ct-Glc antibodies present in NDB sera had a similar relative mean affinity for both proteins (with no more than 1 log difference), suggesting that these antibodies recognize an epitope shared by the two proteins and probably not related to the presence of the N-glycosylations. Peptide CSF114(Glc) could not inhibit NBD antibodies binding to HMW1ct-Glc at the concentrations used in the assay, confirming the hypothesis that N-glycosylation is not a key point for NBD antibodies binding.

Summarizing results obtained in the case of NBD sera, the same antibody levels against HMW1ct-Glc and HMW1ct were revealed by the SP-ELISA and a similar relative mean affinity of anti HMW1ct-Glc antibodies for HMW1ct-Glc and HMW1ct was calculated through the competitive assay. Taken together these results are in agreement with the idea that antibodies recognizing the protein HMW1 were physiologically present in serum of people who contracted *H. influenzae* during their life and that these antibodies were not specific for the N-glycosylated moieties of the bacterial protein.

Bacterial outer membrane proteins were shown to be targets of bactericidal antibodies or to be capable of stimulating the production of protective antibodies in animal models of infection<sup>51</sup>. Being HMW1 adhesin one of the major surface membrane proteins of *H. influenzae*, antibodies specific for this family of high molecular weight proteins are believed to have an important protective role in human host immunity. This idea was supported by different works that demonstrated that HMW1-like adhesion proteins of nontypable *H. influenzae* were the major target of antibodies in serum from children who had recovered from *Haemophilus* otitis<sup>52</sup>, or that anti-HMW1 antibodies had the ability to mediate opsonophagocytic killing of the bacterium<sup>53</sup> and also that they could interrupt the attachment of the bacterium to the epithelial surface of the upper respiratory tract, the first critical step in the colonization of the human host<sup>54</sup>. A deep characterization of surface accessible B-epitopes on HMW1 whole protein was done by using monoclonal antibodies generated by immunizing mice with HMW1 purified from *H. influenzae*

## CHAPTER 4


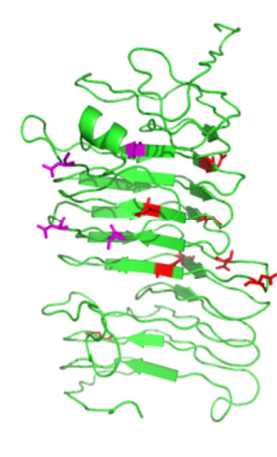

prototype strains. This study demonstrated that the most recognized surface epitope of HMW1 corresponds to a 155 aminoacid segment near the C-terminal region of the protein<sup>55</sup>.

To completely understand the question if antibodies from MS serum recognized conformational epitopes on HMW1ct-Glc, we also performed some competitive ELISA assays using as inhibitor in solution a sample of reduced proteins and another of peptide fragments obtained after tryptic digest of the two proteins. Both sample were produced by the Department of Biology of the Massachusetts Institute of Technology. The binding of two MS sera to peptide CSF114(Glc) was inhibited with the new samples; as expected non glycosylated samples did not inhibit antibodies binding, and reduced or digested HMW1ct-Glc affinity was the same than native HMW1ct-Glc.

The initial hypothesis that in our in vitro system antibodies did not recognize conformational epitopes when proteins were coated on ELISA plates (as explained in 4.5.2) was confirmed by the present competitive experiment because native HMW1ct-Glc, applied as inhibitor in solution and so without any restrictions to its conformation, showed the same inhibition power in terms of  $IC_{50}$  of the reduced and of the digested protein. Results obtained with the digested sample suggested that glycosylated adhesin derived peptides could have the same activity of the whole protein when used as inhibitor in solution and consequently they could be employed to discover the main epitope of the protein HMW1ct-Glc.

### **4.6.4 HMW1ct mutants for competitive ELISA**

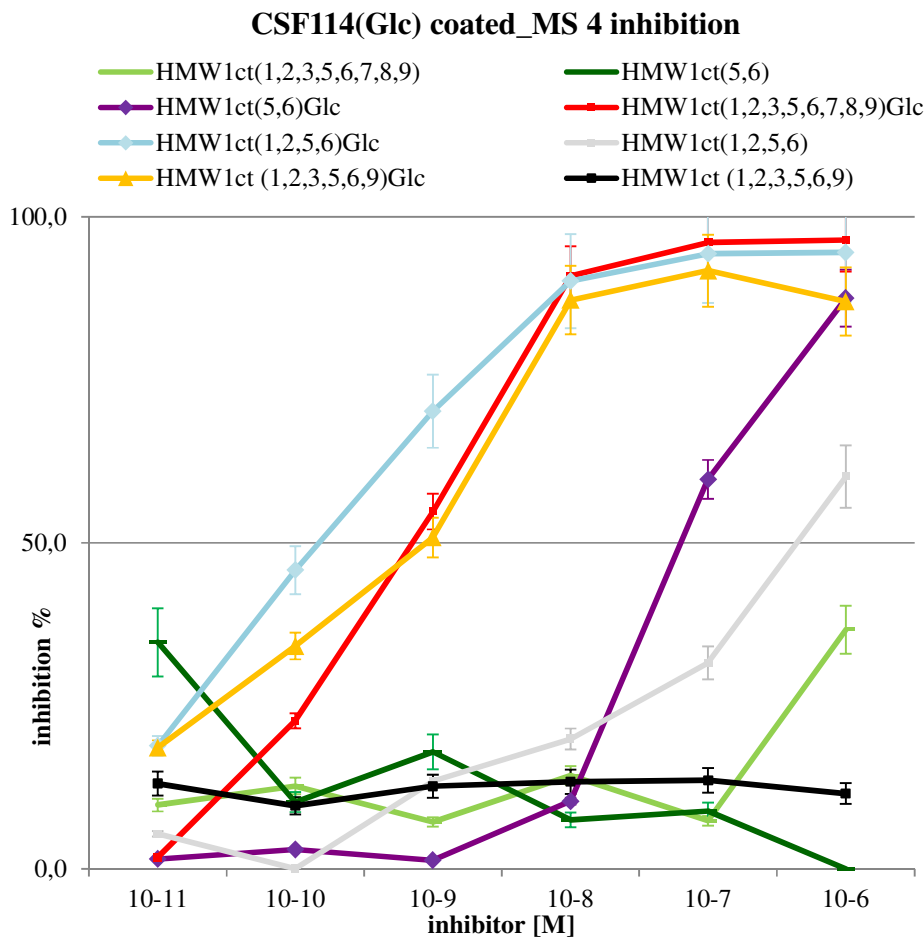
The HMW1ct-Glc protein is characterized by the presence of 8 N-glycosylations on the asparagine side chain of classical Asn-X-Ser/Thr N-glycosylation consensus sequences. The high molecular weight of the protein and the presence of the 8 glucosyl moieties, suggested that it is a multivalent antigen, so with the aim of simplify the potential native epitope represented by HMW1ct-Glc, it was decided to eliminate some N-glycosylation sites sequentially, to understand which particular sugar or which group of them were the most important for antibodies recognition. Accordingly, a series of adhesin mutants containing a different number of N-glycosylation sites, listed in Table 11, were produced in the laboratory of Prof. Barbara Imperiali at the Department of Biology of the Massachusetts Institute of Technology (MIT, Cambridge, USA). We subsequently performed competitive ELISA using these mutants as inhibitors in solution and the corresponding non glycosylated mutants as control.

Mutant name	Structure	Removed glycosylation sites	Remaining glycosylation sites	Number of glycosylations
<b>HMW1ct(1,2,3,5,6,9) Glc</b>		NLS(4) NAT(7) NHT(8) NGA(10) NIT(11) NNT(12)	NVT(1) NVT(2) NAT(3) NVT(5) NTT(6) NAT(9)	Mix of 5 and 6
<b>HMW1ct(1,2,5,6)Glc</b>		NAT(3) NLS(4) NAT(7) NHT(8) NAT(9) NGA(10) NIT(11) NNT(12)	NVT(1) NVT(2) NVT(5) NTT(6)	4
<b>HMW1ct(5,6)Glc</b>		NVT(1) NVT(2) NAT(3) NLS(4) NAT(7) NHT(8) NAT(9) NGA(10) NIT(11) NNT(12)	NVT(5) NTT(6)	2

**Table 11:** HMW1ct-Glc mutants tested in competitive ELISA; the ribbon diagram showing their structure, the removed glycosylation sites (red) and the resulting in vitro glycosylated ones (purple =100% glycosylation, light blue =50% glycosylation) are listed in this table.

The competitive ELISA were performed coating CSF114(Glc) and incubating the same 5 MS sera, tested in the previously described competitive assays, with 6 different concentrations (from  $10^{-6}$  to  $10^{-11}$  M) of the mutants, with and without glycosylations. From the resulting inhibition curves, the  $IC_{50}$  of each inhibitor for each serum was calculated.

As a representative example, the inhibition curves indicating the relative mean affinity of anti CSF114(Glc) antibodies in MS 4 serum for the 6 adhesin mutants, are shown in Figure 30.



**Figure 30:** Inhibition curves obtained from the competitive ELISA incubating MS 4 serum with increasing concentrations of native HMW1ct and of the 3 mutants with and without glycosylations.

As listed in Table 12 the same order of potency of the different inhibitors was conserved among the 5 sera and was the following: HMW1ct-Glc was comparable to HMW1ct(1,2,3,5,6,9)Glc and to HMW1ct(1,2,5,6)Glc and they were stronger inhibitor than HMW1ct(5,6)Glc. The proteins without glycosylation did not inhibit antibodies binding to coated CSF114(Glc) at the tested concentrations, except for HMW1c(1,2,5,6) that had a significantly lower affinity, in the range of  $10^{-6.5}$  M.

	HMW1ct-Glc	HMW1ct	HMW1ct (1,2,3,5,6,9) Glc	HMW1ct (1,2,3,5,6,9)	HMW1ct (1,2,5,6) Glc	HMW1ct (1,2,5,6)	HMW1ct (5,6)Glc	HMW1ct (5,6)
MS 1	$10^{-9.5}$	no inhibition	$10^{-10}$	no inhibition	$10^{-9}$	$10^{-6.5}$	$10^{-8}$	no inhibition
MS 2	$10^{-9.5}$	no inhibition	$10^{-10}$	no inhibition	$10^{-9.5}$	$10^{-6.5}$	$10^{-7}$	no inhibition
MS 3	$10^{-10}$	no inhibition	$10^{-10}$	no inhibition	$10^{-9}$	$10^{-6.5}$	$10^{-7.5}$	no inhibition
MS 4	$10^{-9}$	no inhibition	$10^{-9}$	no inhibition	$10^{-10}$	$10^{-6.5}$	$10^{-7.5}$	no inhibition
MS 5	$10^{-9}$	no inhibition	$10^{-10}$	no inhibition	$10^{-10}$	no inhibition	$10^{-6.5}$	$10^{-6}$

**Table 12:** IC<sub>50</sub> (M) quantifying the relative mean affinity of anti CSF114(Glc) antibodies from 5 MS sera for protein inhibitors applied in solution

The data we obtained comparing all the performed competitive assays, confirmed the relevance of the glucosyl moiety and indicated that the minimum number of glucosylations required to inhibit MS sera binding to CSF114(Glc), with the same high potency of the 8 times glucosylated HMW1ct, was 4. However, we cannot exclude that a protein with only two glucosyl units, different from 5,6 or a protein with four glucosyl residues, different from 1,2,5,6 could have a higher potency than the native HMW1ct-Glc.

#### 4.6.5 Competitive ELISA with adhesin derived peptides.

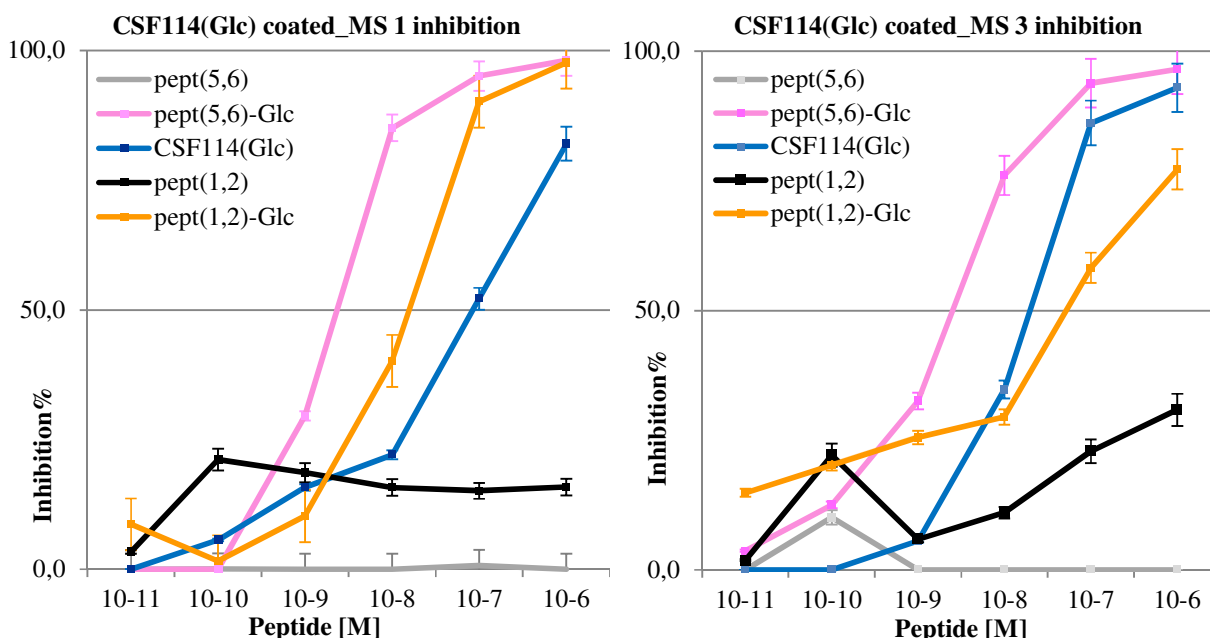
Taking into account the results obtained with HMW1ct(1,2,5,6)Glc, we tried to better understand the role of its glucosylations and we realized that two sub clusters, consisting of two sequons each, could be identified in this mutant: the first formed by sequons 1 and 2, resulting in spatial proximity but connected by a long loop; the second formed by sequons 5 and 6, located at only one amino acid distance along the protein sequence. Considering that peptides fragments deriving from HMW1ct-Glc tryptic digest were able to inhibit MS anti-CSF114(Glc) antibodies binding with the same affinity of the whole glucosylated protein and that the HMW1ct(1,2)Glc mutant was hard to produce because of technical reasons, in order to compare the role of the two sub clusters of sequons and to better understand which of them was the more relevant for antibody recognition, two di-N-glucosylated peptides were synthesized in our laboratory (Table 13). Accordingly, pept(5,6)Glc, derived from sub cluster 5-6, and pept(1,2)Glc, derived from sub cluster 1-2, were prepared by Solid Phase Peptide Synthesis (SPPS) technique. The corresponding non glucosylated sequences were also synthesized as negative controls.

Peptide name	Sequence
Pept(1,2)Glc	Ac-YAN(Glc)VTSATGTIGGTISGNTVN(Glc)VTANKKK-NH <sub>2</sub>
Pept(5,6)Glc	Ac-AN(Glc)VTLN(Glc)TT-NH <sub>2</sub>
Pept(1,2)	Ac-YANVTSATGTIGGTISGNTVNVVTANKKK-NH <sub>2</sub>
Pept(5,6)	Ac-ANVTLNTT-NH <sub>2</sub>

**Table 13:**Sequence of synthetic di-N-glycosylated peptides derived from HMW1ct(1,2,5,6)Glc mutant.

A poli-lysine tag was inserted in pept(1,2) and pept(1,2)Glc to increase their hydrophilicity, but nevertheless their solubility resulted to be poor in the aqueous buffer needed for the competitive assay, consequently we dissolved all the four lyophilized peptides in a stock solution of water and Dimethyl Sulfoxide (DMSO) 1:1 and then we diluted them in the appropriate buffer to perform the test.

The binding of the five MS sera to CSF114(Glc) was inhibited applying six different concentrations of the synthesized peptides, with and without glycosylations, and CSF114(Glc) was used as inhibitor in each plate as an internal control of the performance of the assay. Inhibitor peptides were test at the same concentrations of adhesin proteins (from 10<sup>-6</sup> to 10<sup>-11</sup> M). From the resulting inhibition curves, the IC<sub>50</sub> quantifying the affinity of each peptide for the five sera was calculated and reported in Table 14. The graph illustrating the result of the competitive ELISA with MS 1 and MS 3 sera are shown in Figure 31.



**Figure 31:** Inhibition curves describing the affinity of adhesin derived peptides for anti CSF114(Glc) antibodies in MS1 and MS3 sera.



	<b>Pept(1,2)Glc</b>	<b>Pept(1,2)</b>	<b>Pept(5,6)Glc</b>	<b>Pept(5,6)</b>	<b>CSF114(Glc)</b>
<b>MS 1</b>	$10^{-8}$	no inhibition	$10^{-9}$	no inhibition	$10^{-7}$
<b>MS 2</b>	$10^{-7}$	no inhibition	$10^{-8}$	no inhibition	$10^{-7}$
<b>MS 3</b>	$10^{-7.5}$	no inhibition	$10^{-9}$	no inhibition	$10^{-8}$
<b>MS 4</b>	$10^{-7.5}$	no inhibition	$10^{-8}$	no inhibition	$10^{-7}$
<b>MS 5</b>	$10^{-6}$	no inhibition	$10^{-7.5}$	no inhibition	$10^{-7.5}$

**Table 14:** IC<sub>50</sub> values (M) calculated for the 4 adhesin derived peptides and for CSF114(Glc).

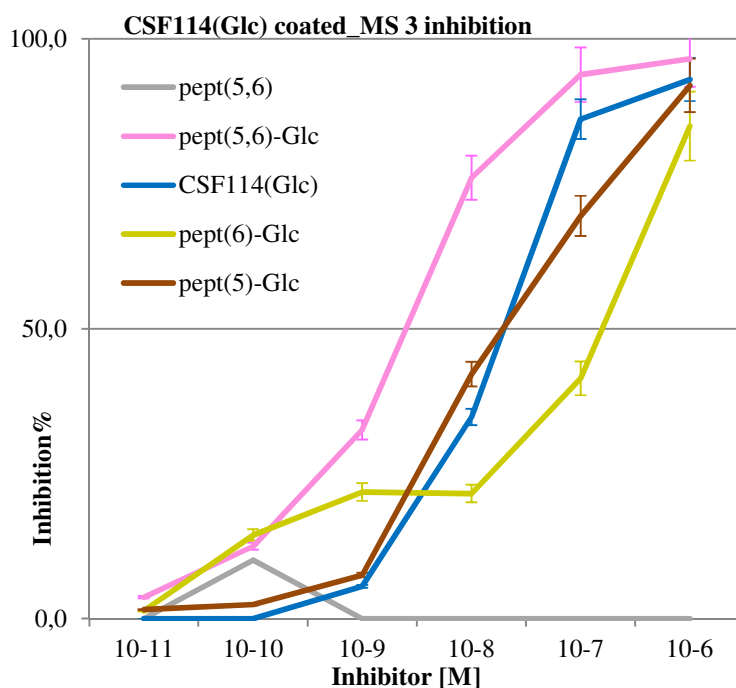
The results of the competitive assay performed with adhesin derived peptides confirmed the importance of the N-glycosylation for the interaction with specific MS antibodies; in fact both peptides containing two Glc residues could inhibit anti CSF114(Glc) antibodies binding to CSF114(Glc) in all the five patients sera, while the non glycosylated control sequences never reach the IC<sub>50</sub> value at the concentrations used in the assay. The second observation is that the same order of potency of the different inhibitors was conserved among the five sera and in particular pept(5,6)Glc was a more potent inhibitor than pept(1,2)Glc, with both peptides showing an affinity 1 or 2 orders of magnitude greater than that of CSF114(Glc); the higher affinity of adhesin derived peptides could be linked to the presence of two Glc units instead of the only one present in CSF114(Glc) sequence.

To understand if one glycosylation site on pept(5,6)Glc was more important than the other for antibody recognition and if both were necessary to inhibit MS sera binding to CSF114(Glc), two peptides bearing a single Glc unit in position 5 or 6, reported in Table 15, were synthesized by PeptLab.

<b>Peptide name</b>	<b>Sequence</b>
<b>Pept(5)Glc</b>	Ac-AN(Glc)VTLNNTT-NH <sub>2</sub>
<b>Pept(6)Glc</b>	Ac-ANVTLN(Glc)TT-NH <sub>2</sub>

**Table 15:** Mono N-glycosylated peptide sequences derived from pept(5,6)Glc.

Both peptides were applied in competitive ELISA with five MS sera and their ability to inhibit the binding of anti CSF114(Glc) antibodies was evaluated. The result of the competitive ELISA performed with MS 3 serum is shown in Figure 32 as a representative example.



**Figure 32:** Inhibition curves obtained incubating MS 3 serum with the 5 peptides listed in the legend.

In the following Table 16 the  $IC_{50}$  values, calculated for the two peptides with the five MS sera, are listed.

	MS 1	MS 2	MS 3	MS 4	MS 5
<b>Pept(5)Glc</b>	$10^{-8}$	$10^{-6.5}$	$10^{-8}$	$10^{-7}$	$10^{-6.5}$
<b>Pept(6)Glc</b>	$10^{-6.5}$	$10^{-6}$	$10^{-7}$	$10^{-7}$	no inhibition

**Table 16:**  $IC_{50}$  values (M) calculated for the two mono-glucosylated adhesin derived peptides.

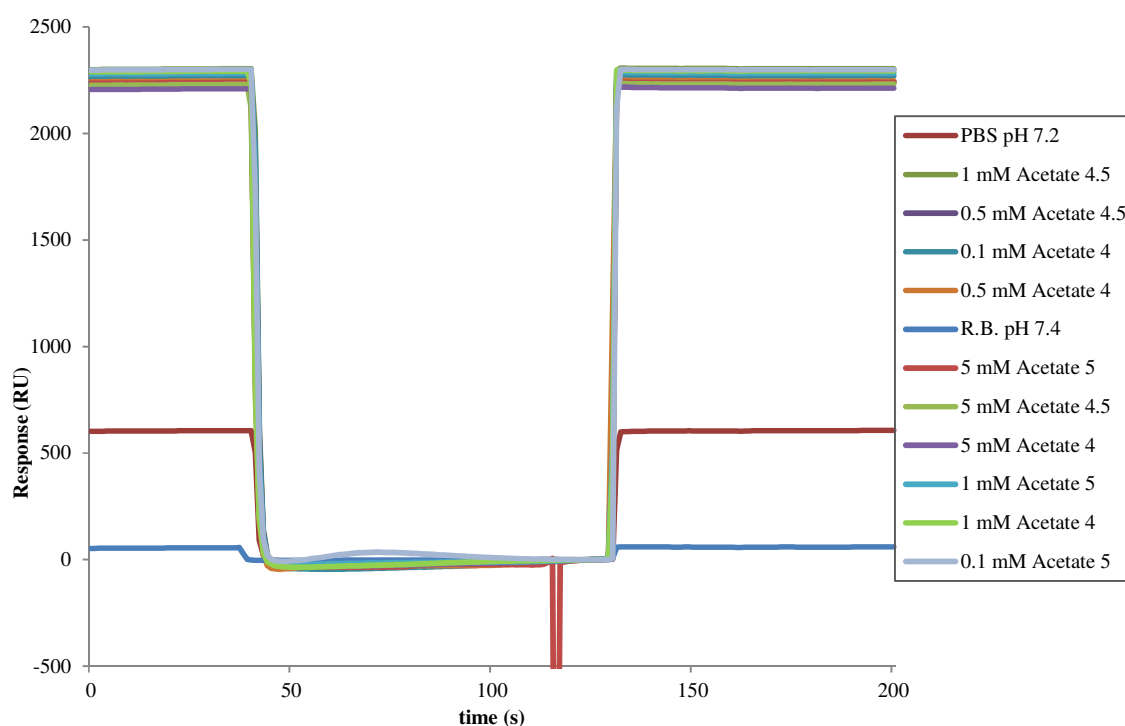
The affinity of anti CSF114(Glc) antibodies present in MS sera for the two peptides was generally lower or comparable to the affinity for CSF114(Glc) itself, but always lower than the affinity for pept(5,6)Glc, indicating that both sites were involved in the interaction with antibodies and so pept(5,6)Glc higher affinity was linked to the presence of two glucose moieties. Comparing the affinity of the two mono-glucosylated peptides, we realized that pept(5)Glc was a stronger inhibitor than pept(6)Glc, consequently the glucosylation in position 5 seems to be more relevant than the other for antibody interaction in our in vitro system.

#### 4.6.6 Adhesin peptides immobilization on Biacore sensor chip

We subsequently decided to characterize the kinetic and the affinity of antibody binding to the immobilized peptide pept(5,6)Glc, since it exhibited the highest affinity for anti CSF114(Glc) antibodies in competitive assays and consequently we thought that it could be used as probe to

detect antibodies in MS sera. With this aim, we planned to synthesize a new version of this peptide with a free N-terminal alanine residue, in order to use its amine group to covalently immobilize the peptide on the carboxylic groups present on Biacore sensor chip surface by the amine coupling strategy. Pept(5,6) with a free N-terminal alanine was also synthesized as negative control.

The pH scouting procedure was separately performed with the two peptides to find the best immobilization buffer maximizing their electrostatic pre-concentration on chip surface. Peptides were diluted in buffers of different pH and molarity but abnormal resonance signals were registered indicating problems of precipitation or peptides aggregation in solution. By adding 5% dimethyl sulfoxide (DMSO) to each solution, we avoided peptides aggregation and we selected 0.1 mM CH<sub>3</sub>COONa at pH 4.0 with 5% DMSO as the best immobilization buffer, although giving a pre-concentration signal of no more than 20 RU (Figure 33). The same problem of aggregation and very low electrostatic interaction with chip surface was observed in the case of the unglucosylated pept(5,6) and therefore we added 5% DMSO to the solutions and we identified 5 mM CH<sub>3</sub>COONa at pH 4.5 as the best immobilization buffer.

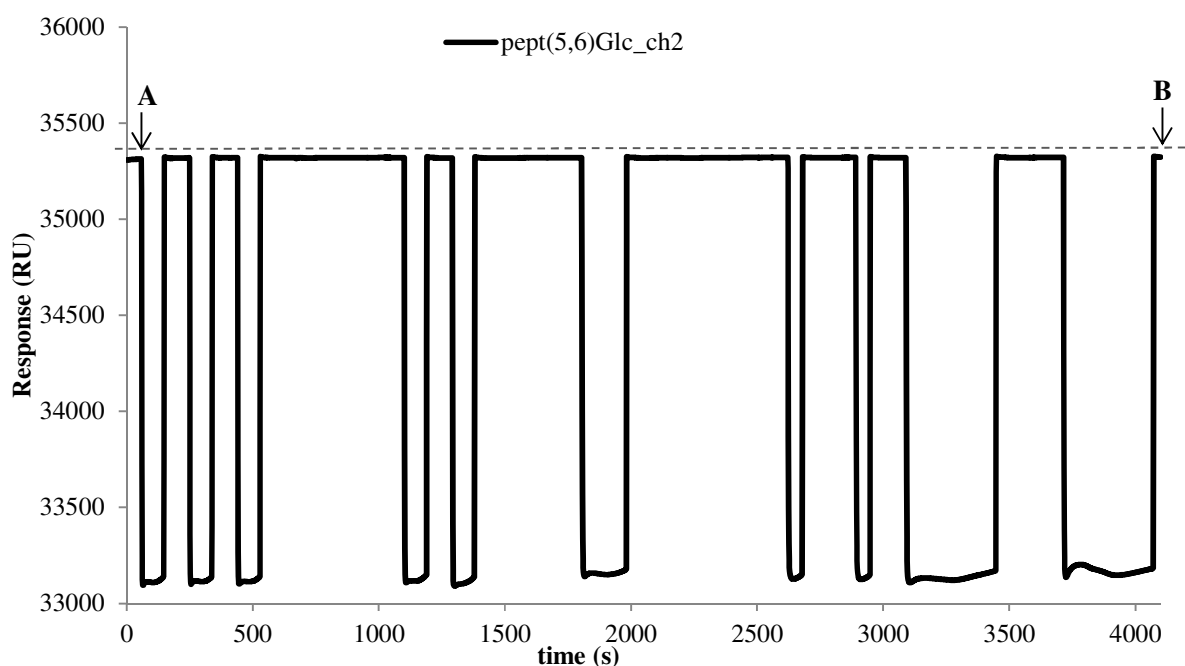


**Figure 33:** Results of the pH scouting performed with pep(5,6)Glc, 5% DMSO was added to each solution and very low electrostatic interaction signals were registered.

## CHAPTER 4

We tried to immobilize pept(5,6)Glc on channel 2 and pept(5,6) on channel 3 of the same sensor chip through the amine coupling strategy. Chip surface was activated and peptides were individually injected several times increasing their concentration in the immobilization buffer and decreasing the flow rate to facilitate the formation of the covalent bond; finally free reactive sites on the surface were blocked.

The same baseline level was registered at the beginning of the immobilization procedure and at the end of the method with pept(5,6)Glc (Figure 34) and with pept(5,6), indicating that no covalent immobilization was achieved.



**Figure 34:** Sensorgram showing the same baseline signal immediately after surface activation (A) and after ten consecutive injection of pept(5,6)Glc (B).

The immobilization of low molecular weight ligands is often hard to achieve in SPR-based system and in this case we thought that the immobilization was not possible also because pept(5,6), solubilized at a pH below its isoelectric point of 9.8, had only one net positive charge due to the presence of a free N-terminal group, so the electrostatic interaction with the chip surface could be too feeble. Another problem could be the presence of DMSO, necessary to solubilize the peptide in the immobilization buffer, but interfering somehow with the coupling reaction.

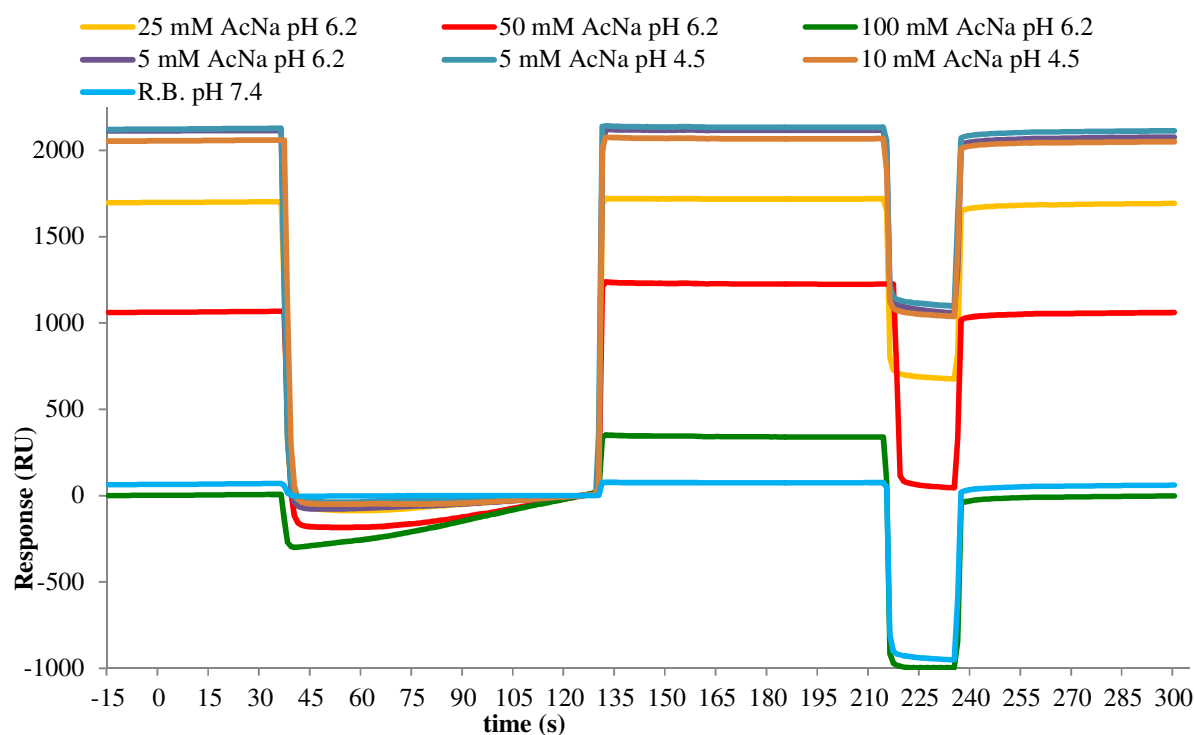
We decided to overcome this problem by synthesizing a new longer adhesin derived peptide, whose sequence is reported in Table 17, and containing the glycosylation sequons 5, 6 and 7 of

HMW1ct-Glc, because those sequons were reported to be the first in vivo glucosylated by the bacterial enzyme<sup>22</sup>. The non glucosylated peptide was also synthesized as negative control.

Peptide name	Sequence
pept(5,6,7)Glc	YAN(Glc)VTLN(Glc)TTGTLTTVKGSNIN(Glc)ATS-NH <sub>2</sub>
pept(5,6,7)	YANVTLNNTTGTLLTTVKGSNINATS-NH <sub>2</sub>

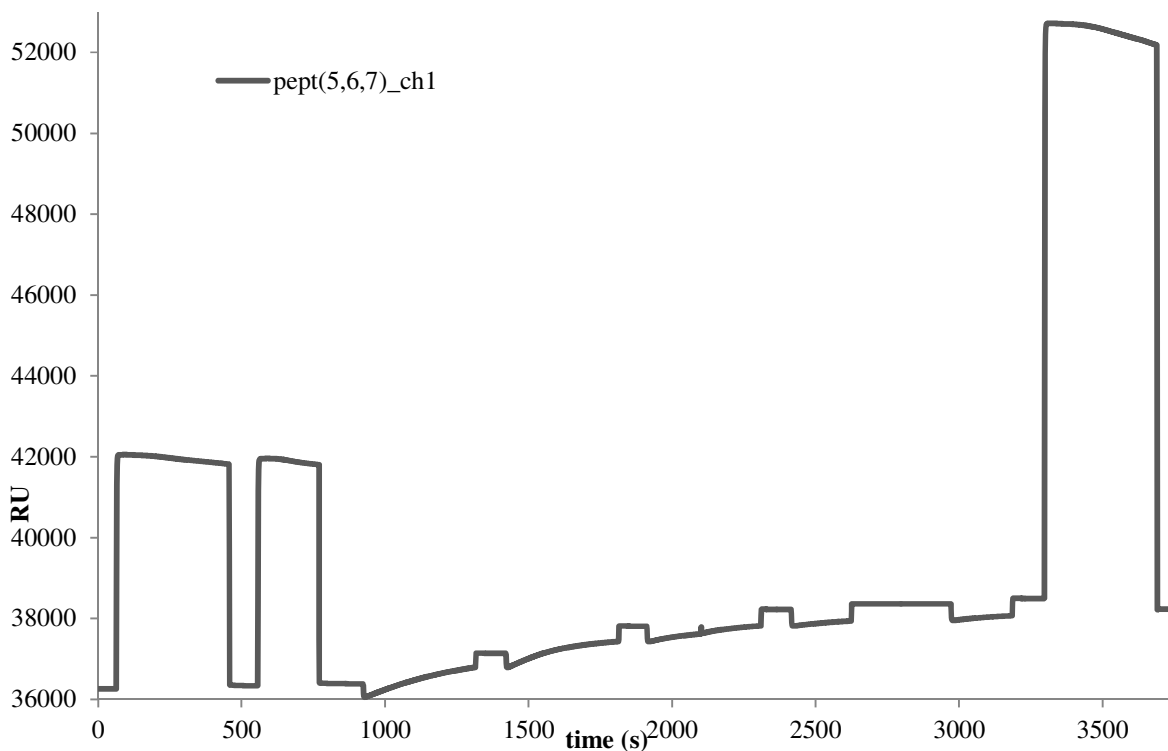
**Table 17:** Sequence of peptides synthesized for Biacore studies; they contain glucosylation sequons 5, 6 and 7 of HMW1ct protein.

Pept(5,6,7) was employed for the optimization of the immobilization protocol. It has an isoelectric point of 10.4 and 2 net positive charges at pH below 8.0 and it was soluble in aqueous buffers. Through the pH scouting procedure, 100 mM sodium acetate at pH 6.2 was selected as the best immobilization buffer giving a satisfactory pre-concentration of the peptide on chip surface (Figure 35).



**Figure 35:** Sensorgrams showing the electrostatic interaction between pept(5,6,7) diluted in different buffers, and Biacore chip surface.

The amine coupling protocol was then applied to covalently immobilize the peptide and at the end of the procedure an immobilization level of 2124 RU was obtained as shown in Figure 36.



**Figure 36:** Resonance signal obtained from the immobilization of pept(5,6,7) on channel 1.

The same immobilization strategy is going to be followed to immobilize the corresponding glycosylated peptide with the idea of performing binding studies with MS sera and affinity and kinetic studies with purified antibodies. For these assays pept(5,6,7) will be used as reference to subtract the signal due to aspecific interactions and pept(5,6,7)Glc will be used as active ligand.

#### 4.6.7 Antibody purification from one MS serum

With the aim of obtaining a very specific fraction of antibodies present in one MS serum and recognizing the N-glycosylated epitopes present on CSF114(Glc) and on HMW1ct-Glc, we set up a purification method consisting of two sequential affinity chromatographies: the first using a column with the non glycosylated antigen to deplete serum from antibodies specific for the unglycosylated portion of the molecule, and the second using a column containing the glycosylated antigen to elute antibodies highly specific for the glucosyl moieties.

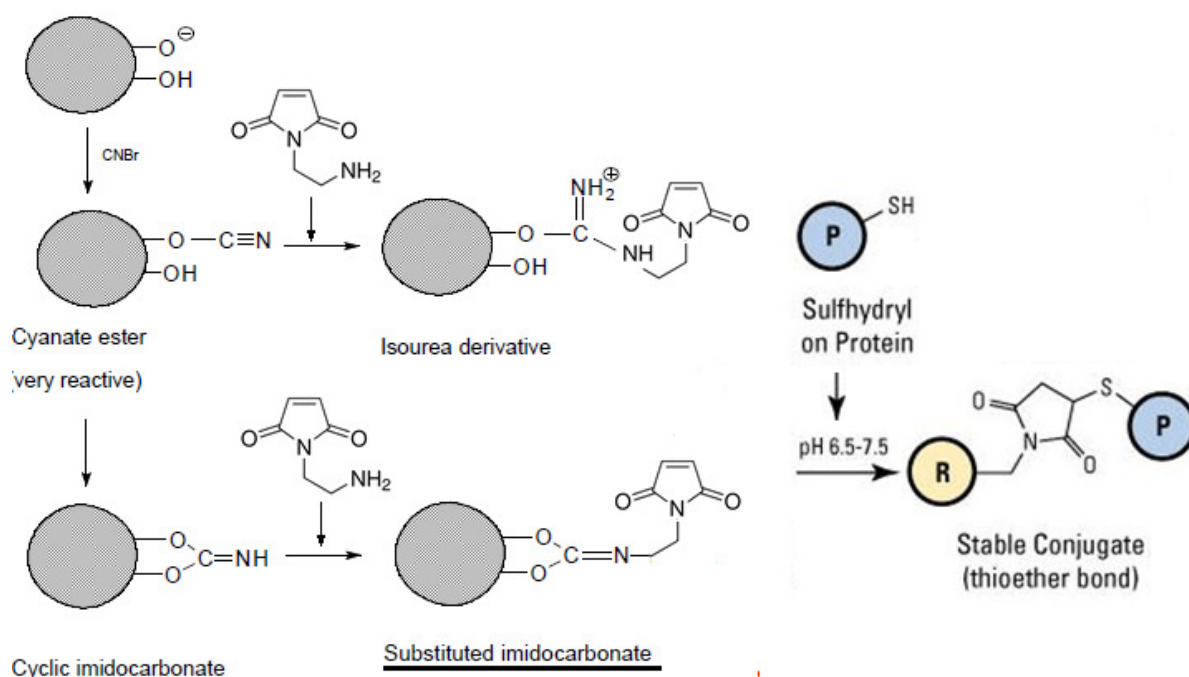
Peptide CSF114(Glc) and non glycosylated peptide CSF114 were used in the past to purify antibodies and their immobilization to sepharose resin, according to the amine coupling strategy, was already optimized .

On the contrary adhesin proteins were never used to purify antibodies, so we investigated two different immobilization strategies: the thiol coupling, because in HMW1ct sequence two

cysteine residues were present and their free thiol groups could be used for the linkage to the sepharose resin; the amine coupling that could involve one of the numerous free primary amine groups present on lysine residues side chains or on the N-terminal alanine residue.

#### 4.6.7.1 Adhesin proteins conjugation to sepharose by thiol coupling

Commercial CNBr-activated sepharose resin was washed and coupled to N-(2-aminoethyl)maleimide previously dissolved in carbonate buffer at pH 8.3, free reactive groups on resin were blocked with a glycine solution at pH 6.0 and the resin was exhaustively washed with two buffers at different pH in order to remove all the not covalently bound reagents. In the meanwhile HMW1ct and HMW1ct-Glc disulfides were reduced by the addition of dithiothreitol (DTT) as reducing agent and each solution was then add to two sepharose resins. The free reactive sites functionalized with maleimide groups were blocked with a cysteine solution at neutral pH. The expected reaction scheme is shown in Figure 37.



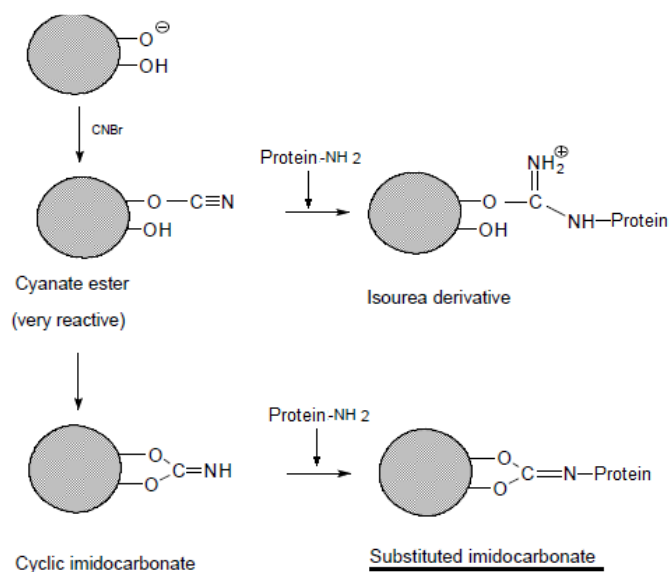
**Figure 37:** Stepwise immobilization of adhesin proteins to CNBr-sepharose resin by the thiol coupling strategy .

After an overnight incubation each protein solution was recovered and its absorbance at 280nm was read and compared to the one registered before the incubation with the resin in order to quantify the protein remained in solution and so to calculate the yield of the coupling step (Table 18).

#### 4.6.7.2 Adhesin proteins conjugation to sepharose by amine coupling

Commercial CNBr-activated sepharose resin was washed and adhesin proteins were diluted in carbonate buffer at pH 8.3 and applied to the resins. After an overnight incubation free reactive sites on resin were blocked with a glycine solution at pH 8.0 and the resin was exhaustively washed with two buffers at different pH in order to remove all the not covalently bound proteins.

In Figure 38 the expected reaction scheme is given.



**Figure 38:** Stepwise immobilization of adhesin proteins to CNBr-sepharose resin by the amine coupling strategy.

Absorbance at 280 nm of every samples in coupling buffer before the coupling and after the reaction with the resin was checked and proteins conjugated to the resin were quantified.

A comparison of adhesin proteins covalently linked to sepharose by the thiol coupling approach and by the amine coupling one is reported in the following Table 18.

Thiol coupling		Amine coupling	
HMW1ct	HMW1ct-Glc	HMW1ct	HMW1ct-Glc
57,0%	37,5%	37,3%	43,8%

**Table 18:** Comparison between the percentage of HMW1ct and HMW1ct-Glc proteins coupled to sepharose according to two different immobilization strategies.

The two immobilization strategies showed similar performances, but we decided to follow the amine coupling strategy for two reasons: at first it is the “cleanest” approach because there was no need to use a reducing reagent such as DTT that could alter the secondary structure of the proteins or that could remain attached to the column and interfere with antibodies binding and consequently with their purification; the second reason is the relative higher quantity of the



glucosylated protein (5%) that we were able to link by the amine coupling approach as compared to the thiol coupling.

#### **4.6.7.3 Sequential affinity chromatography**

MS 1 serum was selected for antibody purification because of its high IgG titer in SP-ELISA against CSF114(Glc) and HMW1ct-Glc. Two affinity columns were prepared to be sequentially used following the selected amine coupling strategy: in the first HMW1ct was linked to the sepharose resin and in the second HMW1ct-Glc was immobilized. The same procedure was used to obtain a CSF114 and a CSF114(Glc) containing column.

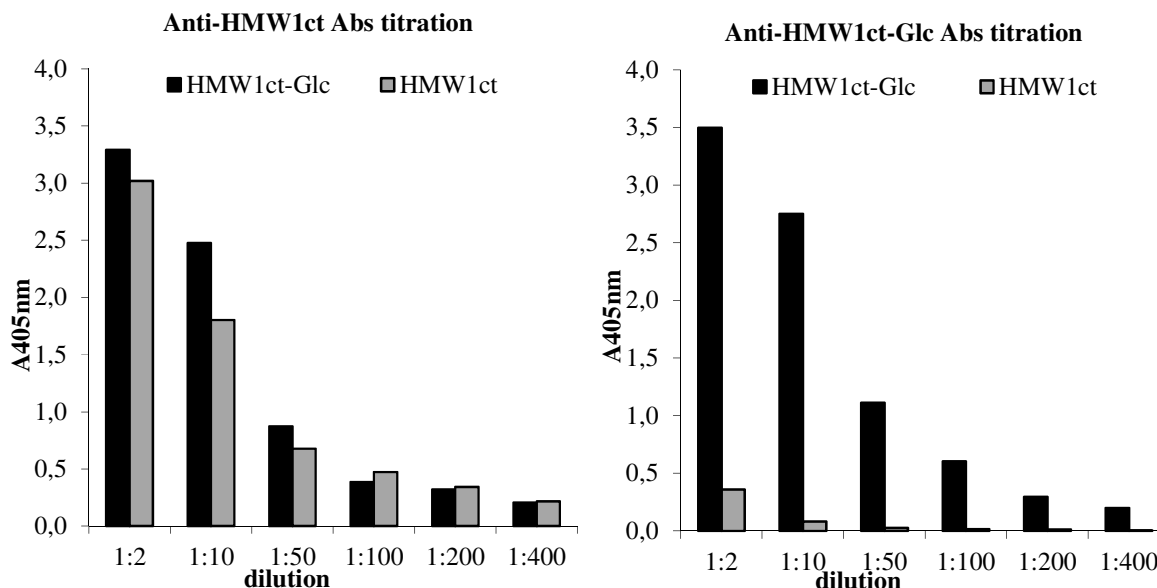
MS 1 serum was diluted, filtered and loaded onto the column functionalized with the protein HMW1ct; after being recirculated three times, the unretained fraction was recovered from the column and directly applied to the second column functionalized with HMW1ct-Glc and recirculated three times. Both columns were extensively washed and antibodies specifically bound to each column were eluted using an acid buffer. Eluted antibodies were neutralized, centrifuged with the appropriate centrifugal filter to remove the elution buffer and immediately recovered with PBS buffer at neutral pH. Purified antibodies concentration was calculated by measuring the absorbance at 280 nm and resulted to be 38.5  $\mu\text{g/mL}$  for 1,5 mL of antibodies eluted from the first column (anti-HMW1ct Abs) and 35.0  $\mu\text{g/mL}$  for 1,7 mL of antibodies eluted from the second column (anti-HMW1ct-Glc Abs).

The same purification procedure was followed using two chromatography columns functionalized with CSF114 and CSF114(Glc), respectively. After serum loading and columns washing, specific antibodies were eluted from the two columns and their concentrations were calculated according to their absorbance at 280 nm. We obtained 1.8 mL of antibodies eluted from the first column (anti-CSF114 Abs) at a concentration of 38.3  $\mu\text{g/mL}$ , and 1.5 mL of antibodies eluted from the second column (anti-CSF114(Glc) Abs) at a concentration of 27.7  $\mu\text{g/mL}$ .

#### **4.6.8 Purified antibodies titration**

The specificity of the four purified antibody fractions for the different antigens was investigated by performing an SP-ELISA titration assay.

Plates were coated with HMW1ct and HMW1ct-Glc and anti-HMW1ct or anti-HMW1ct-Glc Abs were applied at six different dilutions on both coated proteins. The registered absorbance values are shown in Figure 39.

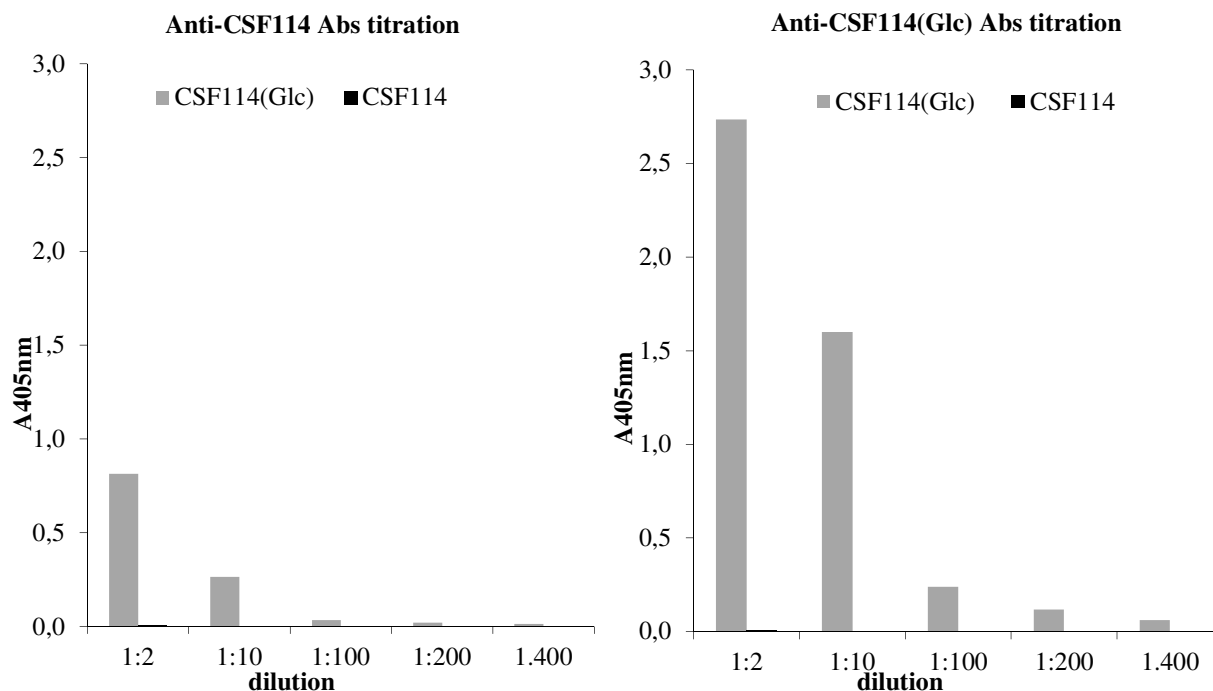


**Figure 39:** SP-ELISA titration of purified anti-HMW1ct and anti-HMW1ct-Glc antibodies.

The result of the titration assay clearly demonstrated the success of the purification procedure based on two sequential affinity chromatographies. Antibodies eluted from the first column showed a very similar titer against HMW1ct as well as against HMW1ct-Glc, suggesting that they recognized some epitopes shared by both proteins and consequently dependent upon their amino acidic sequence. On the contrary antibodies eluted from the second column had a high titer against HMW1ct-Glc only. Considering that HMW1ct-Glc differs from HMW1ct for the presence of 8 glucosyl moieties, antibodies eluted from the second column should bind very specifically those glucosyl units.

An SP-ELISA titration assay was then performed coating CSF114 and CSF114(Glc) and applying five different concentrations of anti-CSF114 and anti-CSF114(Glc) Abs. As reported in Figure 40, the sequential affinity chromatography on peptides was successful in obtaining one antibody fraction specifically recognizing the glucosylated epitope of CSF114(Glc); in fact anti-CSF114(Glc) Abs titer was high on CSF114(Glc) but no absorbance was registered on coated CSF114. Antibodies eluted from the column functionalized with CSF114 displayed a low titer on coated CSF114(Glc) and no titer on CSF114, indicating that the experimental conditions of the

titration assay, probably in terms of incubation time and temperature, were inadequate to detect purified anti-CSF114 Abs.



**Figure 40:** SP-ELISA titration of purified anti-CSF114 and anti-CSF114(Glc) antibodies.

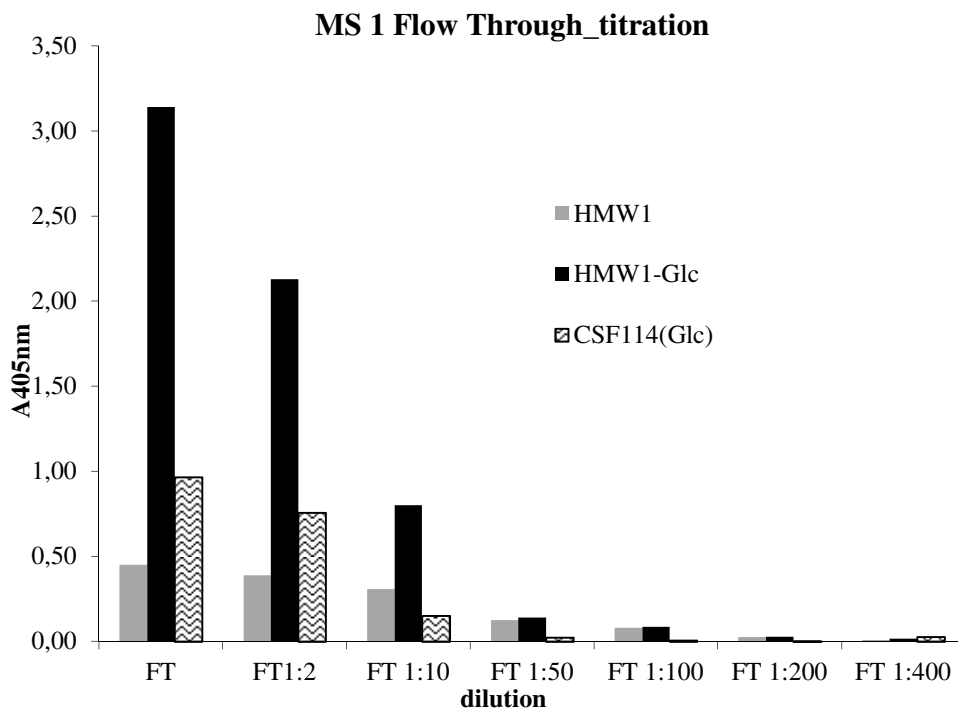
In both sequential affinity chromatographies the initial loading of serum on the column functionalized with the non glycosylated antigen allowed a complete depletion of antibodies recognizing non glycosylated epitopes and consequently to collect antibodies very specific for the glycosyl moieties present on the antigen immobilized on the second column.

#### 4.6.8.1 HMW1ct not retained fraction characterization

During the previously described sequential affinity chromatography process a little amount of the Flow Through (FT) fraction that was not retained from the HMW1ct containing column was preserved for the following analysis.

To confirm the performance of the sequential affinity chromatography process in depleting serum of anti HMW1ct antibodies and to evaluate the relative mean affinity of polyclonal antibodies remained in the FT fraction of MS 1 serum after the depletion step, we decided to perform a titration assay and a competitive ELISA.

For the titration experiment plates were coated with HMW1ct, HMW1ct-Glc and CSF114(Glc) and the FT fraction was applied at seven different final dilutions; absorbance levels registered at the end of the assay are shown in Figure 41.

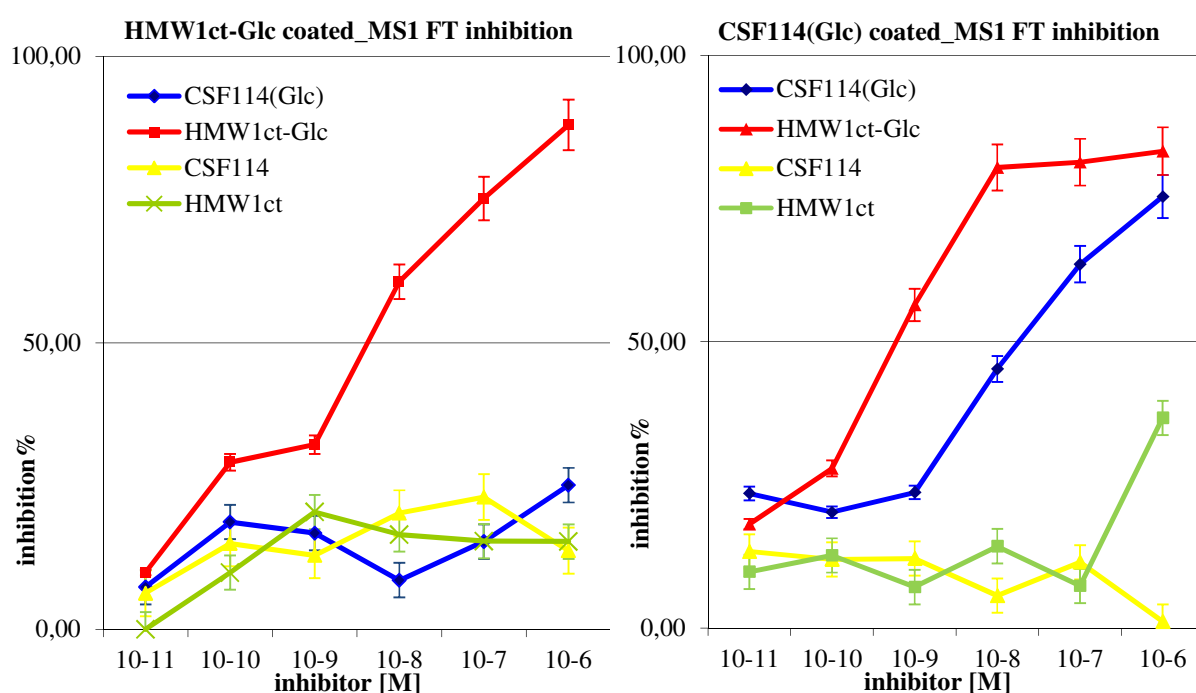


**Figure 41:** SP-ELISA titration of the FT fraction obtained from the HMW1ct-column.

In agreement with results obtained titrating purified anti-HMW1ct-Glc Abs, this FT fraction too had a high concentration dependent antibody titer against the glycosylated protein as compared to the low titer detected against the unglycosylated protein, confirming the performance of the depletion step; as expected antibodies binding to CSF114(Glc) were also present in this sample. The residual absorbance registered on coated HMW1ct could depend on the saturation of the HMW1ct column that did not allow to achieve a complete depletion of anti-HMW1ct antibodies from MS serum or could be due to the presence of antibodies in the FT fraction that recognized some epitopes of HMW1ct that were not accessible when the protein was covalently bound to the sepharose resin but that are better exposed when the same protein was absorbed on the ELISA plate.

A competitive ELISA was then performed coating HMW1ct-Glc and the binding of anti-HMW1ct-Glc antibodies, contained in the FT fraction, was inhibited applying six different concentrations of HMW1ct, HMW1ct-Glc, CSF114 and CSF114(Glc). The inhibition curves indicating the inhibition values (%) for every inhibitor concentrations used are reported in Figure 42. The only molecule that inhibited the binding of anti-HMW1ct-Glc antibodies, at the tested concentrations, was HMW1ct-Glc with an  $IC_{50}$  value of  $10^{-8}$  M. This experiments represented the first attempt to calculate the relative mean affinity of anti-HMW1ct-Glc antibodies from MS

serum in competitive ELISA and interestingly the peptide CSF114(Glc) did not inhibit their binding at the concentration used in this assay. To better understand the reason for the lack of the inhibition ability of the peptide, another competitive assay was performed coating CSF114(Glc) and incubating the same FT fraction with increasing concentrations of HMW1ct-Glc, HMW1ct, CSF114(Glc) and CSF114. As shown in Figure 42, both the glucosylated peptide and the glucosylated protein resulted to be able to inhibit the binding of anti-CSF114(Glc) antibodies with an  $IC_{50}$  of  $10^{-8}$  and  $10^{-9.5}$  M, respectively, thus confirming the previously obtained results with the five MS patients' sera. Non glucosylated molecules never inhibited antibodies binding.



**Figure 42:** Inhibition curves obtained from the competitive ELISA assays and indicating the relative mean affinity of anti HMW1ct-Glc or of anti-CSF114(Glc) antibodies, present in MS 1 FT fraction, for the different inhibitors applied in solution.

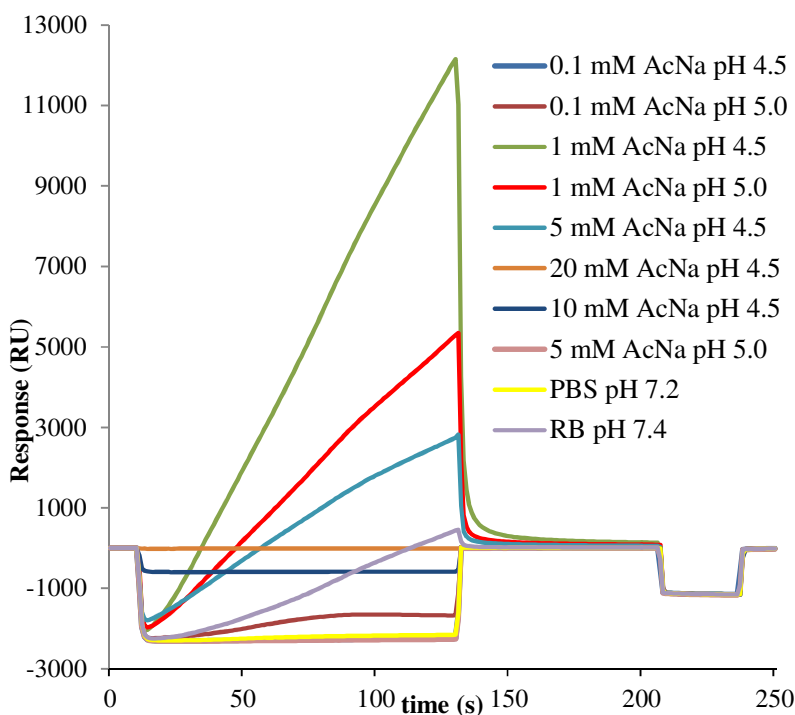
It should be taken into account that the antibody fraction obtained from MS serum is polyclonal and thus contains a family of different immunoglobulins, possibly interacting with different epitopes of the relatively large protein antigen HMW1ct-Glc and only a subgroup of this heterogeneous population of antibodies may cross-react with CSF114(Glc) peptide; this could be the reason why the peptide did not inhibit their binding when HMW1ct-Glc was absorbed on the plate. This hypothesis was in line with the results obtained with the other competitive assay; in fact when CSF114(Glc) was coated, antibodies in the FT fraction interacting with a small antigen like the peptide, were inhibited by both glucosylated molecules.

### 4.6.9 Surface Plasmon Resonance studies with purified antibodies

We decided to exploit the technology of the Surface Plasmon Resonance biosensor Biacore T100 to investigate the cross reactivity of each purified antibody fraction with each antigen and to deeply characterize the kinetic and the affinity of these interactions.

#### 4.6.9.1 Biosensor surface preparation

HMW1ct, HMW1ct-Glc, CSF114 and CSF114(Glc) were individually immobilized onto a different channel of the sensor chip surface. For each ligand the best immobilization buffer, maximizing the electrostatic interaction with chip surface, was selected with the pH scouting procedure consisting in injecting each molecule in buffers of different pH and ionic strength. The pH scouting performed with HMW1ct-Glc is shown in Figure 43 as a representative example.



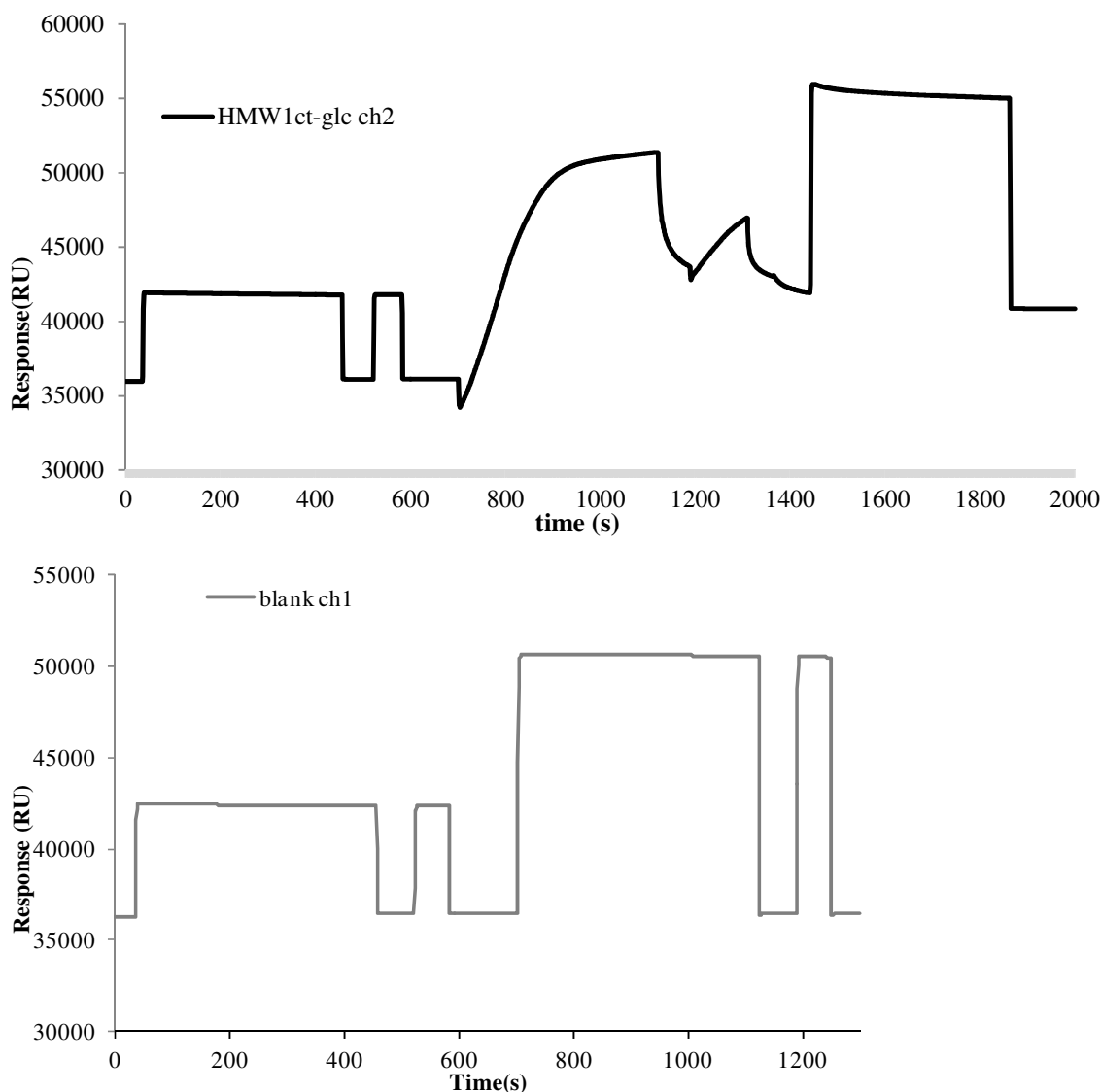
**Figure 43:** Sensorgrams resulting from the pH scouting experiment performed dissolving HMW1ct-Glc in the buffers listed in the legend and injecting it over chip surface.

The optimal selected buffers and the immobilization level of each molecule are reported in Table 19.

	<b>HMW1ct</b>	<b>HMW1ct-Glc</b>	<b>CSF114</b>	<b>CSF114(Glc)</b>
<b>Immobilization buffer</b>	5mM CH <sub>3</sub> COONa pH 4.5	10mM CH <sub>3</sub> COONa pH 4.5	0.5mM CH <sub>3</sub> COONa pH 5	0.1mM CH <sub>3</sub> COONa pH 5.5
<b>Immobilized molecule (RU)</b>	8886	7360	2390	1483

**Table 19:** Optimal immobilization buffer and quantity of proteins and peptides immobilized on chip surface expressed in Resonance Unit (RU).

Ligands were immobilized through the amine coupling strategy, this coupling approach consisted in the activation of carboxylic groups on chip surface and in the injection of the ligand containing at least one free primary amine group in order to allow the amide bond formation between the free amine and an active carboxylic group introduced in the dextran matrix. Remaining free reactive sites on chip surface were then blocked with ethanolamine. Figure 44 shows the resonance signal generated by the immobilization of HMW1ct-Glc on channel 2. The channel 1 of each sensor chip was used as reference to subtract unspecific interaction between samples and gold surface, this channel was activated and directly blocked obtaining the sensorgram showed in Figure 44.



**Figure 44:** Sensorgram illustrating the amine coupling immobilization of HMW1ct-Glc on channel 2 and the blocking of channel 1 used as reference for the studies.

#### 4.6.9.2 Kinetic and affinity studies

The four purified antibody fractions were diluted in running buffer up to four different final concentrations and flowed over the four immobilized ligands in an individual cycle of analysis based on the following steps: sample injection to estimate the association phase, washing with running buffer to evaluate the dissociation phase, and chip surface regeneration to remove all the analyte molecules bound to the ligand. Results were elaborated separately for each sample fitting the experimental values to the 1:1 binding model. This model, describing the interaction between a monovalent analyte molecule and a monovalent immobilized ligand, was validated by three

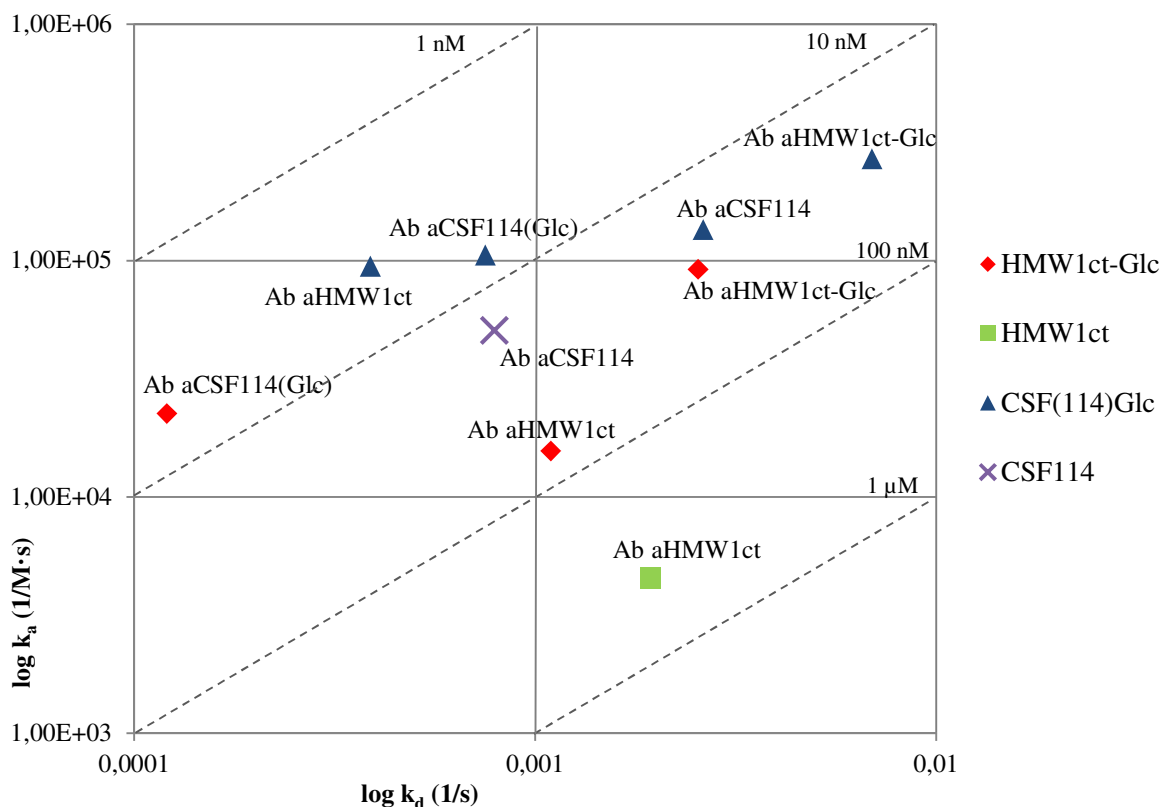


statistical parameters: the residual values between the experimental points and the theoretical ones that were closely distributed around zero, the minimal chi-square value, and the standard errors that were less than 10% of the referred parameter value. The kinetic parameters of the association rate  $k_a$  and dissociation rate  $k_d$  and the affinity constants  $K_D$  ( $k_d/k_a$ ), describing each characterized interaction, were calculate and reported in Table 20.

		<b>HMW1ct-Glc</b>	<b>HMW1ct</b>	<b>CSF114(Glc)</b>	<b>CSF114</b>
<b>Anti-HMW1ct-Glc Abs</b>	$k_a$ (1/Ms)	$(91.8 \pm 0.5) \times 10^3$	no interaction	$(27.0 \pm 0.6) \times 10^4$	no interaction
	$k_d$ (1/s)	$(25.5 \pm 0.1) \times 10^{-4}$		$(69.2 \pm 0.9) \times 10^{-4}$	
	$K_D$ (M)	$2.8 \times 10^{-8}$		$2.6 \times 10^{-8}$	
<b>Anti-HMW1ct Abs</b>	$k_a$ (1/Ms)	$(15.6 \pm 0.2) \times 10^3$	$(45.6 \pm 0.7) \times 10^3$	$(94.8 \pm 3.5) \times 10^3$	no interaction
	$k_d$ (1/s)	$(10.9 \pm 0.1) \times 10^{-4}$	$(19.4 \pm 0.1) \times 10^{-4}$	$(38.8 \pm 2.3) \times 10^{-5}$	
	$K_D$ (M)	$7.0 \times 10^{-8}$	$4.2 \times 10^{-7}$	$4.1 \times 10^{-9}$	
<b>Anti-CSF114(Glc) Abs</b>	$k_a$ (1/Ms)	$(22.5 \pm 0.1) \times 10^3$	no interaction	$(10.6 \pm 0.3) \times 10^4$	no interaction
	$k_d$ (1/s)	$(120.5 \pm 0.9) \times 10^{-6}$		$(75.1 \pm 0.8) \times 10^{-5}$	
	$K_D$ (M)	$5.3 \times 10^{-9}$		$7.1 \times 10^{-9}$	
<b>Anti-CSF114 Abs</b>	$k_a$ (1/Ms)	no interaction	no interaction	$(135.6 \pm 0.6) \times 10^3$	$(50.7 \pm 0.2) \times 10^3$
	$k_d$ (1/s)			$(26.2 \pm 0.2) \times 10^{-4}$	$(79.0 \pm 0.4) \times 10^{-5}$
	$K_D$ (M)			$1.9 \times 10^{-8}$	$1.6 \times 10^{-8}$

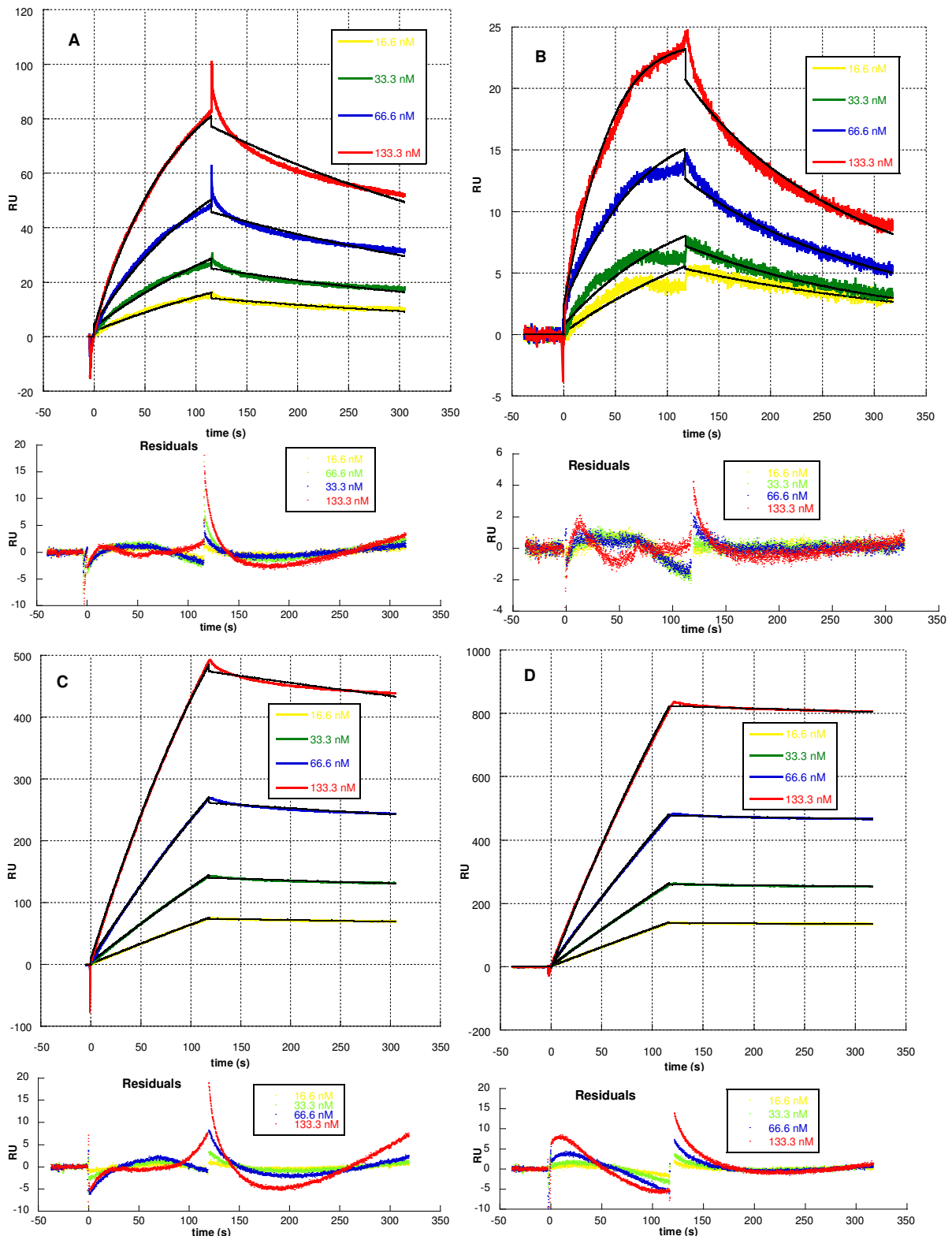
**Table 20:** Affinity constants  $K_D$  and kinetic parameters  $k_a$  and  $k_d$ , calculated according to the 1:1 binding model for each studied interaction.

The kinetic and affinity results were summarized using the Biacore T100 Kinetic Summary application and the  $k_a/k_d$  plot was obtained. This graph showed the association rate parameter ( $k_a$ ) against the dissociation rate parameter ( $k_d$ ), both on logarithmic scale, affinity constants  $K_D$  (calculated as  $k_d/k_a$  ratio) were displayed on diagonal lines. Thus, interactions having the same affinity but different kinetic properties were indicated by points lying in different positions on the same diagonal line. The  $k_a/k_d$  plot summarizing every characterized interactions is shown in Figure 45.

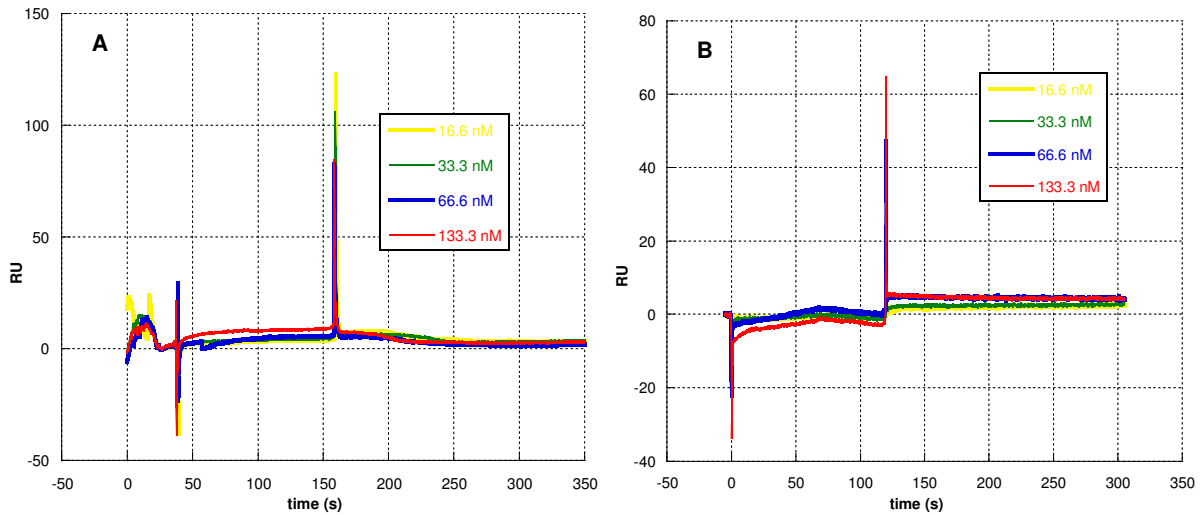


**Figure 45:**  $k_a/k_d$  plot for the 1:1 binding model summarizing interactions between 4 purified antibody fractions and 4 immobilized ligands indicated by different colors in the plot.

The results confirmed the total cross-reactivity of anti-CSF114(Glc) Abs and anti-HMW1ct-Glc Abs: both fractions interacted with CSF114(Glc) and HMW1ct-Glc but they did not bind to the corresponding non glucosylated antigen. The interactions between anti-HMW1ct-Glc Abs and HMW1ct-Glc or CSF114(Glc) (shown in Figure 46 A and B), were characterized by a faster dissociation rate and consequently lower affinity ( $K_D = 2 \times 10^{-8}$  M), as compared to anti-CSF114(Glc) Abs that bound to the same two antigens, as shown in Figure 46 C and Figure 46 D, with higher affinity ( $7 \times 10^{-9}$  M  $> K_D > 5 \times 10^{-9}$  M) because of the slower dissociation rate. The sensorgrams resulting from the kinetic study between anti-HMW1ct-Glc Abs and the non glucosylated HMW1ct and between anti-CSF114(Glc) Abs and CSF114 are showed in Figure 47 A and Figure 47 B, as representative examples of lack of interaction that did not allow calculation of affinity and kinetic parameters.

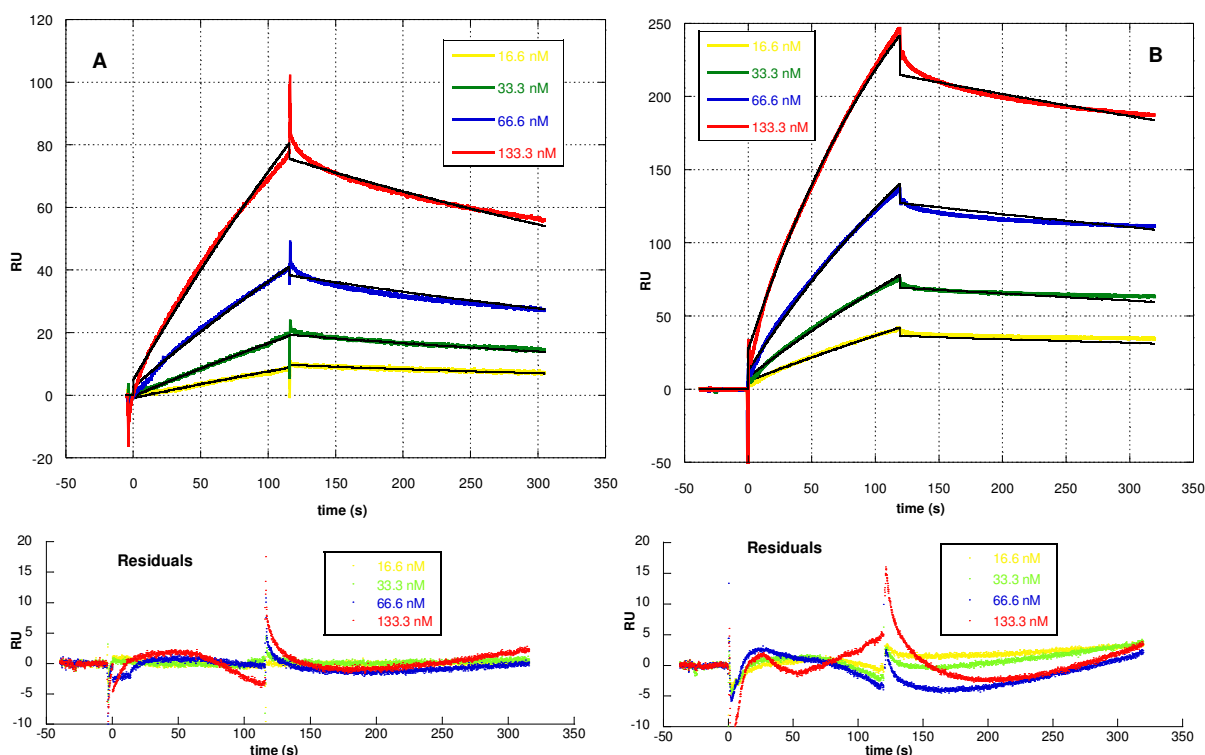


**Figure 46:** Sensorgrams showing the progress of the interaction between: anti-HMW1ct-Glc Abs and HMW1ct-Glc (A) and with CSF114(Glc) (B); anti-CSF114(Glc) Abs with CSF114(Glc) (C); and with HMW1ct-Glc (D). Experimental curves are shown in different colors according to the injected concentrations, black curves indicates the fitted 1:1 binding model. Residuals are shown below each characterized interaction.



**Figure 47:** Sensorgrams showing the lack of binding between anti-CSF114(Glc) Abs and CSF114 (A), and anti-HMW1ct-Glc Abs and HMW1ct (B)

Concerning fractions eluted from the non glucosylated molecules, we observed that anti-CSF114 Abs exhibited the same affinity for CSF114(Glc) and CSF114 ( $K_D = 1 \times 10^{-8}$  M) and that they did not bind to the adhesin proteins. Anti-HMW1ct Abs resulted to be the most heterogeneous fraction, characterized by the presence of antibodies with a different specificity of binding and consequently recognizing all the immobilized ligands, except for CSF114, with a wide difference in affinity ( $10^{-7}$  M  $>$   $K_D$   $>$   $10^{-9}$  M). The kinetics of the interaction of anti-HMW1ct Abs with HMW1ct and of anti-CSF114 Abs with CSF114 are reported in Figure 48 A and B.



**Figure 48:** Sensorgrams showing the interaction between anti-HMW1ct Abs and HMW1ct (A) and between anti-CSF114 Abs and CSF114 (B). Experimental curves are colored according to the injected concentrations, black curves indicates the fitted 1:1 binding model. Residuals are shown below each characterized interaction.

#### 4.6.9.3 Binding studies with sera

18 MS sera and 20 NBD sera, previously tested in SP-ELISA coating HMW1ct-Glc, HMW1ct and CSF114(Glc), were used to perform binding studies on the same three antigens covalently immobilized onto Biacore sensor chips. Each serum was tested at 1:50 and 1:100 dilution in a different cycle of analysis consisting in sample injection, running buffer flow to monitor the dissociation and chip regeneration by washing the surface with two buffers at different pH. The maximum binding level registered at the end of the injection for the 1:100 dilution was determined for each sample with each ligand and is listed in Table 21 for MS sera and in Table 22 for NBD ones.

CHAPTER 4

	BIACORE			SP-ELISA					
	Binding (RU)			IgG			IgM		
	HMW1ct-Glc	HMWct1	CSF114 (Glc)	HMW1ct-Glc	HMWct1	CSF114 (Glc)	HMW1ct-Glc	HMWct1	CSF114 (Glc)
<b>MS1</b>	76.3	12.8	71.2	1.70	0.30	1.50	0.62	0.50	0.43
<b>MS2</b>	52.9	37.1	90.5	1.76	1.43	1.19	0.63	0.67	0.23
<b>MS3</b>	73.1	14.9	117.9	1.48	0.68	1.19	1.58	1.00	0.97
<b>MS4</b>	22.8	3.5	69.0	1.74	0.78	1.06	0.31	0.29	0.11
<b>MS5</b>	47.6	10.2	68.6	1.46	0.90	1.11	0.79	0.60	0.63
<b>MS6</b>	0.0	0.0	42.8	0.89	0.87	0.14	1.80	1.36	1.74
<b>MS7</b>	32.4	23.4	76.0	0.66	0.79	0.21	1.01	0.76	0.67
<b>MS8</b>	20.0	15.6	63.1	0.50	0.50	0.21	0.89	0.93	0.41
<b>MS9</b>	48.6	37.2	101.5	0.54	0.53	0.06	0.52	0.60	0.20
<b>MS10</b>	45.4	31.2	94.4	1.32	0.63	0.83	0.83	0.38	0.26
<b>MS11</b>	47.2	20.3	71.1	2.04	0.53	0.35	1.26	0.74	0.47
<b>MS12</b>	39.7	2.9	64.2	1.56	0.32	0.50	1.40	0.74	0.86
<b>MS13</b>	34.9	20.7	80.9	1.18	0.60	0.59	1.04	0.69	0.45
<b>MS14</b>	37.6	23.3	57.0	1.31	0.94	0.50	0.83	0.73	0.50
<b>MS15</b>	26.5	15.0	54.3	1.26	1.16	0.48	0.29	0.30	0.20
<b>MS16</b>	28.6	9.3	61.6	1.16	0.50	0.44	1.00	0.62	0.96
<b>MS17</b>	30.8	15.3	60.3	1.49	0.89	0.59	0.83	0.71	0.41
<b>MS18</b>	28.8	8.5	62.3	1.58	0.56	0.46	1.00	0.53	0.73

**Table 21:** Comparison between binding levels of MS sera registered with SPR studies and IgG or IgM titer obtained in SP-ELISA.

	BIACORE			SP-ELISA					
	Binding (RU)			IgG			IgM		
	HMW1ct-Glc	HMWct1	CSF114 (Glc)	HMW1ct-Glc	HMWct1	CSF114 (Glc)	HMW1ct-Glc	HMWct1	CSF114 (Glc)
<b>NBD1</b>	8.4	0.4	62.3	0.45	0.45	0.32	0.39	0.39	0.29
<b>NBD2</b>	16.6	5.7	114.9	0.5	0.26	0.13	0.83	0.43	0.18
<b>NBD3</b>	13.7	5.5	109.8	0.66	0.53	0.04	0.29	0.25	0.08
<b>NBD4</b>	0.7	0.0	36.9	0.29	0.98	0.18	0.37	0.33	0.28
<b>NBD5</b>	14.0	7.9	48.3	1.62	1.43	0.91	0.86	0.41	0.89
<b>NBD6</b>	41.6	25.5	54.0	1.82	0.72	0.57	1.49	1.43	0.73
<b>NBD7</b>	38.3	18.9	64.8	0.62	0.72	0.62	0.28	0.34	0.41
<b>NBD8</b>	16.3	0.0	45.3	0.5	0.34	0.09	0.36	0.29	0.24
<b>NBD9</b>	21.5	10.1	51.7	0.32	0.47	0.12	0.65	0.28	0.44
<b>NBD10</b>	14.9	5.6	53.8	0.22	0.23	0.02	0.19	0.19	0.09
<b>NBD11</b>	40.9	12.3	47.6	0.92	0.49	0.28	0.72	0.65	0.91
<b>NBD12</b>	14.0	1.6	45.2	0.8	0.54	0.31	0.24	0.25	0.36
<b>NBD13</b>	17.0	8.8	35.4	0.75	0.93	0.14	0.87	0.51	0.44
<b>NBD14</b>	29.9	16.2	59.5	1.03	0.85	0.35	0.45	0.34	0.14
<b>NBD15</b>	35.3	11.4	50.8	1.16	0.62	0.2	0.48	0.49	0.16
<b>NBD16</b>	21.0	3.0	44.2	1.31	0.85	0.08	1.69	1.44	0.22
<b>NBD17</b>	29.9	9.5	53.8	0.56	0.62	0.14	0.49	0.4	0.28
<b>NBD18</b>	24.0	6.6	56.9	0.94	0.55	0.2	1.1	0.92	0.33
<b>NBD19</b>	3.6	0.0	37.7	0.39	0.21	0.05	0.34	0.36	0.13
<b>NBD20</b>	28.7	8.0	51.2	0.75	0.55	0.08	0.28	0.23	0.04

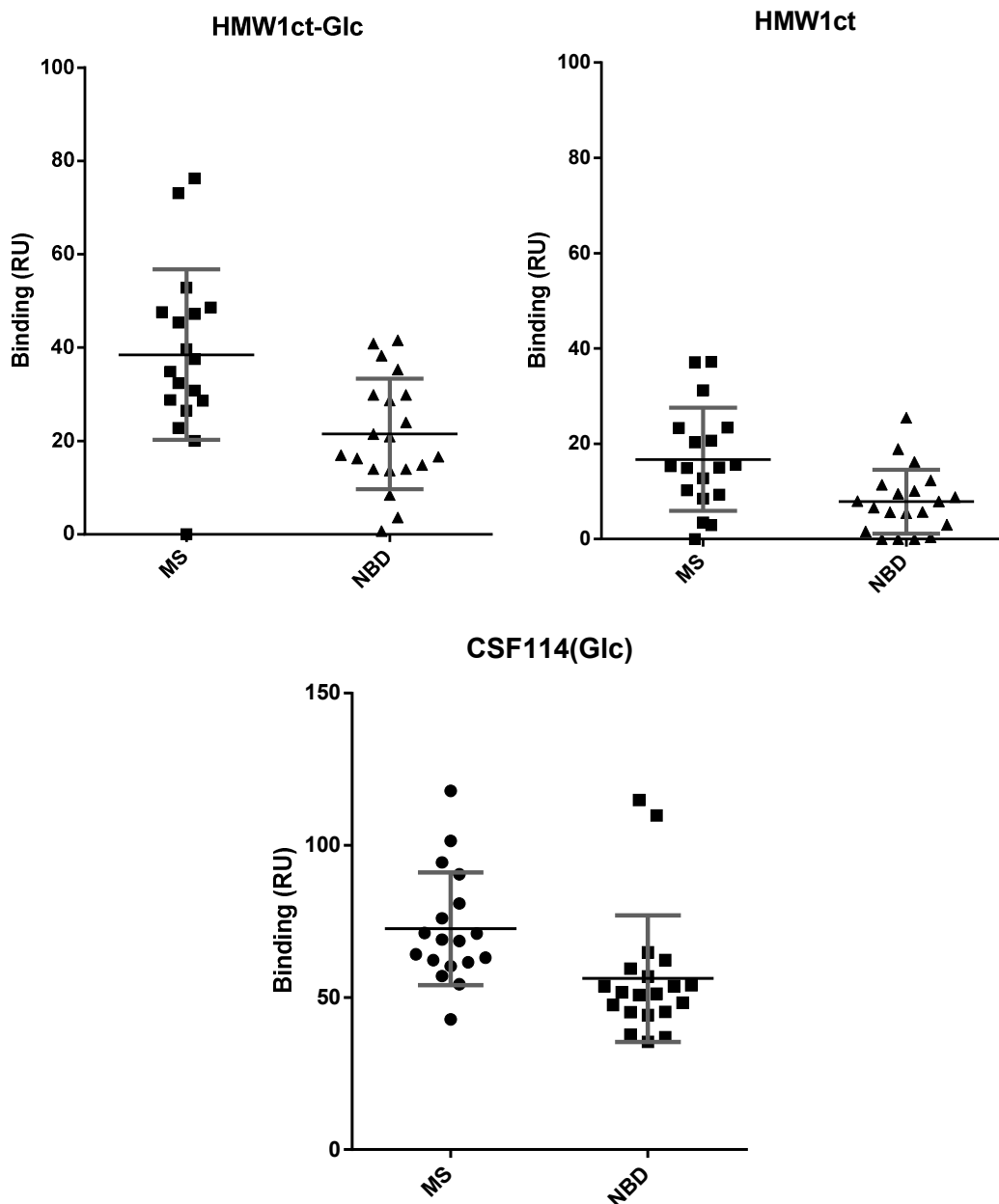
**Table 22:** Comparison between binding levels of NBD sera registered with SPR studies and IgG or IgM titer obtained in SP-ELISA.

In Table 23 we reported the mean and the relative Standard Deviation (SD) of the binding values registered with the two groups of sera on the three immobilized antigens with the present SPR assay.

Binding level (RU)				
Immobilized antigen	MS		NBD	
	Mean	SD	Mean	SD
<b>HMW1ct-Glc</b>	38.5	18.2	21.5	11.8
<b>HMW1ct</b>	16.7	10.8	7.8	6.7
<b>CSF114(Glc)</b>	72.6	18.5	56.2	20.8

**Table 23:** Mean binding levels and SD registered with the biosensor assay.

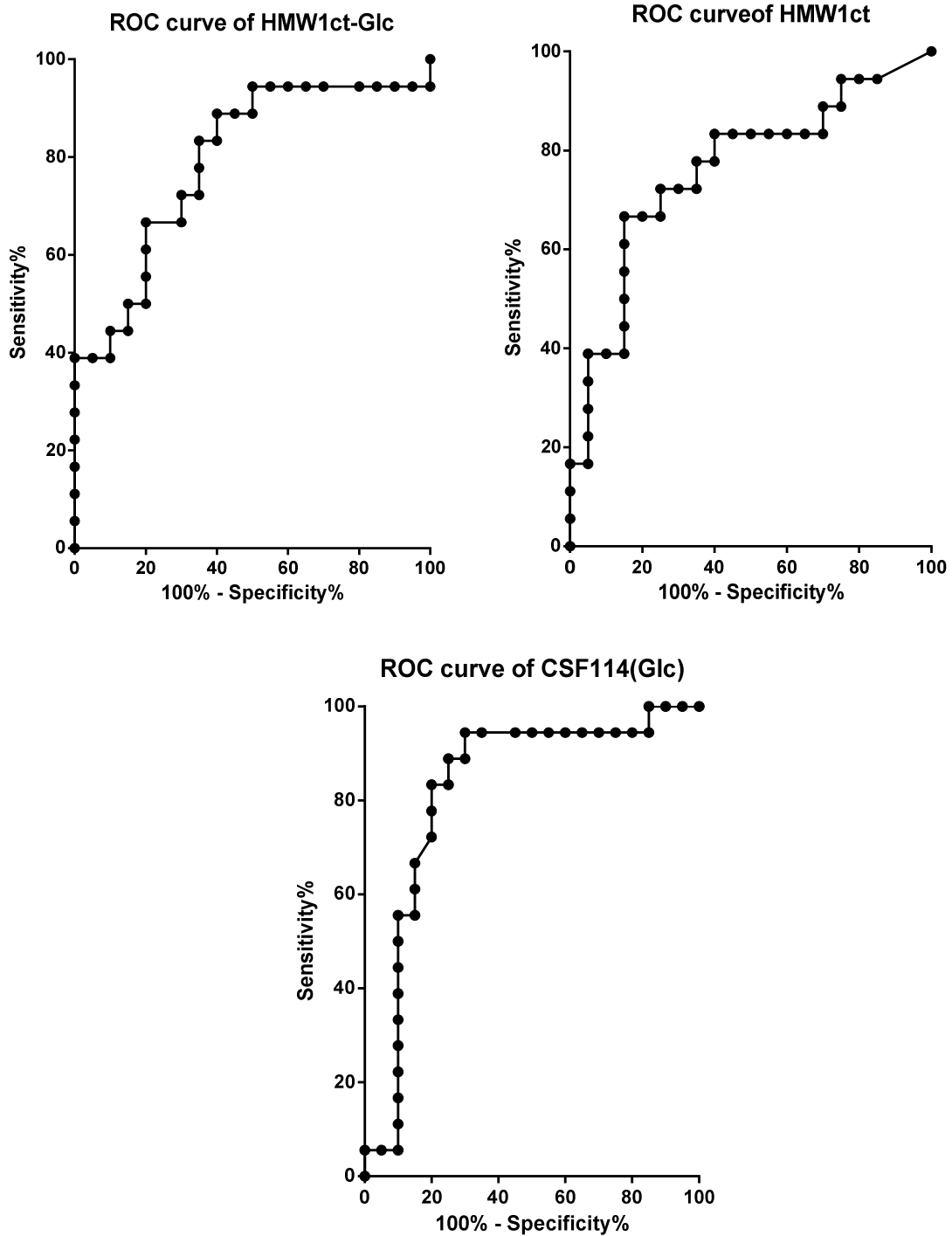
A significant difference of binding signals between the two groups was registered on each immobilized molecule, observing the higher values in MS sera (Figure 49).



**Figure 49:** Column scatters for the distribution of the binding levels registered on immobilized HMW1ct-Glc, HMW1ct and CSF114(Glc) with MS and NBD sera; mean values and Standard Deviation are shown for each group. Because a difference between the two groups of sera was detected with CSF114(Glc) and with both immobilized proteins, a receiver operating characteristic (ROC)-based analysis was employed comparing different combinations of cut-off values, specificities and sensitivities.



Three ROC curves for anti-HMW1ct-Glc, anti-HMW1ct and anti-CSF114(Glc) activities were constructed based on 18 cases of MS versus 20 controls (Figure 49).



**Figure 50:** ROC curves analysis of antibodies interacting with HMW1ct-Glc, HMW1ct and CSF114(Glc) in MS versus NBD sera.

## CHAPTER 4

A discriminative power for the anti-HMW1ct-Glc antibodies was found with an area under the curve of 0.79 and a p-value of 0.002; the optimal diagnostic cut-off for the method was 41.2 RU with a sensitivity of 38.9% and a specificity of 95.0%. According to this cut-off value, an increased antibody level was detected in 7/18 MS sera (38.9%) and in 1/20 NBD sera (5%).

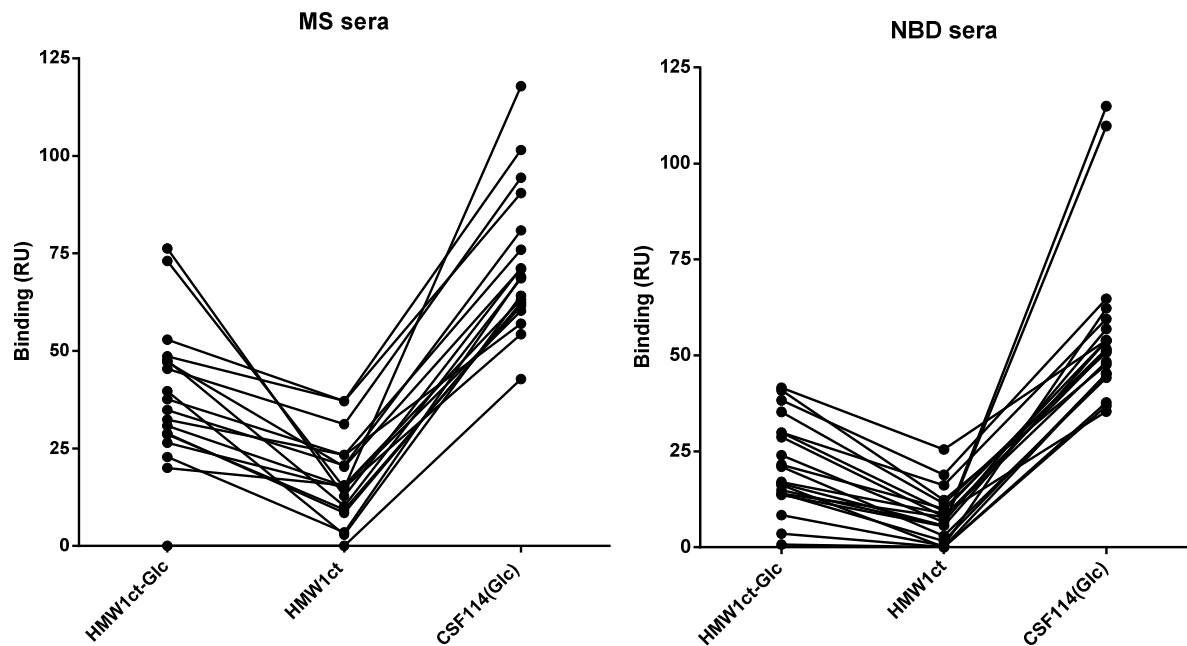
In the case of the non-glycosylated protein, a discriminative power was also found: the area under the curve was 0.76 and the p-value 0.006, the diagnostic cut-off for this method was 22.0 RU with a sensitivity of 27.8% and a specificity of 95.0%. Consequently an increased antibody level was registered in 5/18 MS sera (27.8%) and in 1/20 NBD sera (5%).

Analyzing the data obtained with immobilized CSF114(Glc), we obtained a discriminative power indicated by an area under the curve of 0.82 and a p-value of 0.0007; the diagnostic cut-off for the method was set at 71.1 RU with a sensitivity of 38.9% and a specificity of 90%. We registered an increased antibody level in 7/18 MS sera (38.9%) and in 2/20 NBD sera (10.0%).

The results of the present binding study confirmed the ability of SPR biosensor to specifically detect autoantibodies in MS patients' sera as compared to health subjects, when CSF114(Glc) was covalently immobilized on the chip surface<sup>46</sup>.

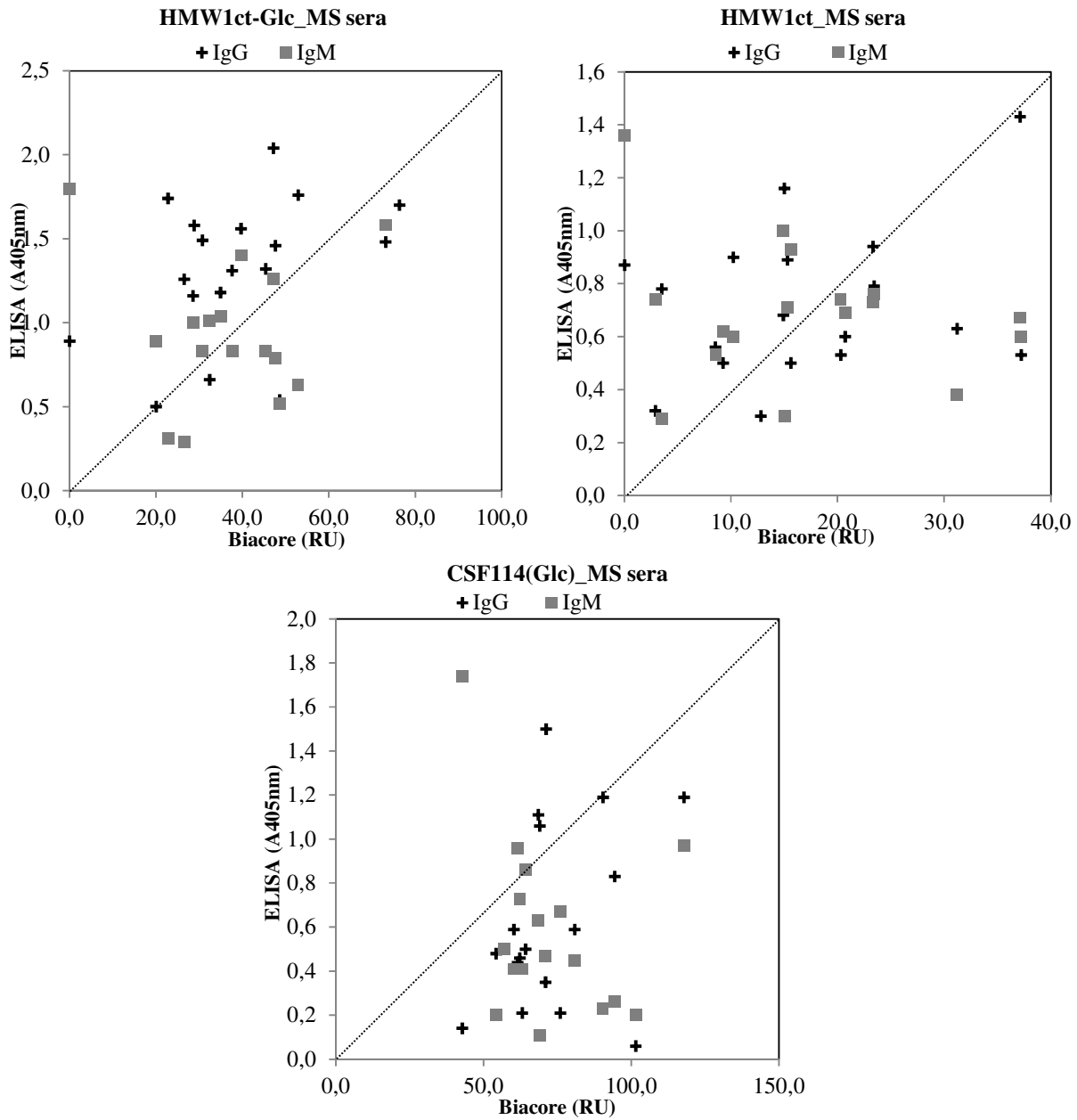
Another interesting aspect was that, from this preliminary screening assay, both adhesin proteins resulted to be able to detect antibodies in MS patients' sera compared to NBD ones with a specificity of 95.0% but with a higher sensitivity in the case of glycosylated HMW1ct.

From the graph shown in Figure 51 we could see that the same trend of binding values was conserved among the different injected sera on the three immobilized antigens and, in particular, they were generally higher on the glycosylated protein than on the non glycosylated one and the highest binding values were registered on CSF114(Glc) both in NBD and in MS groups. The wide difference in binding values among MS sera was registered with MS 1 and MS 3 which showed the highest signal on HMW1ct-Glc and a low signal on HMW1ct indicating that the two sera contained a high concentration of antibodies recognizing the glycosyl moieties of HMW1ct-Glc. Concerning the NBD group, a significant difference in binding level was obtained with NBD 2 and NBD 3 sera displaying the highest interaction signal on CSF114(Glc), but resulting below the cut-off value on both immobilized adhesin proteins.



**Figure 51:** Comparison between binding signals obtained with each MS serum or each NBD serum on the different immobilized ligands

IgG and IgM levels detected in SP-ELISA coating the same three antigens and applying the 18 MS sera and the 20 NBD used in the present SPR assay, were compared with SPR binding data. As indicated by the correlation graphs for MS sera shown in Figure 52, the two methods exhibited different overall results.



**Figure 52:** Biacore-ELISA correlation of the reactivity of HMW1ct-Glc, HMW1ct and CSF114(Glc) for MS patients' sera. IgM and IgG observed in ELISA are indicated by different symbols and plotted against the total antibody fraction detected in Biacore assay.

Comparing data obtained with both methods when CSF114(Glc) was used as probe, 5 positive cases in ELISA (IgM and/or IgG) were recognized as border line samples by the biosensor, 1 positive case in ELISA was negative by the SPR assay; 3 positive cases according to the biosensor were not recognized as positive in ELISA and 1 positive case by biosensor resulted border line in ELISA.

Considering data obtained with both methods when HMW1ct-Glc was used as probe, 2 positive cases in ELISA were also recognized as positive with the biosensor analysis, 1 positive case in ELISA was negative and the other positive case in ELISA resulted to be border line with the present SPR assay.

When HMW1ct was used as probes in SP-ELISA very similar absorbance values were registered applying NBD sera or patients' sera in the case of IgG and IgM, and when HMW1ct-Glc was coated no discriminative power was found for IgG antibodies, so a diagnostic cut-off was not established for SP-ELISA in these three cases and a precise correlation between positive or negative cases according to both methods could not be done.

Nevertheless, we noticed that the best correlation between antibody levels detected with the two assays was registered with the IgM fraction interacting with the protein HMW1ct-Glc.

Considering the results of the biosensor assay a general increase in antibody level was revealed in MS sera compared to NBD sera with the two proteins and the difference in antibody levels between the two groups was higher in the case of immobilized HMW1ct-Glc, confirming the importance of glucosyl moieties for MS antibodies detection.

We could conclude that when the same antigens were non covalently adsorbed on ELISA plates or covalently immobilized on biosensor chip surface, different families of antibodies were detected, probably because of the different immobilization strategy that resulted in a different final orientation of the antigens on the solid supports. In addition low affinity antibodies were usually removed during the washing steps of the ELISA assay, but they could be revealed when continuously flowing over the antigen in the SPR assay. Furthermore the SPR study had the advantage of monitoring in real time the interaction, of using a few microliters of biological material and of limiting the variability of the assay because the same sample solution contemporary flows over the three immobilized ligands thanks to the complex system of valves that control the instrument flow. In our SP-ELISA information was provided by the use of a specific anti-IgM or anti-IgG secondary antibody, this was not the case of the SPR assay in which antibody binding was directly registered thanks to the change in mass over the surface, without the need of adding a secondary antibody.

#### **4.6.10 Immunohistochemistry assay**

In collaboration with Dr. S. Matà of the Department of Neurology, Azienda Ospedaliera Universitaria Careggi, Florence, we performed some immunohistochemistry assays on normal rat

## CHAPTER 4

fixed tissues to understand if antibodies present in one whole serum (patient MS 1) or antibodies purified with the sequential affinity chromatography process, from the same MS serum, and recognizing glucosylated epitopes in our *in vitro* assays, could also bind *in situ* to some structures expressed in nervous tissues.

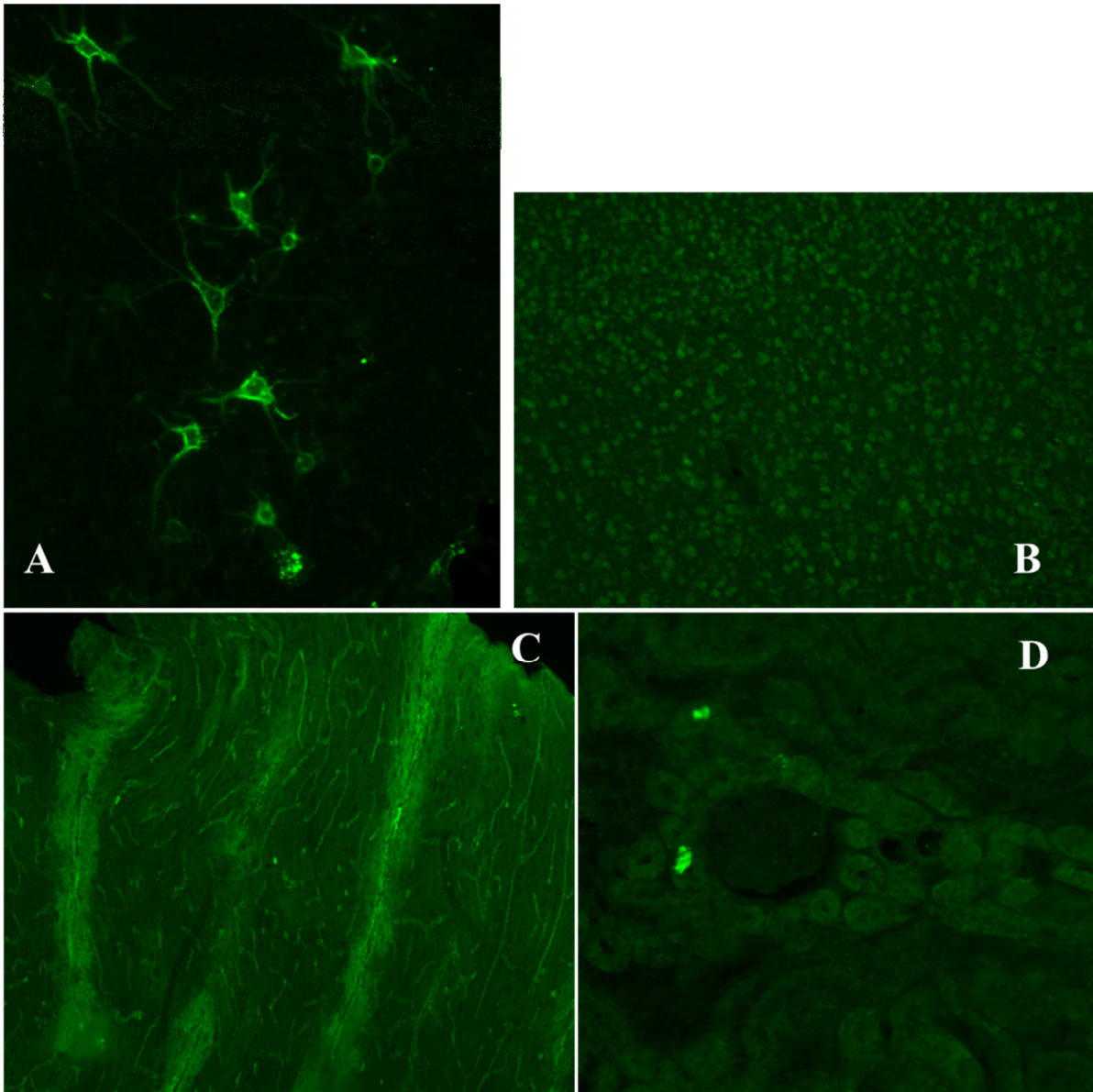
Tissues were obtained from one healthy rat that was euthanized by an injection of an overdose of anesthetic and transcardially perfused with fixative solution. Brain, kidney, stomach, spinal cord and cerebellum were surgically removed, fixed overnight and finally stored at -80°C. Thirty micron coronal sections from every tissues were then cut using a cryostat and collected in the anti-freeze solution until use.

### 4.6.10.1 Validation of tissues

To understand if we succeeded in the fixation process and if tissues could be used for the following immunohistochemistry assay with MS 1 serum and purified antibodies, we decided to validate them by applying some positive controls. We chose four previously tested sera containing antibodies with different known specificity and recognizing the following antigens on rat tissues: the trisaccharide Human Natural Killer-1 (HNK-1), that is associated to different glycoproteins or glycolipids in the nervous system, the aquaporin 4 (AQ4), an integral membrane protein expressed on cell membrane, the Glutamic Acid Decarboxylase (GAD) which is present at nerve terminals and synapses, and cell nuclei.

Immunohistochemistry was performed on free-floating tissue sections, the positive control sera were diluted in PBS buffer 1:200 and incubated with tissues. After washing, a Fluorescein Isothiocyanate (FITC) conjugated secondary antibody was added and primary antibodies bound to the tissues were detected with a fluorescence microscope.

As shown in Figure 53 a specific green fluorescence signal was detected with each serum in the different tissues, confirming that rat fixed tissues could be used for the next experiments.



**Figure 53:** Fluorescence signal generated after the incubation of positive control samples on different rat tissues: A) anti HNK1 antibody detected in the limbic cortex of brain section, B) anti nucleus antibody in the brain cortex, C) anti AQ4 antibodies around the medium vessels of the cortex, D) anti GAD antibodies in the glomerulus of the kidney.

Negative controls were also performed with each tissue by omitting the primary antibody; as expected, no fluorescence signal was registered.

#### 4.6.10.2 Immunohistochemistry with MS 1 serum

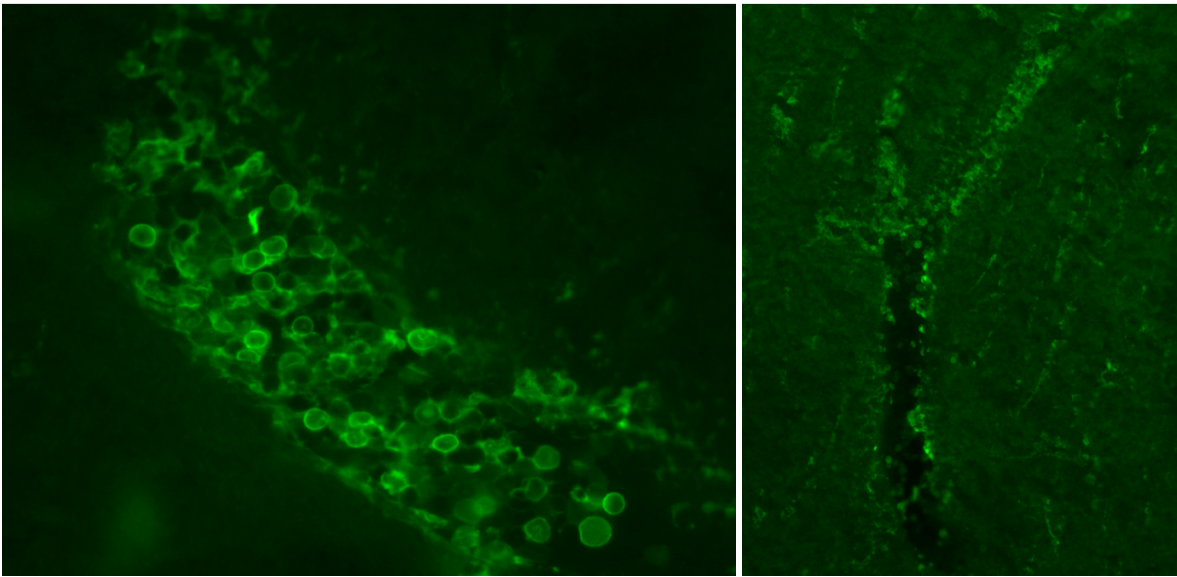
MS 1 serum was diluted in PBS 1:50 and 1:200 and incubated with free floating rat tissues.

After washing, double immunofluorescence was performed by applying the appropriate FITC-conjugated secondary antibody to detect bound primary antibodies and then the 4',6-diamidino-2-

## CHAPTER 4

phenylindole (DAPI) reagent was added to specifically stain cells' nuclei. Immunostaining for MS 1 serum at the higher dilution gave no detectable signals in nervous sections nor in the other tested tissues, but some fluorescence signals were registered in the brain vessels zone, when serum was incubated at the lower dilution. In each section the DAPI reagent enabled the visualization of cells' nuclei.

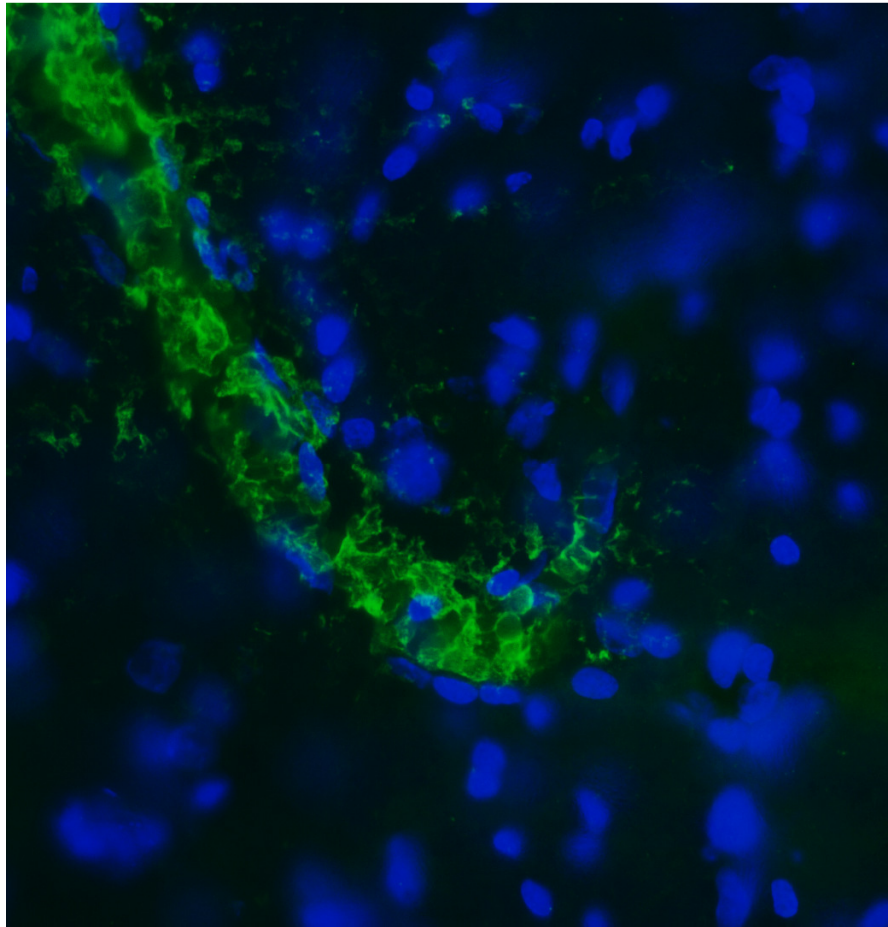
In Figure 54 we reported FITC dependent signal obtained because of the interaction between antibodies present in MS 1 serum and medium or small vessels in brain sections.



**Figure 54:** FITC fluorescence signal registered on vessels incubating rat brain sections with MS 1 serum at 1:50 dilution.

Antibodies could theoretically bind to structures localized on epithelial cells around the vessels or to some other targets inside the vessels; to deeply understand this point we overlapped the fluorescence signal generated by FITC with the one produced by DAPI obtaining the image shown in Figure 55.





**Figure 55:** FITC (green) and DAPI (blue) fluorescence signals overlapped. No correlation seemed to be present.

No co-localization was found between the two signals indicating that antibodies probably bound to anucleate cells inside blood vessels (e.g. erythrocytes or platelets). This result is surprising, since these cells should have been fully removed by the initial perfusion process, so this hypothesis has to be confirmed with further studies and with the application of specific markers to stain the different kinds of blood cells.

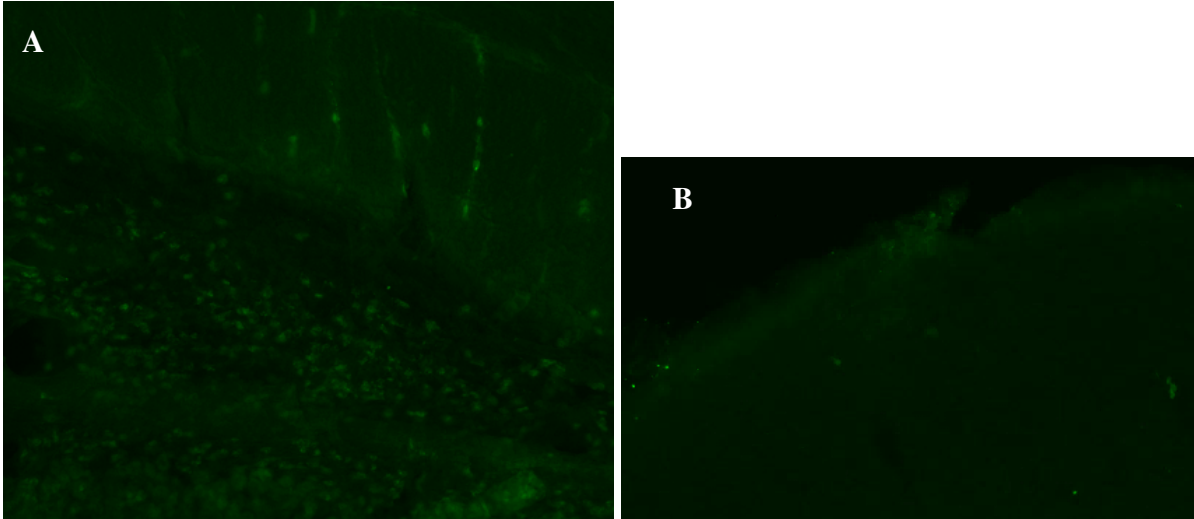
#### **4.6.10.3 Immunohistochemistry with purified antibody fractions**

We performed the immunohistochemistry assay with the 4 purified antibody fractions obtained through the sequential affinity chromatography process: anti-HMW1ct Abs, anti-HMW1ct-Glc, anti-CSF114 Abs and anti-CSF114(Glc) Abs. Each sample was incubated with rat fixed sections at a concentration of 10  $\mu\text{g}/\text{mL}$ . The FITC-conjugated secondary antibody was added and fluorescence was read at the appropriate wavelength.

Analyzing the fluorescence signal registered with the four antibody samples on the different fixed rat tissues, we could summarize that anti-HMW1ct-Glc Abs not specifically interacted with

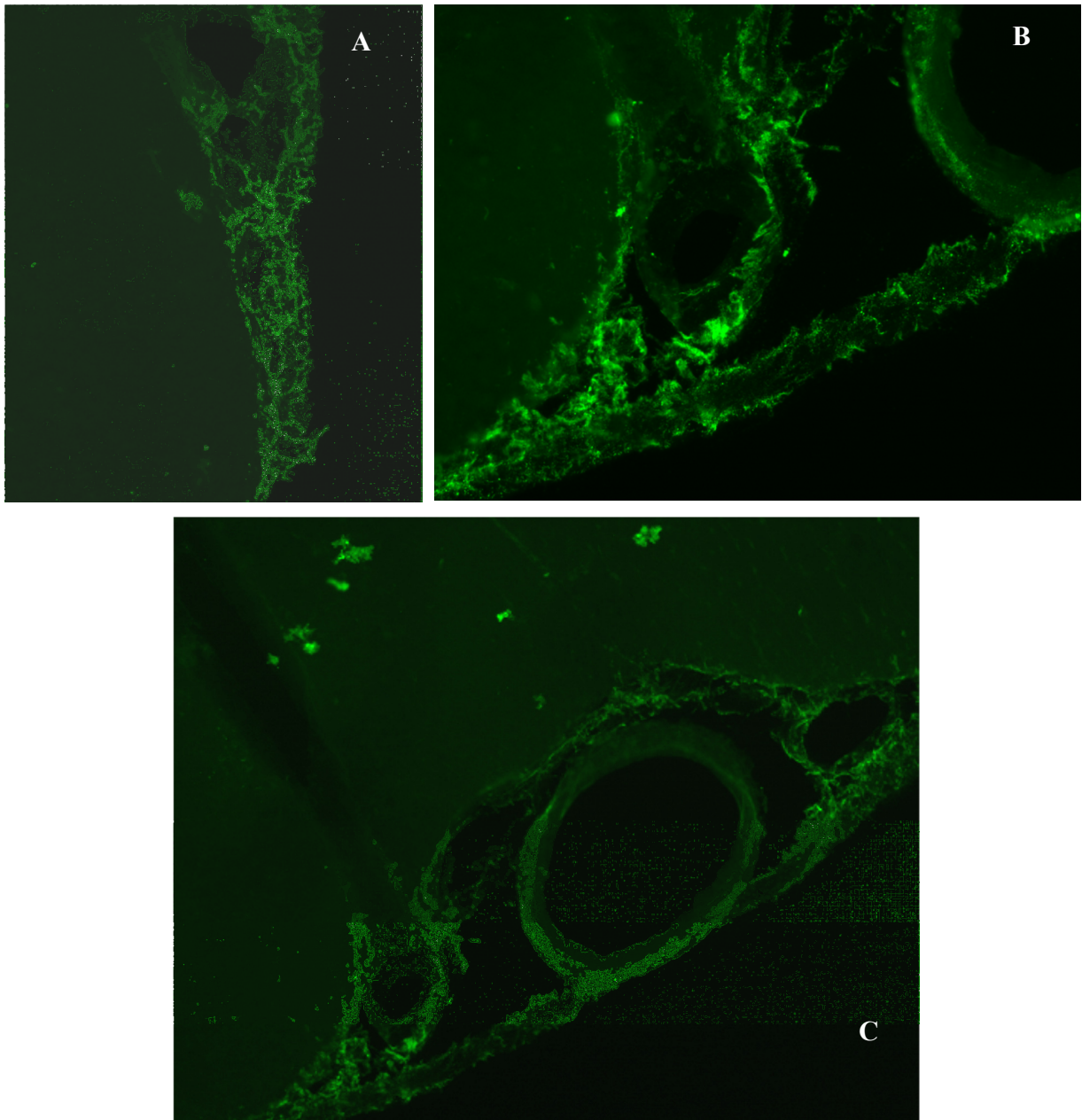
## CHAPTER 4

stomach sections (Figure 56 A) but they didn't bind to nervous tissues as shown in Figure 56 B. Applying anti-CSF114 Abs and anti-CSF114(Glc) Abs no fluorescence signal was registered on any tissues.



**Figure 56:** Results of the immunohistochemistry assay performed with anti-HMW1ct-Glc Abs purified from MS 1 patient. A) unspecific signal on stomach section; B) lack of signal on brain section.

From the immunohistochemistry assay performed with anti-HMW1ct Abs we observed a specific interaction signal on brain and spinal cord sections (Figure 57). This signal was localized along the pia mater, a thin highly vascular membrane composed of fibrous connective tissue that closely envelops the brain and spinal cord, hosting a large number of blood vessels, which pass through the pia mater to go inside the brain or the spinal cord.



**Figure 57:** FITC fluorescence signal registered incubating anti-HMW1ct Abs with spinal cord (A) and brain (B,C) sections.

As expected, anti-CSF114 Abs did not recognize any structure on tested tissues, but no interaction signal on nervous sections (brain, cerebellum and spinal cord) was detected applying anti-HMW1ct-Glc and anti-CSF114(Glc) Abs that, through in vitro studies, we demonstrated to be highly specific for N-glycosylated epitopes. To understand if this lack of reactivity was due to low sample concentration, the assay was repeated by incubating samples at their initial concentration without dilution, but the same results were obtained. We were sure that

## CHAPTER 4

glucosylated epitopes were preserved on fixed tissues because in the validation step a specific fluorescence signal was obtained with the serum containing antibodies recognizing the HNK1 epitope, whose antigenic portion was known to be its terminal sulfated trisaccharide. The most consistent explanation for this lack of signal could be that N-glycosylated proteins, or unglycosylated structures mimicked by the N-glycosylated molecules used to characterize the antibodies, were not present in the nervous tissues from the selected normal healthy rat. To clarify this point we decided to repeat the study on tissues from Experimental Autoimmune Encephalomyelitis (EAE) mice, animal model of the disease. This part of the work is going to be performed by the Immunology Department of the Weizmann Institute of Science in Israel.

The interaction registered between anti-HMW1ct Abs and the pia mater membrane of the brain and of the spinal cord, could indicate that structures mimetic of the bacterial protein were present on the pia mater membrane. A certain level of antibodies recognizing the non glucosylated bacterial protein were detected in MS sera with the SP-ELISA assay and with the SPR binding study and, in line with results obtained from competitive ELISA, this immunohistochemistry assay confirmed that they did not recognize the same epitope as anti-HMW1ct-Glc Abs. We believed that anti-HMW1ct Abs are not related to MS disease and to confirm this point, the same immunohistochemistry assay is going to be repeat by the Immunology Department of the Weizmann Institute of Science, incubating tissues with the total antibody fraction purified from one normal blood donor by protein G chromatography. If the same interaction with the pia membrane is detected, it will be definitively proved that anti-HMW1ct antibodies are physiologically present in serum of each person having been in contact with *H. influenzae*, and that they are not involved in the autoimmune response typical of the disease. On the other hand we can speculate that only if adhesin mimetic structures, which could be present somewhere on nervous tissue (e.g. on the pia membrane), are aberrantly N-glycosylated, they can be recognized by specific anti-HMW1ct-Glc antibodies (that we demonstrated to be exclusively of MS patients); those anti-HMW1ct-Glc antibodies could trigger the harmful autoimmune response typical of Multiple Sclerosis disease that lead to the destruction of myelin. It has already been shown that B cell activation in MS may be dependent on bacterial or viral antigens<sup>56</sup> and a pathogenic link between the antibody responses to bacterial carbohydrate products and those to myelin antigens has been documented<sup>57</sup>. This considerations could support the idea that, together with the molecular mimicry between pathogen structures and self-molecules, one or more aberrant N-glycosylations of endogenous proteins caused by a bacterial enzyme (such as

HMW1C glycosyltransferase of *H.influenzae*), could be the possible mechanisms responsible for the activation of the immune response involved in the development of MS disease.

#### 4.7 Conclusions

This study demonstrated, with different *in vitro* assays, the cross-reactivity between the autoantibodies detected in MS patients' sera with the use of the synthetic N-glycosylated peptide probe CSF114(Glc) and the N-glycosylated protein HMW1ct corresponding to the C-terminal portion of the adhesion protein HMW1 that is expressed on the outer membrane of the human pathogen *Haemophilus influenzae*.

More in detail the following considerations emerged from the experiments performed during the study:

- SP-ELISA assay's results indicated that unglucosylated HMW1ct was not able to detect specific antibodies in MS sera as compared to NBD ones, while glucosylated HMW1ct-Glc could discriminate between MS and NBD group only in the case of serum IgM. Another important aspect was that in the case of NBD a similar level of antibodies interacting with HMW1ct-Glc and with HMW1ct was registered, suggesting that those antibodies did not recognize glucosylated epitopes;
- Competitive ELISA assays showed that HMW1ct-Glc bearing eight N-linked glucose moieties were able to inhibit the binding of anti CSF114(Glc) antibodies in 5 representative MS sera. Similar results were obtained with all the HMW1ct mutants containing a lower number of glucose units and the minimal number of glycosylations required to inhibit MS antibodies binding with the same high affinity of the fully glucosylated HMW1ct (average  $IC_{50}=10^{-9}$  M) was four. On the other hand non-glycosylated proteins did not inhibit MS sera binding, confirming the importance of the presence of the glucosyl moiety on the proteins and on the peptide for the interaction with MS antibodies. In the case of NBD sera, antibody binding to HMW1ct-Glc was inhibited with similar affinity by both proteins, glucosylated and unglucosylated, thus confirming that these antibodies were physiologically present in the blood of people who probably were infected by the very common pathogen *H. influenzae* during their life and consequently developed antibodies able to recognize an epitope shared by the two proteins and not related to the presence of N-glycosylation moieties;

## CHAPTER 4

- The adhesin derived peptide pept(5,6)glc was selected to perform SPR-binding study, but because of its poor solubility in the immobilization buffer and of the too low electrostatic interaction with chip surface, peptide covalent immobilization failed. A longer version of that peptide with and without three glucosylation units were synthesized and the non glucosylated sequence was successfully immobilized on chip surface. The same immobilization strategy is going to be applied for the immobilization of the glucosylated peptide;
- Antibody purification from one MS serum by two sequential affinity chromatographies was successfully set up, enabling us to obtain an antibody fraction recognizing exclusively the glucosyl units of HMW1ct-Glc and of CSF114(Glc);
- SP-ELISA titration assay with purified antibody fractions confirmed the ability of the sequential affinity chromatography process to deplete serum from antibodies recognizing the non glucosylated epitopes and consequently to obtain two fractions containing antibodies highly specific for the glucosylated moieties of HMW1ct-Glc and CSF114(Glc), respectively;
- SPR kinetic and affinity studies demonstrated the cross-reactivity between anti-CSF114(Glc) and anti-HMW1ct-Glc antibody fractions: in particular anti-CSF114(Glc) antibodies interacted with both glucosylated molecules with one fold higher affinity ( $K_D=10^{-9}$  M) than anti-HMW1ct-Glc antibodies, which bound the same two molecules with lower affinity ( $K_D=10^{-8}$  M);
- SPR binding study on immobilized HMW1ct and HMW1ct-Glc indicated that both adhesin proteins were able to detect antibodies in MS patients' sera as compared to NBD ones with the same specificity but with a higher sensitivity in the case of HMW1ct-Glc. Binding values registered with the different sera did not correlate with absorbance levels obtained with the SP-ELISA assay, indicating that when the same antigens were non covalently adsorbed on ELISA plates or covalently immobilized on the biosensor chip, different families of antibodies were detected;
- The immunohistochemistry assay performed with the whole MS serum showed an interaction signal with anucleate cells inside the blood vessels of brain sections, but this result has to be confirmed by further experiments. In the case of purified antibodies, a fluorescence signal was obtained only with anti-HMW1ct antibodies, which appear to stain putative mimetic structures of the HMW1ct protein, present on the pia mater

membrane; a control experiment with antibodies purified from one normal blood donor serum will be performed to confirm the hypothesis that the registered interaction is not specific of MS disease. No interaction was revealed applying anti-HMW1ct-Glc antibodies probably because N-glycosylated proteins or non glycosylated structures mimicked by HMW1ct-Glc were absent in the nervous tissues of the selected normal rat. Further assays will be performed to deeply investigate this aspect.

The overall results suggested that the induction of the specific autoantibodies observed in MS patients' sera within this study could be ascribed either to a molecular mimicry process between bacterial N-glycosylated proteins and endogenous structures on nervous tissues or to an aberrant N-glycosylation of endogenous human proteins caused by a bacterial enzyme. The immunohistochemistry assays that are planned to be performed with purified anti-HMW1ct-Glc antibodies on nervous tissues from experimental autoimmune encephalomyelitis mice, will be fundamental to choose between these two hypothesis.

Taken together, these results contribute to understand if pathogen delivered innate immune signals could have important implications in triggering the pathogenic self-reactive response of Multiple Sclerosis. In this context it is important to consider that proteins from neurotropic pathogens could be possible candidate target antigens only if they derive from an intracellular pathogen that must enter the CNS and persist there without being associated with any life-threatening diseases and indeed the bacterium *Haemophilus influenzae* fulfills these requirements.

## **4.8 Materials and methods**

### **4.8.1 SP-ELISA**

Peptides were diluted in Coating Buffer (12 mM Na<sub>2</sub>CO<sub>3</sub>, 35 mM NaHCO<sub>3</sub>, 3 mM NaN<sub>3</sub>, pH 9.6) and proteins in PBS buffer pH 7.2 up to a final concentration of 10 µg/mL and 100 µL solution/well were dispensed on Nunc MaxiSorp 96 wells immunoplates. Incubation was at +4C overnight. Plates were washed 5 times with the automatic washer Hydroflex (Tecan) using the washing buffer (NaCl 0.9%, Tween 20 0,05%). Immediately after drying, the potential aspecific binding sites were blocked using 120 µL/well of FBS Buffer (10% Fetal Bovine Serum in Washing Buffer) for 1 hour at room temperature. FBS solution were manually removed and 100µL/well sera were dispensed in duplicate at 2 dilutions (1:100 and 1:1000 in FBS Buffer) and incubated overnight at +4C. Plates were automatically washed 5 times.100µL/well of secondary

## CHAPTER 4

antibody diluted in FBS Buffer were added: anti human IgG-Alkaline Phosphatase(Sigma) 1:8000 and anti-human IgM-Alkaline Phosphatase (Invitrogen) 1:1200; incubation was 3 hours at room temperature. Plates were automatically washed 5 times. 100 $\mu$ L/well of p-nitrophenilosphate [1mg/mL] in Substrate Buffer (1 M diethanolamine, 1 mM MgCl<sub>2</sub>, 3 mM NaN<sub>3</sub>, pH 9.8) were added. After about 30 minutes the colorimetric reaction was quenched by adding 50  $\mu$ L/well of 1 M NaOH and the absorbance was read at 405 nm with a multichannel ELISA reader (Tecan Sunrise).

### 4.8.2 SP-ELISA denaturant conditions

100  $\mu$ L/well of HMW1ct and HMW1ct-Glc proteins were diluted in PBS buffer up to a final concentration of 10  $\mu$ g/mL and incubated overnight at +4C. Plates were automatically washed 5 times with PBS buffer. 100  $\mu$ L/well of denaturing solution (8 M urea, 10 mM  $\beta$ -mercaptoethanol) was added and incubated 4 hours at room temperature. Plates were washed 5 times with Washing Buffer. 100  $\mu$ L/well of 25 mM iodoacetamide solution were added and plates were incubated overnight at room temperature. Plates were washed 5 times and remaining free sites on plate were blocked with 120  $\mu$ L/well of FBS buffer. Following the standard SP-ELISA protocol absorbance was read at 405 nm

### 4.8.3 Titration ELISA

Peptides and proteins were coated on plate surface and free sites on plate were blocked according to the same protocol used for a classical SP-ELISA assay. 100  $\mu$ L/well of sera were applied in triplicate at 6 different dilutions (1:100, 1:200, 1:300, 1:400, 1:600 and 1:800), flow through fraction was applied at 7 dilutions (without dilution, 1:2, 1:10, 1:50, 1:100, 1:200 and 1:400) and purified antibodies were applied at 6 final dilutions (1:2, 1:10, 1:50, 1:100, 1:200 and 1:400); samples were incubated on the plate for 1 hour at room temperature. The assay kept on following the standard SP-ELISA protocol and using only the human anti IgG-alkaline phosphatase antibody as secondary antibody.

### 4.8.4 Competitive ELISA

The protocol used for this assay is the same followed for the titration ELISA; the only difference is about sample application. For the competitive ELISA the selected sera were used at the semi-saturating dilution (corresponding to the dilution giving an absorbance of around 0.5 in the titration test). Serum and inhibitor in FBS buffer were mixed (50:50) and 100  $\mu$ L/well were



immediately dispensed. Each inhibitor were tested at 6 final concentrations:  $10^{-6}$ ,  $10^{-7}$ ,  $10^{-8}$ ,  $10^{-9}$ ,  $10^{-10}$  and  $10^{-11}$  M, prepared by serial dilution.  $IC_{50}$  was calculated for each inhibitor as the molar concentration need to obtain half of the maximum absorbance signal.

#### **4.8.5 Proteins conjugation to sepharose: thiol coupling**

100 mg of CNBr-sepharose resin (Sigma) were washed twice with 1 mM HCl 1.5 mL and cetrifugated at 4000 rpm for 3 minutes; the washing step was repeated with 1.5 mL of Milliq water and with 1.5 mL of coupling buffer (0.1 M  $NaHCO_3$ , 0.5 M NaCl, pH 8.3).

5 mg of N-(2-Aminoethyl)maleimide (Sigma) were dissolved in 1.5 mL of coupling buffer and applied to the resin overnight at room temperature. The resin was twice washed with 1.5 mL of coupling buffer and free sites on resin were blocked adding 1,5 mL of 0.2 M glycine pH 8.0 for 2 hours at room temperature. The resin was twice washed with 1.5 mL of coupling buffer and 1.5 mL of acetate buffer (0.1 M  $CH_3COO-Na^+$ , 0.5 M NaCl, pH 4.3). 1.5 mg of proteins were reduced by the addiction of DTT (1:2) in 1.5 mL of 10 mM HEPES pH 7.2 for 2.5 hours at room temperature; this solution was then added to 100 mg of previously washed sepharose resin. Free sites on sepharose were blocked with 1.5 mL of 0.2 M cysteine 10 mM HEPES pH 7.2 for 2 hours at room temperature. The resin was twice washed with 1.5 mL of coupling buffer and 1.5mL of acetate buffer.

#### **4.8.6 Proteins and peptides conjugation to sepharose: amine coupling**

200 mg of CNBr-sepharose resin (Sigma) were washed twice with 1.5 mL of 1 mM HCl and centrifuged at 4000 rpm for 3 minutes; the washing step was repeated with 1.5 mL of Milliq water and with 1.5 mL of coupling buffer (0.1 M  $NaHCO_3$ , 0.5 M NaCl, pH 8.3).

2 mg of proteins or peptides were dissolved in 2 mL of coupling buffer and applied to the resin overnight at room temperature. The resin was twice washed with 2 mL of coupling buffer and free sites on resin were blocked adding 2 mL of 0.2 M glycine pH 8.0 for 2 hours at room temperature. Finally the resin was twice washed with 2 mL of coupling buffer and 2 mL of acetate buffer (0.1M  $CH_3COO^-Na^+$ , 0.5M NaCl, pH 4.3).

#### **4.8.7 Sequential affinity chromatography**

The resins functionalized with the different antigens were transferred to chromatography columns of approximately 4 mL volume. 2 mL of serum were filtered with a 0.22  $\mu$ m filter and diluted 1:10 in PBS buffer pH 7.2. Diluted serum was applied three times to the first resin containing the

## CHAPTER 4

non glycosylated antigen; the not retained fraction was directly applied to the second column containing the glycosylated antigen for three times at room temperature. Both columns were washed with 12 mL of PBS buffer and specific antibodies were eluted with 12 mL of 0.2 M glycine at pH 2.6 and immediately neutralized adding 1.2 mL of 0.5M NaHCO<sub>3</sub>. Eluted fractions were concentrated with 50K amicon centrifugal filter and recovered in PBS buffer. IgG concentration was calculated by A<sub>280nm</sub>, considering 1.4 as mg/mL extinction coefficient.

### 4.8.8 Surface Plasmon Resonance studies

All experiments were conducted using a Biacore T100 instrument from GE Healthcare. All solutions and buffers were prepared with milliQ water obtained by the Sartorius system (arium 611 VF). Sensor chips CM5, amine coupling kit and Running Buffer HBS-EP+ 10x (0.1 mol/L HEPES, 1.5 mol/L NaCl, 30 mmol/L EDTA, 0.5% v/v p20) were purchased by GE Healthcare. Running Buffer was diluted ten times with MilliQ water at pH 7.4 and filtered daily with a Millipore Express™ PLUS 0.22µm system.

#### 4.8.8.1 Antigen immobilization on CM5 sensor chip

Immobilization buffers were selected separately for each peptide and protein through the pH scouting procedure, using the following buffers: PBS pH 7.2, Running Buffer pH 7.4, 0.1 mM CH<sub>3</sub>COO<sup>-</sup>Na<sup>+</sup> pH 4.5 and pH 5.0, 1 mM CH<sub>3</sub>COO<sup>-</sup>Na<sup>+</sup> pH 4.5 and pH 5.0, 5 mM CH<sub>3</sub>COO<sup>-</sup>Na<sup>+</sup> pH 4.5 and pH 5.0, 10 mM CH<sub>3</sub>COO<sup>-</sup>Na<sup>+</sup> pH 4.5 and 20 mM CH<sub>3</sub>COO<sup>-</sup>Na<sup>+</sup> pH 4.5. Molecules were solubilized in each buffer at a final concentration of 10 µg/mL and injected over the non-activated sensor chip surface for 120 s at a flow rate of 10 µL/min; after each injection chip surface was regenerated with a pulse of 0,1 M NaOH for 30 s at a flow rate of 10 µL/min. The selected buffer and the immobilized peptide quantities are reported in Table 19.

Each molecule were covalently linked on the surface of a chip CM5-type according to the amine coupling strategy that includes: sensor chip surface activation with two injections of 0.1 M N-hydroxysuccinimide and 0.4 M 1-ethyl-3-(3-dimethylaminopropyl)-carbodiimide (50:50) for 420 and 240 s at a flow rate of 10 µL/min; ligand injection at a concentration of 10 µg/mL in the previously selected immobilization buffer for 420 s and 60 s at a flow rate of 10 µL/min; free reactive sites block with two pulses of ethanolamine-HCl 1 M pH 8.5 for 420 s and 60 s at a flow rate of 10 µL/min.

Reference channel was activated and directly blocked with ethanolamine-HCl 1 M pH 8.5

#### **4.8.8.2 Binding studies with sera**

Binding studies were conducted on the immobilized ligands diluting each serum 1:50 and 1:100 in Running Buffer. Each serum was tested in a different cycle of analysis formed by the following steps: sample injection for 120 s, running buffer flow for 200 s, surface regeneration with one injection of 10 mM glycine at pH 2.5 for 30 s and one injection of 0.1 M NaOH for 60 s; for every step a flow rate of 30  $\mu\text{L}/\text{min}$  was used. Binding values were registered at the end of every sample injection.

#### **4.8.8.3 Kinetic and affinity studies with purified antibodies**

The 4 purified antibody fractions were diluted in running buffer to obtain the final concentrations of 20.0, 10.0, 5.0 and 2.5  $\mu\text{g}/\text{mL}$ . Each concentration was injected over the immobilized ligands in a different cycle of analysis based on: sample injection for 120 sec, Running Buffer flow for 200 s and sensor surface regeneration with 10 mM Gly pH 2.5 for 30 s and 0.1 M NaOH for 60 s; for every step a flow rate of 30  $\mu\text{L}/\text{min}$  was used.

#### **4.8.9 Tissues fixation**

One normal health rat was anesthetized with 1 mL/g of a 4% chloriol solution and then perfused using a peristaltic pump with fixative solution (4% paraformaldehyde in PBS buffer). Brain, cerebellum, spinal cord, kidney and stomach were surgically removed and kept in fixative for 24 hours at +4°C. Tissues were washed with 9% NaCl and put in 30% sucrose in PBS buffer for 3 days at +4°C. 3 days later, tissues were washed again with 9% NaCl, frozen in isopentane and stored at -80°C.

Frozen tissues were then cut with a cryostat in order to obtain some slices of 30  $\mu\text{m}$  thickness; slices were stored at -20°C in the anti-freeze solution (40% PBS, 30% glycerol and 30% ethylene glycol).

#### **4.8.10 Immunofluorescence test with paraformaldehyde-fixed tissues**

Paraformaldehyde-fixed tissue's slices were transferred from the anti-freeze solution (40% PBS, 30% glycerol and 30% ethylene glycol) to a 24 wells plate (Greiner). 2 slices were applied in each well and 1,5 mL of TBS Buffer (20 mM TRIS, 135 mM NaCl) were add. The plate was left in slight oscillation for 15 minutes; the washing step was repeated 3 times.

## CHAPTER 4

Free sites on tissues were blocked with 400  $\mu\text{L}$ /well of FBS buffer (10% FBS, TBS buffer, 0.15% Triton) and incubate at room temperature in slight oscillation for 30 minutes. Serum were diluted in FBS buffer 1:200 and 1:50, purified antibodies were tested at 10  $\mu\text{g}/\text{mL}$  or at their starting concentration and incubated with the tissues overnight at  $+4^{\circ}\text{C}$ .

After 3 washing with 1.5 mL/well of TBS buffer, 400  $\mu\text{L}$ /well of secondary antibody (polyclonal rabbit anti human IgG-FITC (Dako) or polyclonal rabbit anti human IgM-FITC (Sigma) 1:275 in FBS buffer, were applied for 2 hours at room temperature in slight oscillation in the dark.

Tissues were washed 3 times with 1,5 mL/well of TBS buffer.

To stain nuclei 4',6-diamidino-2-phenylindole (DAPI) stock solution (1 mg/mL DAPI in dimethylformamide (DMF) stored at  $-20^{\circ}\text{C}$ ) was diluted 1:1000 in TBS buffer and 400  $\mu\text{L}$ /well were incubated with tissues for 30 minutes at room temperature in slight oscillation.

After 3 washing with 1.5 mL/well of TBS buffer, each slice was transferred to a gelatin-coated glass slide and put at  $4^{\circ}\text{C}$  overnight in the dark. 200  $\mu\text{L}$  of anti-fade mounting medium (DiaMedix) were then applied on each slide and an appropriate glass cap was put on them.

Slides were observed at a fluorescence microscope using an incident wave of light at  $494_{\text{nm}}$  to obtain a green fluorescent light at  $518_{\text{nm}}$  because of the FITC presence and using an incident wave of light at  $358_{\text{nm}}$  to obtain a blue fluorescent light at  $461_{\text{nm}}$  because of DAPI optical properties.

## 4.9 References

- <sup>1</sup> H. Nothaft, C.M. Szymanski; Protein glycosylation in bacteria: sweeter than ever; *Nat. Rev. Microbiol.*, 2010 (8): 765-778.
- <sup>2</sup> C.M. Szymanski, R. Yao, C.P. Ewing, T.J. Trust, P. Guerry; Evidence for a system of general protein glycosylation in *Campylobacter jejuni*; *Microbiology* 1999 (32): 1022-1030.
- <sup>3</sup> C.D. Brimer, T.C. Montie; Cloning and comparison of *fliC* genes and identification of glycosylation in the flagellin of *Pseudomonas aeruginosa* a-type strains; *J. Bacteriol.* 1998 (180): 3209–3217.
- <sup>4</sup> M.A.Schmidt, L.W. Riley, I. Benz; Sweet new world: glycoproteins in bacterial pathogens; *Trends Microbiol.* 2003 (11): 554–561.
- <sup>5</sup> E. Bause; Structural requirements of N-glycosylation of proteins. Studies with proline peptides as conformational probes; *Biochem. J.* 1983 (209): 331-336.
- <sup>6</sup> Y.Gavel, G. von Heijne; Sequence differences between glycosylated and non-glycosylated Asn-X-Thr/Ser acceptor sites: implication for protein engineering; *Protein Eng.* 1990 (3): 433-442.
- <sup>7</sup> B. Imperiali, K.L Shannon, M. Unno, K.W. Rickert; A mechanistic proposal for asparagine-linked glycosylation; *J. Am. Chem. Soc.* 1992 (114): 7044-7945.
- <sup>8</sup> D.F. Zielinska, F. Gnad, J.R. Winsiewski, m. Mann; Precision mapping of an in vivo N-glycoproteome reveals rigid topological and sequence constraints; *Cell* 2010 (141): 897-907.
- <sup>9</sup> H.H. Freeze; Genetic defects in the human glycome; *Nat. Rev. Genet.* 2006 (7): 537-551.
- <sup>10</sup> M.E. Ackerman, M. Crispin, X. Yu, K. Baruah, A.W. Boesch, D.J. Harvey; Natural variation in Fc glycosylation of HIV-specific antibodies impacts antiviral activity; *J. Clin. Invest.* 2013 (123): 2183–2192.
- <sup>11</sup> S.R. Silva, A. Casabuono, J.F. Jacysyn, B.C. Favoretto, I. Fernandes, M.S. Macedo;. Sialic acid residues are essential for the anaphylactic activity of murine IgG1 antibodies; *J. Immunol.* 2008 (181): 8308–8314.
- <sup>12</sup> M. Blank, I. Krause, N. Dotan, L. Anafi, M. Eisenstein, R. Cervera; Anti-GalNAc $\beta$ : a novel anti-glycan autoantibody associated with pregnancy loss in women with antiphospholipid syndrome and in a mouse experimental model; *J. Autoimmun.* 2012 (39): 420–427.
- <sup>13</sup> T. Grader-Beck, F. Boin, S. von Gunten, D. Smith, A. Rosen, B.S. Bochner; Antibodies recognising sulfated carbohydrates are prevalent in systemic sclerosis and associated with pulmonary vascular disease; *Ann. Rheum. Dis.* 2011 (70): 2218–2224.
- <sup>14</sup> B. Brynedal, J. Wojcik, F. Esposito, V. Debailleul, J. Yaouanq, F. Martinelli-Boneschi; MGAT5 alters the severity of multiple sclerosis; *J. Neuroimmunol.* 2010 (220): 120–124.
- <sup>15</sup> D.C. Turk; The pathogenicity of *Haemophilus influenzae*; *Med. Microbiol.* 1984 (18): 1-16.
- <sup>16</sup> J.W. St. Geme III, S. Falkow, S.J. Barenkamp; High-molecular-weight proteins of nontypable *Haemophilus influenzae* mediate attachment to human epithelial cells; *Proc. Natl. Acad. Sci. USA* 1993 (90): 2875–2879.
- <sup>17</sup> J.W. St. Geme III; The HMW1 adhesin of nontypeable *Haemophilus influenzae* recognizes sialylated glycoprotein receptors on cultured epithelial cells; *Infect. Immun.* 1994 (62): 3881-3889.
- <sup>18</sup> J.W. St. Geme III, S. Grass; Secretion of the *Haemophilus influenzae* HMW1 and HMW2 adhesins involves a periplasmic intermediate and requires the HMWB and HMWC proteins; *Mol. Microbiol.* 1998 (27): 617–630.
- <sup>19</sup> J. R. Mc Cann, J.W. St. Geme III; The HMW1C-Like Glycosyltransferases: an Enzyme Family with a Sweet Tooth for Simple Sugars; *Plos Pathog.* 2014 (10): 1-4.
- <sup>20</sup> S. Grass, A.Z. Buscher, W.E. Swords, M.A. Apicella, S.J. Barenkamp; The *Haemophilus influenzae* HMW1 adhesin is glycosylated in a process that requires HMW1C and phosphoglucomutase, an enzyme involved in lipooligosaccharide biosynthesis; *Mol. Microbiol.* 2003 (48): 737-751.
- <sup>21</sup> Julia Gross, Susan Grass, Alan E. Davis, Petra Gilmore-Erdmann, R. Reid Townsend and Joseph W. St. Geme III; The *Haemophilus influenzae* HMW1 Adhesin Is a Glycoprotein with an Unusual N-Linked Carbohydrate Modification; *J. Biol. Chem.* 2008 (283): 26010-26015.
- <sup>22</sup> K.J. Choi, S. Grass, S. Paek, J.W.St. Geme, H.J. Yeo; The *Actinobacillus pleuropneumoniae* HMW1C-like glycosyltransferase mediates N-linked glycosylation of the *Haemophilus influenzae* HMW1 adhesin; *Plos One* 2010 (5): 1-12.

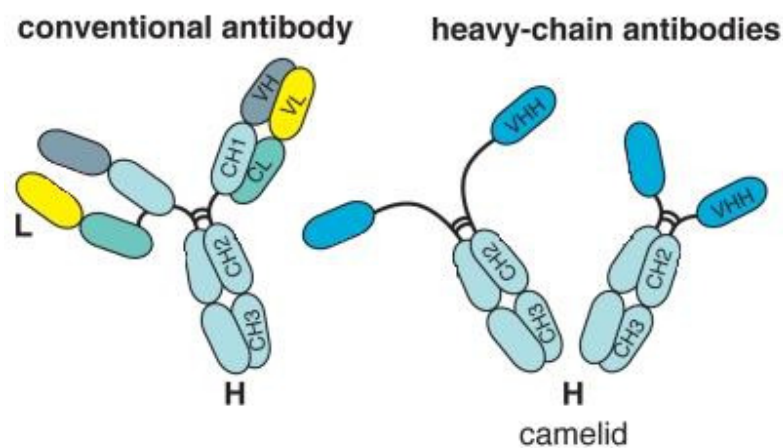
- 
- <sup>23</sup> A.J. Clarke, R. Hurtado-Guerrero, S. Pathak, A.W. Schuttelkopf, V. Borodkin; Structural insights into mechanism and specificity of O-GlcNAc transferase; *EMBO J.* 2008 (27): 2780-2788.
- <sup>24</sup> S. Grass, C.F. Lichti, R.R. Townsend, J. Gross, J.W. St. Geme III; The Haemophilus influenzae HMW1C protein Is a glycosyltransferase that transfers hexose residues to asparagine sites in the HMW1 Adhesin; *Plos Pathog.* 2010 (6): 1-9
- <sup>25</sup> C. Lucchinetti, W. Bruck, J. Parisi, M. Rodriguez, H. Lassmann; Heterogeneity of multiple sclerosis lesions: implications for the pathogenesis of demyelination; *Ann. Neurol.* 2000 (47): 707-717.
- <sup>26</sup> S. Cepok, M. Jacobsen, S. Schock; Patterns of cerebrospinal fluid pathology correlate with disease progression in multiple sclerosis; *Brain* 2001 (124): 2169-2176.
- <sup>27</sup> F. Frazekas, F. Barkhof, M. Filippi, R.I. Grossman, D.K Li, W.I. McDonald, D.H. Miller; The contribution of molecular resonance imaging to the diagnosis of multiple sclerosis; *Neurology* 1999 (53): 448-456.
- <sup>28</sup> O. Olerup, J. Hillert; HLA class II-associated genetic susceptibility in multiple sclerosis: a critical evaluation; *Tissue Antigens* 1991 (38): 1-15.
- <sup>29</sup> D. Buljevac, H.Z. Flach, W.C. Hop; Prospective study on the relationship between infections and multiple sclerosis exacerbations, *Brain* 2002 (125): 952-960.
- <sup>30</sup> Kurtzke, J. F.. 1993. Epidemiologic evidence for multiple sclerosis as an infection. *Clin. Microbiol. Rev.* 6:382
- <sup>31</sup> L. Steinman; Multiple sclerosis: a coordinated immunological attack against myelin in the central nervous system; *Cell* 1996 (85): 299-302.
- <sup>32</sup> K.W. Wucherpfennig, J.L. Strominger; Molecular mimicry in T cell-mediated autoimmunity: viral peptides activate human T cell clones specific for myelin basic protein; *Cell* 1995 (80): 695-705.
- <sup>33</sup> Croxford, J. L., J. K. Olson, S. D. Miller; Epitope spreading and molecular mimicry as triggers of autoimmunity in the Theiler's virus induced demyelinating disease model of multiple sclerosis; *Autoimmun. Rev.* 2002 (1): 251-260.
- <sup>34</sup> M.V. Ejada-Simon, Y.C. Zang, J. Hong, V.M. Rivera, J.Z. Zhang; Cross-reactivity with myelin basic protein and human herpesvirus-6 in multiple sclerosis; *Ann. Neurol.* 2003 (53): 189-197.
- <sup>35</sup> J. L. Croxford, H.A. Anger, S.D. Miller; Viral delivery of an epitope from Haemophilus influenza induces central nervous system autoimmune disease by molecular mimicry; *J. Immunol.* 2005 (174): 907-917.
- <sup>36</sup> P.V. Lehmann, E.E. Sercarz, T. Forsthuber ; Determinant spreading and the dynamics of the autoimmune T-cell repertoire; *Immunol. Today* 1993 (14): 203-208.
- <sup>37</sup> Medana, M.A. Martinic, H. Wekerle, H. Neumann; Transection of major histocompatibility complex class I-induced neurites by cytotoxic T lymphocytes; *Am. J. Pathol.* 2001 (159): 809-815.
- <sup>38</sup> M. Kerschensteiner, E. Gallmeier, L. Behrens; Activated human T cells, B cells, and monocytes produce brain-derived neurotrophic factor in vitro and in inflammatory brain lesions: a neuroprotective role of inflammation?; *J. Exp. Med.* 1999 (189): 865-870.
- <sup>39</sup> N. A. Ponomarenko, O. M. Durova, I. I. Vorobiev; Catalytic antibodies in clinical and experimental pathology: human and mouse models; *J. Immunol.Methods* 2002 (269): 197-211.
- <sup>40</sup> A.J. Bieber, A. Warrington, L.R. Pease, M. Rodriguez; Humoral autoimmunity as a mediator of CNS repair; *Trends Neurosci.* 2002 (24): 39-44.
- <sup>41</sup> R. Martin, H.F. Mc Farland, D.E. Mc Farlin; Immunological aspects of demyelinating diseases; *Annu. Rev. Immunol.* 1992 (10): 153-187.
- <sup>42</sup> J.J. Archelos, M.K. Storch, H.P. Hartung; The role of B cells and autoantibodies in multiple sclerosis; *Ann. Neurol.* 2000 (47): 694-706.
- <sup>43</sup> J. de Seze, S. Dubucquoi, D. Lefranc, L. Prin; IgG reactivity against citrullinated myelin basic protein in multiple sclerosis; *J. Neuroimmunol.* 2001 (117): 149-155.
- <sup>44</sup> H. A. Doyle, M.J. Mamula; Post-translational protein modifications in antigen recognition and autoimmunity; *Trends immunol.* 2001 (22): 443-449.
- <sup>45</sup> F.Lolli, B.Mulinacci, A. Carotenuto, B. Bonetti, G. Sabatino, B. Mazzanti, A.M. D'Ursi, E. Novellino, M. Pazzagli, L. Lovato, M.C. Alcaro, E. Peroni, M.C. Pozo-Carrero, F. Nuti, L. Battistini, G. Borsellino, M. Chelli, P. Rovero, A.M. Papini; An N-glycosylated peptide detecting disease-specific autoantibodies, biomarkers of multiple sclerosis; *Proc. Natl. Acad. Sci.* 2005 (102): 10273-10278.

- 
- <sup>46</sup> F. Real-Fernández, I. Passalacqua, E. Peroni, M. Chelli, F. Lolli, A.M. Papini, P. Rovero; Glycopeptide-based antibody detection in Multiple Sclerosis by surface plasmon resonance; *Sensors* 2012 (5): 5596-5607.
- <sup>47</sup> S. Pandey, I. Dioni, D. Lambardi, F. Real-Fernández, E. Peroni, G. Pacini, F. Lolli, R. Seraglia, A.M. Papini, P. Rovero; Alpha actinin is specifically recognized by Multiple Sclerosis autoantibodies isolated using an N-glycosylated peptide epitope; *Mol. Cell. Proteomics* 2013 (12): 277–282.
- <sup>48</sup> A. Carotenuto, A.M. D’Ursi, E. Nardi, A.M. Papini, P. Rovero; Conformational analysis of a glycosylated human myelin oligodendrocyte glycoprotein peptide epitope able to detect antibody response in multiple sclerosis; *J. Med. Chem.* 2001 (44): 2378-2381.
- <sup>49</sup> F. Lolli, B. Mazzanti, M. Pazzagli, E. Peroni, M.C. Alcaro, G. Sabatino, R. Lanzillo, V. Brescia Morra, L. Santoro, C. Gasperini, et al.; The glycopeptide CSF114(Glc) detects serum antibodies in multiple sclerosis; *J. Neuroimmunol.* 2005 (167): 131–137.
- <sup>50</sup> S.Rath, C.M. Stanley, M.W. Steward; An inhibition enzyme immunoassay for estimating relative antibody affinity and affinity heterogeneity; *J. Immunol. Method* 1988 (106): 245-249.
- <sup>51</sup> S.J. Barenkamp; Protection by serum antibodies in experimental nontypable H.influenzae otitis media; *Infect. Immun.* 1986 (52): 572-578.
- <sup>52</sup> S.J. Barenkamp, F.F. Bodor; Development of serum bactericidal activity following nontypeable Haemophilus influenzae acute otitis media; *Pediatr. Infect. Dis. J.* 1990 (9): 333-339.
- <sup>53</sup> L.E. Winter, S.J. Barenkamp; Human antibodies specific for the high-molecular weight adhesion proteins of nontypeable Haemophilus influenza mediate opsonophagocytic activity; *Infect. and Immun.* 2003 (12): 6884-6891.
- <sup>54</sup> E.H. Beachei; Bacterial adherence: adhesin receptor interaction mediating the attachment of bacteria to mucosal surface; *J. Infect. Dis.* 1981 (143): 325-345.
- <sup>55</sup> S.J. Barenkamp, J.W. St. Geme III; Identification of surface exposed B-cell epitopes on high molecular weight adhesion proteins of nontypeable Haemophilus influenzae; *Infect. Immun.* 1996 (64): 3032-3037.
- <sup>56</sup> M.A. Persson, M.A. Laurenzi, D. Vranjesevic; Extended repertoire of specific antibodies in CSF of patients with subacute sclerosing panencephalitis compared to those with multiple sclerosis: anti-bacterial antibodies are also increased; *J. Neuroimmunol.* 1989 (22): 135-142.
- <sup>57</sup> L.E. Huges, P.A. Smith, S. Bonell, R.S. Natt, C. Wilson, T. Rashid, A. Ebringer; Cross-reactivity between related sequences found in Acinetobacter sp., Pseudomonas aeruginosa, myelin basic protein and myelin oligodendrocyte glycoprotein in multiple sclerosis; *J. Neuroimmunol.* 2003 (144): 105-115.

## 5: Affinity determination of human recombinant domain antibodies specific for CSF114(Glc)

### 5.1 Human single domain antibodies: origins and applications

Most of the antibodies present in vertebrates are composed of two heavy and two light chains and both chains contribute to two identical antigen binding sites. In addition to these conventional antibodies, camelids produce a significant proportion of functional antibodies composed of heavy chains only<sup>1</sup>, consequently their antigen binding sites are formed by a single domain defined  $V_HH^2$  that is directly linked to the Fc-domain. Camelid heavy chain antibodies come in two variants, distinguished on the basis of the lengths of their hinge region and designated as long- and short-hinge isotypes (Figure 58).



**Figure 58:** Structural feature of a conventional antibody formed by heavy (H) and light (L) chains and of a heavy chain antibody formed by heavy chains only.

This discovery raised interest in isolating soluble and functional human antibody domains. The human formats ( $hV_H$ ) have many advantages from a genetic engineering point of view, since they can be easily cloned and amplified, because they are encoded by a single coding sequence. Other advantageous features of  $hV_H$  include high solubility, thermal stability, refolding capacity, and, because of their small size (molecular weight is approximately 15 kDa), they have a better tissue penetration *in vivo* and they can recognize epitopes that are inaccessible to conventional antibodies<sup>3</sup>. Lastly, being derived from human scaffolds,  $hV_H$  are promising for a potential use in immunotherapy because of their reduced immunogenicity<sup>4</sup>.



It has already been demonstrated that in vitro panning procedures allow to obtain structure sensitive antibody fragments<sup>5</sup>, and it is widely accepted that a single variable heavy domain isolated from natural antibodies may contribute to antigen binding with comparable affinities and specificities to the whole antibody<sup>6</sup>.

## **5.2 Objective**

The immunoenzymatic assay based on the synthetic probe CSF114(Glc) was shown to identify Multiple Sclerosis specific autoantibodies, and it is actively used in diagnostics and research to monitor and quantify MS associated Ig levels. We reasoned that high affinity engineering hV<sub>H</sub> raised against the same probe, could be relevant for the development of antigen detection strategies to be used in MS diagnosis. The aim of the present research was to detect and to quantify the interaction between some phage clones and the glucosylated peptide CSF114(Glc) and subsequently to determine the affinity and the kinetic of binding of one selected hV<sub>H</sub> fragment for CSF114(Glc) and for its unglucosylated version, using the Surface Plasmon Resonance biosensor Biacore T100.

## **5.3 Results and discussion**

In collaboration with the Department of Experimental and Clinical Biomedical Sciences of the University of Florence (Prof. Donatella Degl'Innocenti), we received eight different phage clones expressing on their surface a different hV<sub>H</sub> antibody specific for the CSF114(Glc) peptide.

The ability of every phage to specifically bind to CSF114(Glc) was previously tested in SP-ELISA assay and we tried to understand if these phages, when injected in a continuous flow, could recognize the glucosylated peptide immobilized on the surface of the chip of the biosensor. Then, soluble hV<sub>H</sub> fragments, produced from the phages selected thanks to SPR binding studies, were deeply characterized through affinity and kinetic studies on immobilized CSF114(Glc) and CSF114.

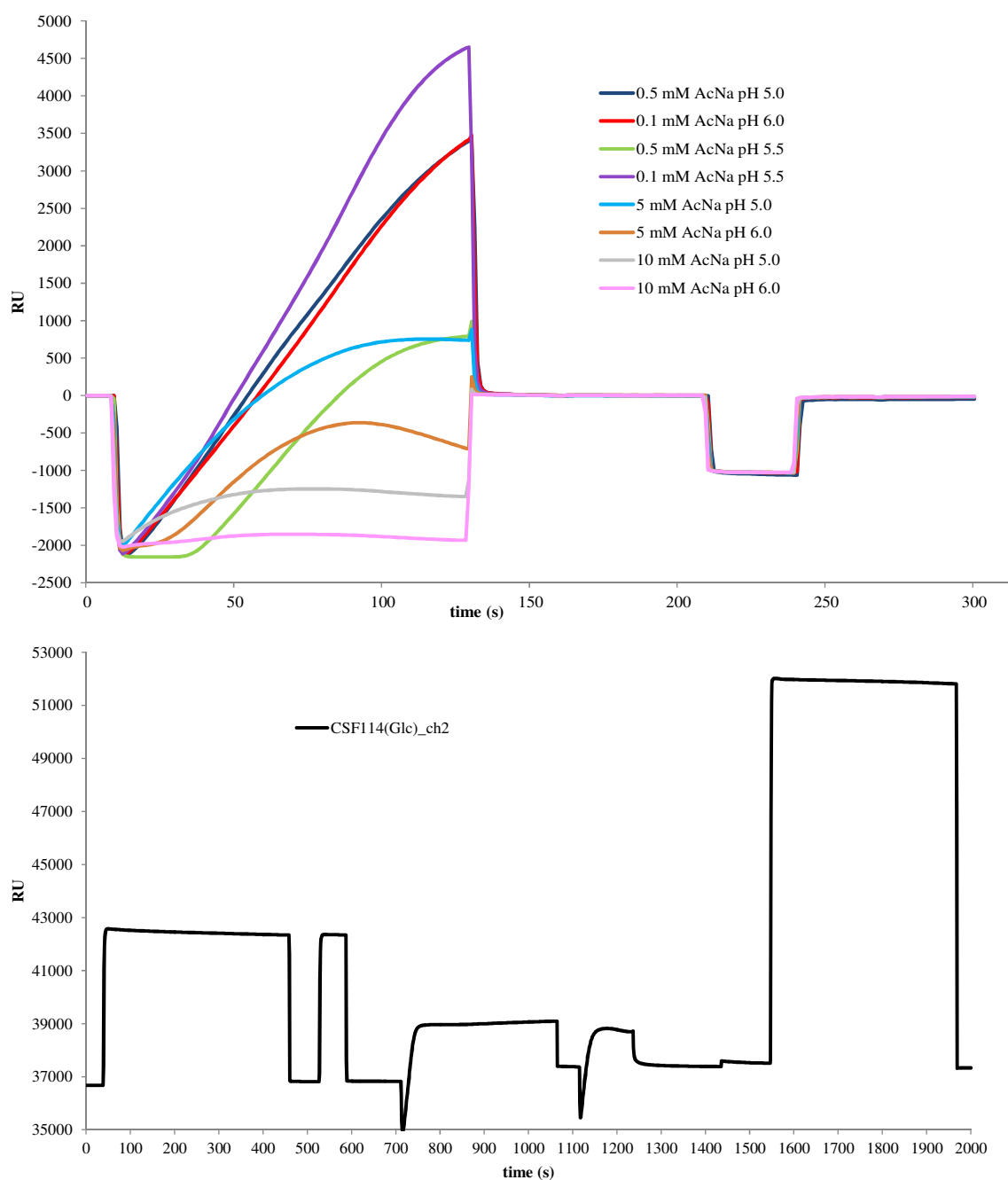
### **5.3.1 Peptides immobilization on Biacore chip**

The CSF114(Glc) peptide and its unglucosylated counterpart CSF114, whose sequences are reported in Table 24, were immobilized on two different channels of a CM5-type sensor chip.

Peptide	Sequence
CSF114(Glc)	TPRVERN(Glc)GHSVFLAPYGWMVK-NH <sub>2</sub>
CSF114	TPRVERNGHSVFLAPYGWMVK-NH <sub>2</sub>

**Table 24:** Sequence of peptides covalently immobilized on sensor chip surface.

Peptides were covalently linked according to the amine coupling strategy. An amine bond was formed between one primary amine group of each peptide and the previously activated carboxylic group on chip surface. Immobilization buffers were selected separately for each peptide using the pH scouting procedure in order to maximize electrostatic interactions between chip and peptides. At the end of the coupling protocol an immobilization level of 1126 RU was obtained for CSF114 in 0.5 mM in sodium acetate buffer pH 5.0 and 1327 RU for CSF114(Glc) in 0.1 mM sodium acetate buffer pH 5.5. The instrumental signal registered with the pH scouting procedure and the amine coupling immobilization of CSF114(Glc) is reported in Figure 59.

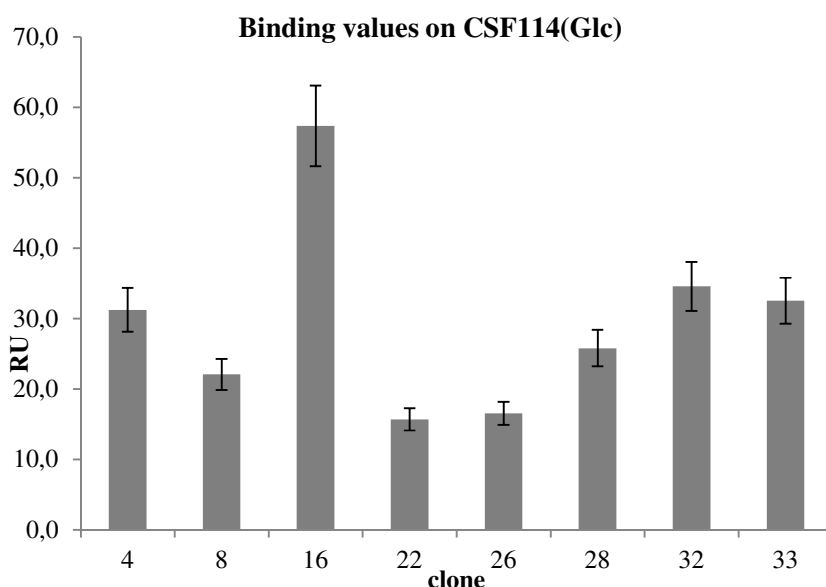


**Figure 59:** Sensorgrams showing the electrostatic pre-concentration on chip surface and the covalent immobilization of CSF114(Glc) on channel 2 of a CM5-type chip.

For SPR binding studies with phages and kinetic and affinity studies with soluble hV<sub>H</sub> fragments, the channel containing the unglycosylated peptide CSF114 was used as reference and the channel with immobilized CSF114(Glc) was used as the active one. To better quantify the binding between soluble hV<sub>H</sub> fragments and each single peptide, SPR binding studies were performed considering as reference one ethanolamine containing channel.

### 5.3.2 SPR binding studies with specific hV<sub>H</sub>-CSF114(Glc) phages

Binding studies with phages were conducted diluting each phage up to the same final concentration in running buffer and flowing it at a low flow rate over the immobilized peptides. Each phage was tested in a different cycle of analysis formed by the sample injection, the running buffer flow and finally the chip surface regeneration. The interactions between phages and peptides were quantified, considering the maximum binding values registered at the end of the injection (Figure 60).



**Figure 60:** Binding values (RU) registered on immobilized CSF114(Glc) for the eight selected phages.

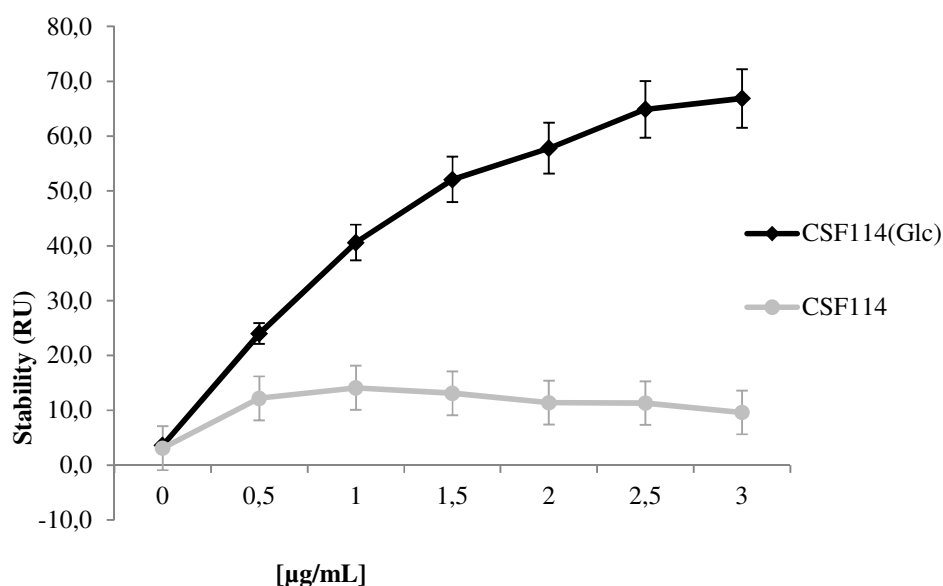
Binding study results, in line with SP-ELISA ones, confirmed the positivity of all tested phages for CSF114(Glc), and indicated phage 16 as the most promising for the expression of hV<sub>H</sub> soluble antibodies.

### 5.3.3 Kinetic and affinity characterization of hV<sub>H</sub>-CSF114(Glc)6xHis

Phage 16, selected from the previous study, could not be obtained in the soluble form because of technical problems; so the characterization of the interaction was continued with clone 22, the only one from which it was possible to express in high concentration the soluble form of hV<sub>H</sub>-CSF114(Glc)6xHis.

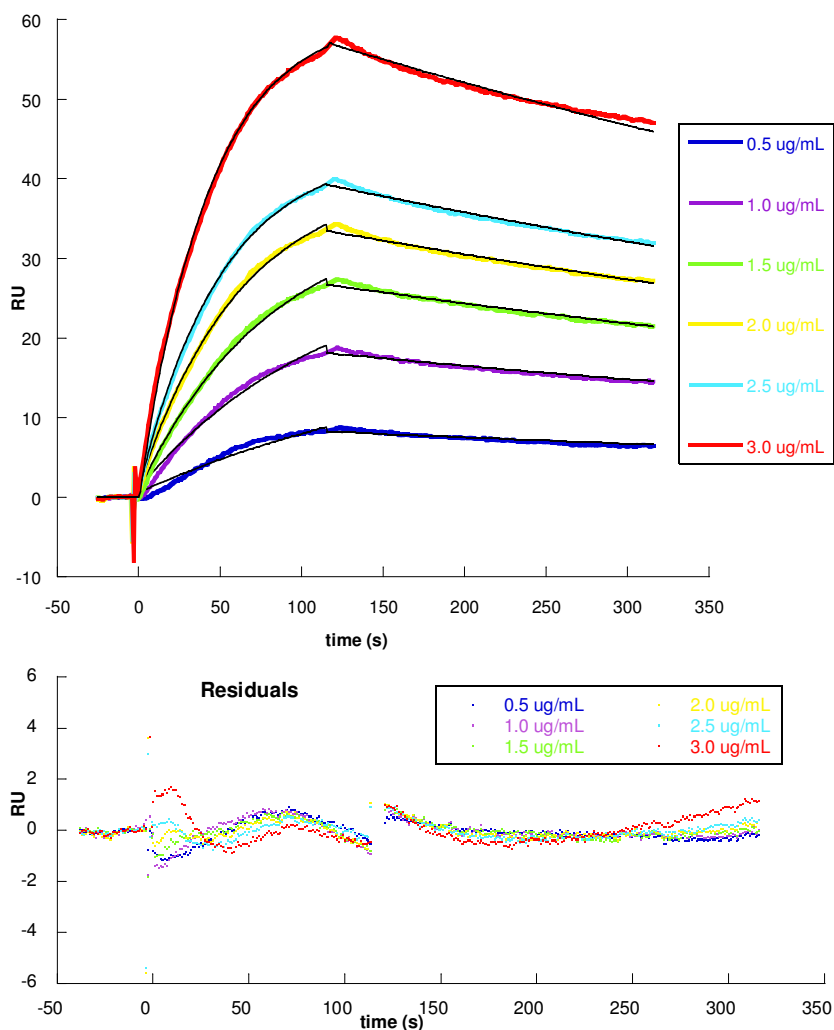
Biosensor analysis started diluting the hV<sub>H</sub>-CSF114(Glc)6xHis sample in running buffer at six different final concentrations and considering the *stability* signal registered on both single channel 15 s after the end of the injection of each sample concentration. As shown in Figure 61,

for each tested antibody concentration, we obtained an instrumental signal that was directly proportional to hVH-CSF114(Glc)6×His bounded to glucosylated peptide. Stability signals were found to be significantly higher (5-fold to 10-fold) for CSF114 (Glc) than for CSF114. The direct dependence of signals on antibody concentration further indicated a specific interaction mainly linked to the presence of the N-glucosyl moiety. On the contrary, signals generated by the association with the unglucosylated sequence CSF114 were not proportional to hVH-CSF114(Glc)6×His concentration, a behavior typical of a non-specific interaction.



**Figure 61:** Stability values registered on CSF114(Glc) (black) and CSF114 (light grey) at the different tested concentration (µg/mL).

Considering the results of the SPR binding study, we decided to characterize the kinetic and affinity of the interaction between hV<sub>H</sub>CSF114(Glc)6×His antibody and CSF114(Glc) peptide. According to the same method applied for binding experiments, the hV<sub>H</sub>CSF114(Glc)6×His was injected in different concentrations and final results were elaborated with the software associated to the instrument to obtain the affinity constant and the kinetic parameters. Fitting experimental curves to the theoretical 1:1 interaction model as shown in Figure 62,  $k_a$  was found to be  $1.20 \pm 0.10 \times 10^5 \text{ M}^{-1} \text{ s}^{-1}$  and  $k_d$  was  $1.09 \pm 0.07 \times 10^{-3} \text{ s}^{-1}$ , resulting in an overall equilibrium dissociation constant ( $K_D = k_d/k_a$ ) of  $9.08 \pm 0.13 \times 10^{-9} \text{ M}$ .



**Figure 62:** In the upper part sensorgrams showing the interaction between hV<sub>H</sub>-CSF114(Glc)6xHis and peptide CSF114(Glc); the graph represents experimental curves corresponding to six different antibody concentrations in different colors and the corresponding curves obtained by fitting with a theoretical 1:1 interaction kinetic model (black); in the lower part the residual values indicating the difference between experimental and mathematical curves are shown and they are closely distributed along the zero.

Affinity measurements indicated that hV<sub>H</sub>-CSF114(Glc)6xHis antibody established a very strong interaction with CSF114(Glc) peptide. Another experimental aspect that confirmed the strength of the interaction between hV<sub>H</sub>-CSF114(Glc)6xHis antibody and CSF114(Glc) was the difficulty of regenerating the sensor chip after measurements; three consecutive regeneration steps were needed to completely detach the antibody from the sensor chip surface instead of the one or two regeneration cycles, usually used in similar experiments<sup>7</sup>.

Previous attempts to use the SPR technology to characterize purified human anti-CSF114(Glc) antibodies from MS patient sera confirmed the specificity of auto-antibodies for the glycosylated peptide and provided a  $k_d$  parameter of  $2.2 \times 10^{-4} \text{ s}^{-1}$ <sup>8</sup>.  $K_d$  parameter obtained in the present study

was in the range of  $10^{-3} \text{ s}^{-1}$ , indicating that hV<sub>H</sub>CSF114(Glc)6×His antibody dissociated from CSF114(Glc) about five times faster than human autoantibodies obtained from MS patients' sera. This observation could be at least in part explained taking into account that the mass transport that influences the SPR signals is influenced by several factors, among which the molecular weight of the analyte and the observation that the dissociation rate inversely correlates to the analyte size. In this case, the molecular weight of the hV<sub>H</sub> (~15 kDa) is at least 10-fold lower than that of a common human immunoglobulin, leading to a faster dissociation rate.

Considering the obtained results, we could suggest some application in humans; in fact, since the peptide CSF114(Glc) has been used as an immunological probe to develop a patented immunoenzymatic diagnostic assay to detect specific autoantibodies in MS patients' sera (MS PepKit), a human anti-CSF114(Glc) hV<sub>H</sub> domain antibody could be effectively exploited as a positive standard/calibrator of this assay. In addition, because the current form of the assay is a classical ELISA sandwich, we may speculate on a possible evolution into a competitive assay based, for example, on a labeled recombinant antibody pre-coupled to CSF114(Glc) that is displaced by patients' MS specific autoantibodies, with evident benefits in terms of speed and accuracy. Interesting perspectives could also be the possible use of antibody constructs for blocking in vivo the interaction of auto-antibodies with small antigenic structures within the brain, diminishing or suppressing the antibody mediated damage. In this perspective, a human domain antibody characterized by a high affinity for antigens in MS, lacking the effector region of a normal Ig molecule and with a low overall immunogenicity in the human body, could be ideal to block the auto-antibodies and display beneficial effects in vivo.

#### 5.4 Conclusions

In this part of the work some phages coming from a previously panned human domain antibody library and the soluble form of one human domain antibody was characterized with an SPR biosensor, looking for the antibody clone that could recognize the N-glycosylated CSF114(Glc) peptide with high affinity, to be used for further studies in MS.

From a technical point of view, the results obtained from binding experiments with hV<sub>H</sub>-CSF114(Glc) phages indicate that this kind of biosensor can successfully be used to quantify the interaction of immobilized ligands with high molecular weight analytes such as phages; indeed in the present study the most promising phage, that could be used to express a soluble antibody, was selected considering its interaction with the glycosylated peptide.

## CHAPTER 5

In a recent publication<sup>9</sup> we reported affinity and kinetic measurements of hV<sub>H</sub>-CSF114(Glc)6xHis showing that the soluble antibody specifically recognized the glucosylated peptide with high affinity as indicated by the equilibrium dissociation constant K<sub>D</sub> that is in the nanomolar range.

Considering these aspects it could be interesting to use the selected hV<sub>H</sub>-CSF114(Glc)6xHis as a positive control in diagnostic tests, or as a molecular probe in immunohistochemistry assays and more importantly it could be test in vivo as a competitive probe for MS autoantibodies.

### 5.5 Materials and methods

#### 5.5.1 Production of hV<sub>H</sub> soluble antibodies

Soluble hV<sub>H</sub> antibodies were produced by the Department of Experimental and Clinical Biomedical Sciences of the University of Florence (Prof. Donatella Degl'Innocenti) starting from a commercial human domain antibody library according to manufacturer instructions<sup>10</sup>. Briefly, after phage manipulation, selection was performed thanks to a magnetic beads-based biopanning using 50 pmol of the biotinylated CSF114(Glc); then individual phage clones were grown and tested in ELISA against CSF114(Glc). Phagemides from positive clones were sequenced, amplified and ligated into an expression vector used to transform competent *E.Coli* in order to express hV<sub>H</sub> specific for CSF114(Glc) as a 6xHis tagged antibody (hV<sub>H</sub>-CSF114(Glc)6xHis). Purified hV<sub>H</sub>-CSF114(Glc)6xHis specificity for the glucosylated peptide was confirmed in SP-ELISA assays.

#### 5.5.2 Peptides immobilization on Biacore CM5 chip

The pH scouting procedure was employed to select the optimal immobilization buffer for each peptide using PBS buffer pH 6.5 and 7.2 and sodium acetate buffers 0.1, 0.5, 5.0 and 10 mM pH 5.0, 5.5 and 6.0. The CSF114 peptides (with or without glucosyl moiety) were dissolved in each buffer to a final concentration of 10 µg/mL and injected for 120 s at a flow rate of 10 µL/min. After this step, chip surface was regenerated with 0.1 M NaOH for 30 s at a flow rate of 10 µL/min. Buffer selection was based on the maximal RU signal observed at the end of the injection. Peptide were immobilized on the surface of a chip CM5-type according to the amine coupling strategy that includes: sensor chip surface activation with two injections of a solution of (1:1) N-hydroxysuccinimide 0.1 M and 1-ethyl-3-(3-dimethylaminopropyl)-carbodiimide 0.4 M for 420 s and 240 s at a flow rate of 10 µL/min; peptide injection at a concentration of 10 µg/ml



in the previously selected immobilization buffer for 420 s at a flow rate of 10  $\mu\text{L}/\text{min}$ ; free reactive sites block with two pulses of ethanolamine-HCl 1 M pH 8.5 for 420 s and 60 s at a flow rate of 30  $\mu\text{L}/\text{min}$ . This procedure was used on both active and reference channels, containing glucosylated and non-glucosylated CSF114 peptides, respectively.

### 5.5.3 SPR binding studies with specific hV<sub>H</sub>-CSF114(Glc) phages

Binding studies were conducted on the immobilized CSF114(Glc) peptide with 8 phages, previously selected with the phage display technique for their positivity versus the same peptide and with 1 negative control. Each phage was diluted up to the final concentration of  $5 \times 10^{10}$  Colony Forming Unit in running buffer (0.1M HEPES, 1.5 M NaCl, 30mM EDTA, 0.5% v/v Surfactant p20) and tested in a different cycle of analysis. One cycle was formed by the following steps: phage injection for 420 s at a flow rate of 5  $\mu\text{L}/\text{min}$ , running buffer flow for 200 s, surface regeneration with one injection of 10mM glycine solution pH 2.5 for 30 s and one injection of 0.1 M NaOH for 60 s. Binding values were registered at the end of every sample injection.

### 5.5.4 SPR characterization of hV<sub>H</sub>-CSF114(Glc)6xHis

hV<sub>H</sub>-CSF114(Glc)6xHis antibody was diluted in running buffer to final concentrations of 3.0, 2.5, 2.0, 1.5, 1.0 and 0.5  $\mu\text{g}/\text{mL}$ . Each concentration was injected over immobilized peptides in both active and control channels for 120 s at a flow rate of 30  $\mu\text{L}/\text{min}$ . Running buffer was then flushed for 200 s at a flow rate of 30  $\mu\text{L}/\text{min}$  to allow dissociation, and finally, chip surface was regenerated by injecting a 0.1 M NaOH solution for 60 s followed by a 10 mM glycine solution pH 2.5 for 30 s and then again a 100 mM NaOH solution for 60 s at a flow rate of 30  $\mu\text{L}/\text{min}$ . Obtained results were elaborated using the Biacore T100 Evaluation software 2.0 fitting experimental data to a theoretical 1:1 interaction kinetic model in order to calculate the association rate ( $k_a$ ), the dissociation rate ( $k_d$ ) and the equilibrium dissociation constant ( $K_D = k_d/k_a$ ).

## 5.6 References

- 
- <sup>1</sup> J. Wesolowski, V. Alzogarai, J. Rejelt, F. Koch-Nolte; Single domain antibodies: promising experimental and therapeutic tools in infection and immunity; *Med. Microbiol. Immunol.* 2009 (198): 157-174.
- <sup>2</sup> M. Arbabi, A. Desmyter, L. Wyns, R. Hamers; Selection and identification of single domain antibody fragment from camelid heavy chain antibodies; *FEBS Letter* 1997 (414): 521-526.
- <sup>3</sup> B. Stiljemans, K. Conrath, V. Cortez-Retamozo, S. Mages; Efficient targeting of conserved cryptic epitopes of infectious agents by single domain antibodies. African trypanosomes as paradigm; *J.Biol.Chem.* 2004 (279): 1256-1261.
- <sup>4</sup> R. To, T. Hirama, M. Arbabi-Ghahroudi, J. Tahna; Isolation of monomeric human V(H)s by a phage selection; *J.Biol.Chem.* 2005 (280): 41395-41403.
- <sup>5</sup> D. degl'Innocenti, N. Taddei, M. Ramazzotti, M. Stefani, F. Chiti, G. Ramponi; Selection of antibody fragments specific for an alpha-helix region of acylphosphatase; *J. Mol. Recognit.* 2004 (17): 62-66.
- <sup>6</sup> E.S. Ward, D. Güssow, A.D. Griffiths, G. Winter; Binding activities of a repertoire of single immunoglobulin variable domains secreted from *Escherichia coli*; *Nature* 1989 (341): 544-546.
- <sup>7</sup> F. Real-Fernández, I. Passalacqua, E. Peroni, M. Chelli, F. Lolli, A.M. Papini, P. Rovero; Glycopeptide-based antibody detection in multiple sclerosis by surface plasmon resonance; *Sensors* 2012 (12): 5596-5607.
- <sup>8</sup> E.S. Bulukin, E. Peroni, M. Minunni, M. Pazzagli, P. Rovero, M. Mascini, A.M. Papini; Development of an efficient multiple sclerosis diagnostic technology based on an optical glucopeptide immunosensor; *Understanding Biology Using Peptides, American Peptide Symposia* 2006 (9): 785-786.
- <sup>9</sup> **F. Niccheri, F. Real-Fernández, M. Ramazzotti, F. Lolli, G. Rossi, P. Rovero, D. Degl'Innocenti; Human recombinant domain antibodies against multiple sclerosis antigenic peptide CSF114(Glc); *J. Mol. Recognit.* 2014 (27): 618-626.**
- <sup>10</sup> C.M. Lee, N. Iorno, F. Sierro, D. Christ; Selection of human antibody fragments by phage display; *Nature protocols* 2007 (2): 3001-3008.

## **6: SP-ELISA detection of anti N-glycosylation antibodies in Rett Syndrome patients' sera**

### **6.1 Proposed correlation between Multiple Sclerosis and Rett syndrome**

Rett syndrome is an X-linked dominant postnatal severe and disabling neurodevelopmental disorder, which is the second most common cause for genetic mental retardation in girls and the first pervasive disorder with a known genetic basis. The classical variant is characterized by apparently normal development for the first 6-18 months, accompanied then by early deceleration of head growth, followed by loss of acquired cognitive, social and motor skills and other neurological and related symptoms, together with development of autistic behavior<sup>1</sup>. Rett syndrome is formerly placed in the heterogeneous group of Autism Spectrum Disorders (ASD), but is now regarded as a distinct pathological entity. To date, no effective therapy for preventing or arresting the neurologic regression in the disease in its various clinical presentations is available. The syndrome is primarily associated to a single monogenic mutation in the Methyl CpG binding protein 2 (MeCP2) gene in up to 95% of cases<sup>2</sup>, more rarely by mutation in Cyclin-Dependent Kinase-Like 5(CDKL5)<sup>3</sup> or in Forkhead box protein G1 (FOXG1)<sup>4</sup>. Rett patients with atypical clinical presentation, usually harbor CDKL5 or FOXG1 mutations, while the preserved speech variant is usually linked to MeCP2 mutations<sup>5</sup>. Despite almost two decades of research into the functions and role of MeCP2, little is known about the mechanisms leading from MeCP2 deficiency to disease development.

MeCP2 protein product acts as a transcriptional repressor or activator depending on the target gene associated. Overall, the evidence in both MeCP2 deficient patients and knock-out mice implies that loss of MeCP2 causes malfunction of numerous synapses throughout the brain, which creates less efficient neuronal networks and gives rise to Rett-like phenotypes<sup>6</sup>.

Recent studies on MeCP2 null mice identified the Brain Derived Neurotrophic Factor (BDNF), playing a major role in neuronal survival, neurogenesis and plasticity, as a major MeCP2 target, consequently abnormalities in BDNF homeostasis are believed to contribute to the neurologic phenotype and to the pathophysiology of part of the symptoms of Rett syndrome. In the last year a clinical correlation between Rett and Multiple Sclerosis has been suggested on the basis of preliminary results obtained with Glatiramer acetate, an immunomodulator with proven safety

and efficacy in Multiple Sclerosis treatment, that has been reported to cause elevated secretion of BDNF in Rett animal model too<sup>7</sup>.

## 6.2 Objective

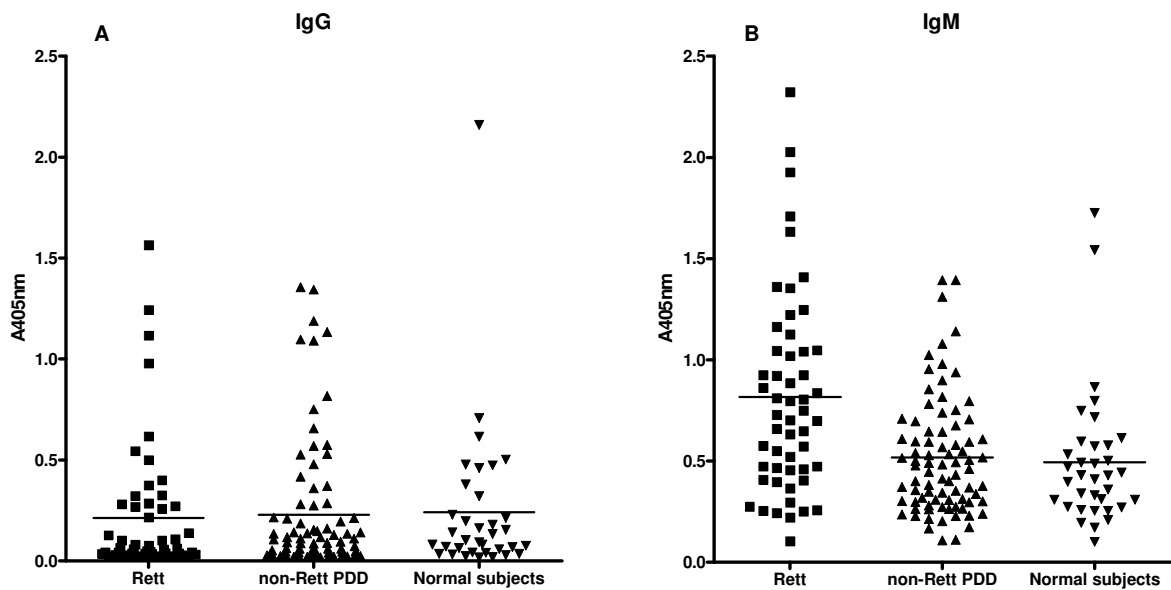
Taking care of the above mentioned clinical correlation and considering that both Rett and Multiple Sclerosis are central nervous system pathologies and that the synthetic N-glycosylated peptide CSF114(Glc) has successfully been used to detect specific autoantibodies in a subgroup of MS patients<sup>8</sup>, the ability of the same probe to reveal antibodies in Rett patients' sera, by comparison to healthy controls and pathological controls, was investigated. Subsequently, taking into account the results obtained during the present PhD research, indicating that specific antibodies that recognize the N-glycosylated HMW1ct protein from *H.influenzae* were present in MS sera and that they cross-reacted with CSF114(Glc), we investigated if this bacterial protein could also be used to reveal antibodies in Rett patients' sera.

This study could be useful to understand if a putative perturbation of the humoral response is present in Rett patients and if specific antibodies could be revealed for diagnostic or prognostic purpose.

## 6.3 Results and discussion

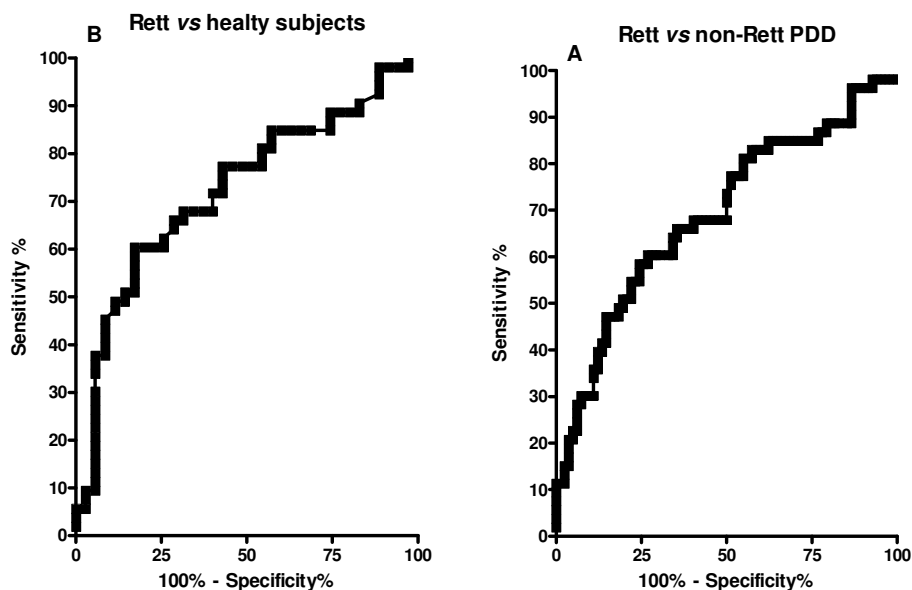
### 6.3.1 Determination of specific anti N-glycosylated peptide antibodies by SP-ELISA

The presence of serum antibody in patients' sera was evaluated by a SP-ELISA assay according to a standard optimized procedure, the N-glycosylated peptide probe CSF114(Glc) was coated to the plates and a total of 164 human sera consisting of Rett patients, normal health children and pathological controls were applied. The IgG and IgM titer of anti-CSF114(Glc) antibodies was determined thanks to the application of a specific enzyme labeled secondary antibody; after the addition of its substrate the colorimetric reaction was measured at 405nm; absorbance values were directly dependent on the quantity of the antibodies that bound the adsorbed peptide. In Figure 63 the absorbance values for IgG and IgM are reported for each group of sera.



**Figure 63:** Distribution graphs of the anti-CSF114(Glc) IgG (A) and IgM (B) revealed by the immunoenzymatic assay in each group of sera; horizontal line indicate the median absorbance value for each group.

The IgM antibody titer found in Rett patients was significantly higher than those observed in the control groups, both healthy subjects and non-Rett PDD patients. Calculated Receiver-Operating Characteristic (ROC) curves indicated that anti-CSF114(Glc) IgM were able to discriminate Rett syndrome from either non-Rett PDD patients and control subjects (Figure 64). Considering a cut-off value of 0.61 this test can distinguish between Rett and non-Rett pervasive developmental disorder (non-Rett PDD) groups with a sensitivity of 60.4% and a specificity of 71.9%, the area under the curve was 0.669 and the p-value 0.0006. When comparing Rett and normal health subjects group, setting a cut-off of 0.62 a specificity of 82.9% and a sensitivity of 60.4% were obtained, with an area under the curve of 0.697 and a p-value of 0.0016.



**Figure 64:** Receiver-Operating Characteristic analysis for anti CSF114(Glc) IgM in Rett vs non-Rett PDD groups(A) and in Rett vs normal subjects groups (B).

At variance, the CSF114(Glc) antigen failed to detect a significant IgG serum antibody population in both patient groups and healthy controls; a higher but not significant IgG titer was only found in 3 Rett patients and interestingly they were the oldest inside their group.

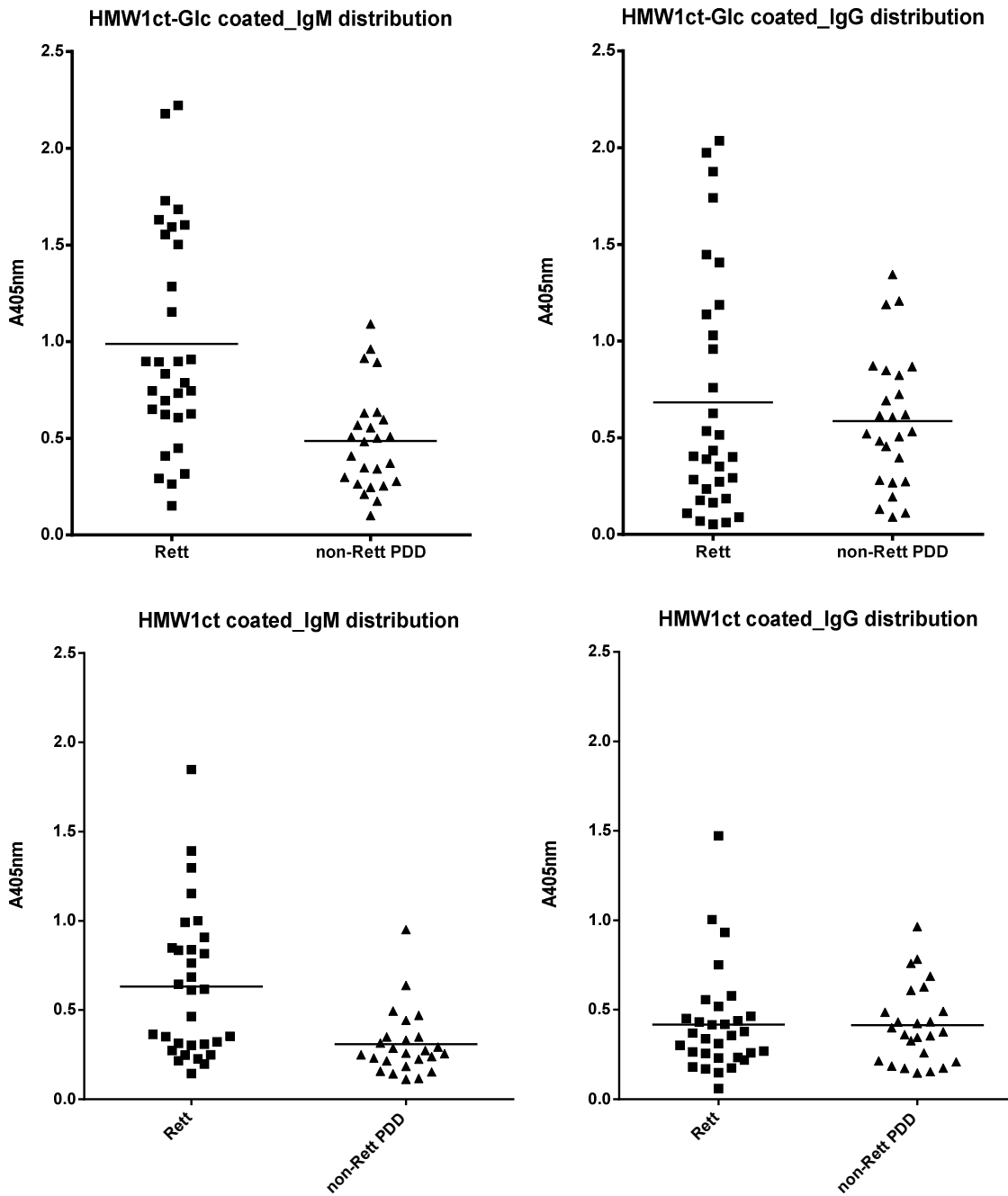
Although, a number of studies have addressed the relationship between Rett syndrome and immune system dysfunction, these have mainly focused on their influence on peripheral immune cells<sup>9</sup>, although some recent reports investigated humoral immunity in RTT patients, observing evidences of immune system activation<sup>10</sup>. Results obtained by this SP-ELISA screening indicated that Rett patients showed a consistent and highly significant increase of the serum IgM relative to both healthy controls and non-Rett PDD patients group.

The specificity of interaction between CSF114(Glc) and IgM antibodies was demonstrated by the ROC curve, widely considered a test of accuracy for discriminating between patients and normal subjects. Thus, it appears that the Rett patients group can be distinguished with confidence on the basis of serum IgM titer detected by the CSF114(Glc)-based assay. It is of interest that the large serum IgM increases, noted here, were also observed with the same assay, in a subset of multiple sclerosis patients. It is plausible that the IgM changes, noted in these CNS pathologies, could be linked to a common mechanism based on a pervasive neuroinflammation. Maybe the association between neuroinflammation and the observed serum IgM rise could be causal to the Rett disease initiation and/or progression together with the combination of epigenetic modification and environmental factors.

### 6.3.2 Determination of specific anti N-glycosylated adhesin antibodies by SP-ELISA

A significant cross-reactivity was found, during this PhD research, between anti-CSF114(Glc) antibodies in MS patients' sera and the 8 times N-glycosylated protein HMW1ct corresponding to the C-terminal fragment (aa 1205 – 1536) of the HMW1 adhesion protein of *H. influenzae*. Considering also the above described pathophysiological relevance of antibodies recognizing CSF114(Glc) in Rett patients' sera, we investigated if those antibodies could cross-react with the protein HMW1ct-Glc.

With this aim, the presence of serum antibodies in Rett patients' sera was estimated by SP-ELISA coating HMW1ct-Glc and the corresponding non glycosylated sequence HMW1ct. 31 Rett patients' sera and 25 non-Rett PDD control sera were applied in this preliminary screening phase. Antibodies recognizing the adsorbed proteins were revealed thanks to the application of appropriate enzyme labeled secondary antibodies and quantified according to the absorbance values registered at 405nm as illustrated in Figure 65 for each group of sera.



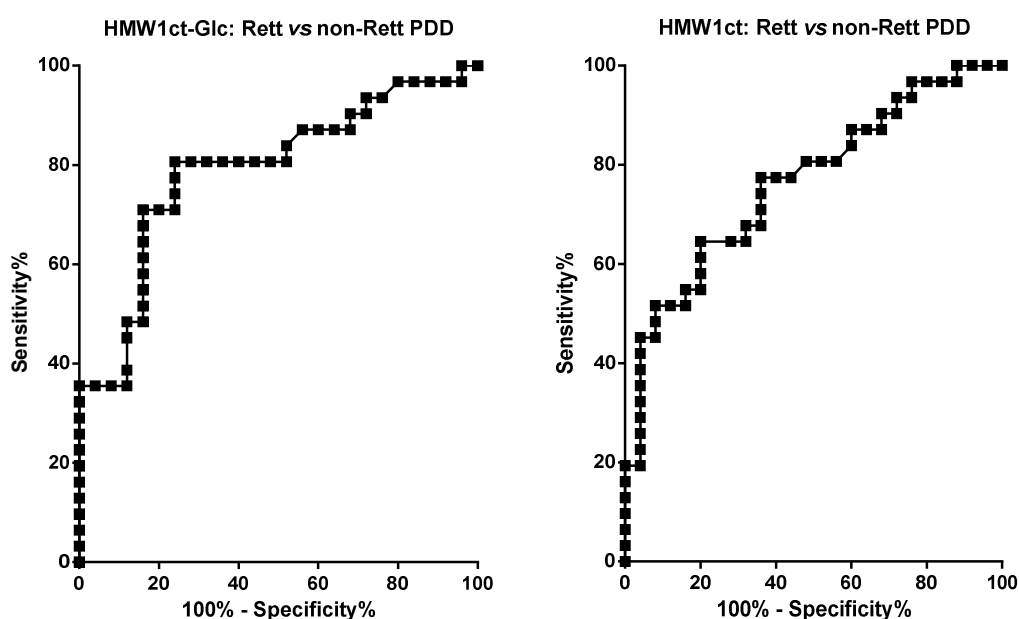
**Figure 65:** Distribution graphs of the anti-HMW1ct-Glc IgM or IgG and of the anti-HMW1ct IgM or IgG revealed by the immunoenzymatic assay in Rett and non-Rett PDD sera; horizontal line indicate the mean absorbance value for each group.

The IgM antibody titer against both HMW1ct proteins found in Rett patients was higher than those in the control non-Rett PDD patients; on the other hand, high levels of serum IgG were found in both groups coating both proteins, indicating that anti-adhesin antibodies of IgG isotype were present in the most part of tested sera independently of patient disease.



Calculated Receiver-Operating Characteristic (ROC) curve indicated that anti-HMW1ct-Glc IgM antibodies were able to discriminate Rett syndrome from non-Rett PDD with an area under the curve of 0.79 and a p-value of 0.0002; the diagnostic cut-off for the method was set at 1.0 with a sensitivity of 35.5% (11/31) and a specificity of 96.0% (1/25).

From the ROC analysis of anti-HMW1ct IgM antibodies, we obtained a discriminative power indicated by an area under the curve of 0.76 and a p-value of 0.0007; the cut-off of 0.93 was selected with a sensitivity of 19.4% (6/31) and a specificity of 96.0% (1/25). ROC curves are shown in Figure 66.



**Figure 66:** ROC analysis for anti HMW1ct-Glc and anti-HMW1ct IgM in Rett vs non-Rett PDD groups.

The same specificity in detecting serum IgM in Rett patients was found for both HMW1ct and HMW1ct-Glc proteins adsorbed on the ELISA support, but a higher sensitivity and a higher statistical significance for the test was calculated for the N-glycosylated protein.

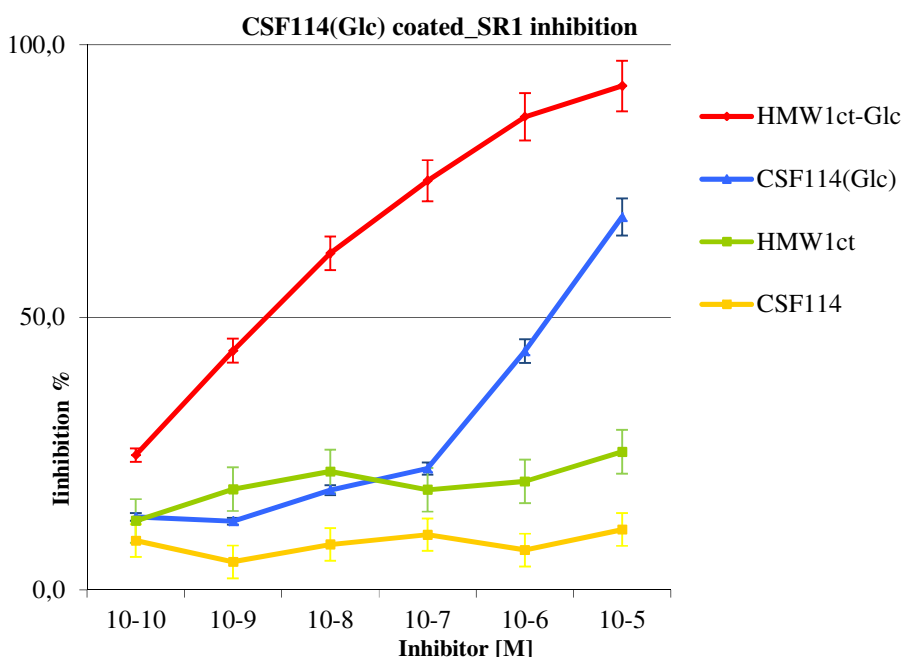
From the screening of this small cohort of sera an overall higher IgG and IgM antibodies level was detected with the two proteins as compared to the coated peptide CSF114(Glc); probably because when a high molecular weight antigen is used as probe on the solid support, heterogeneous families of antibodies, recognizing a variety of epitopes, are revealed and it is not possible to know if the absorption on the plastic support alters the natural conformation of the proteins, masking real epitopes or creating new ones. For this reason, we decided to continue the project by coating on the solid support peptide CSF114(Glc) that was the best performing probe

in detecting specific antibodies in Rett sera, and by testing the two proteins as inhibitors in solution.

### 6.3.3 Competitive ELISA assay with Rett sera

Two Rett sera, showing a high IgG level against CSF114(Glc), were selected to be used in competitive ELISA assays according to the method of Wrath, Stanley and Steward<sup>11</sup>.

At first, sera were titrated by testing them at four different dilutions in order to find the semi-saturating dilution giving an absorbance of around 0.5, to be used in competitive ELISA. The competitive ELISA was then performed on coated CSF114(Glc) with the only one serum (SR 1) showing a sufficient IgG titer in the experimental conditions required to perform the assay. SR 1 was incubated with six different concentrations (from  $10^{-5}$  to  $10^{-10}$  M) of HMW1ct, HMW1ct-Glc, CS114 and CSF11(Glc). From the inhibition curves reported in Figure 67, the  $IC_{50}$  for each inhibitor was calculated.



**Figure 67:** Inhibition curves describing the relative mean affinity of anti-CSF114(Glc) antibodies from SR1 serum for the four inhibitors applied in solution.

This experiment confirmed the proposed cross-reactivity of anti-CSF114(Glc) antibodies with the protein HMW1ct-Glc, and indicated that N-glycosylation moieties were fundamental for the interaction with antibodies; indeed non glycosylated CSF114 and HMW1ct were not able to inhibit antibody binding. From the calculated  $IC_{50}$  values, as in the case of Multiple Sclerosis

sera, we observed a significant higher affinity of anti-CSF114(Glc) antibodies for the glucosylated protein ( $10^{-8.5}$  M) than for the glucosylated peptide ( $10^{-6}$  M).

## 6.4 Conclusions

The SP-ELISA assay based on the N-glucosylated CSF114(Glc) that was recently reported in a scientific paper by our research group<sup>12</sup>, provided evidence for an increase in IgM titer, but not in IgG, in Rett patients relative to both healthy controls and non-RTT PDD ones, suggesting that this synthetic probe was able to specifically detect IgM antibodies that are relevant for the Rett syndrome.

The other interesting aspect was that this study contributed to elucidate that two disease conditions such as Rett and the diffuse autism (non-Rett PDD patients), seemingly contiguous as they share some behavioral traits, are in fact different for their severity, life-span expectancy and, as we demonstrated, immune system derangement.

Preliminary results obtained when the bacterial proteins HMW1ct-Glc and HMW1ct were used in SP-ELISA, indicate the presence of high IgG levels in the majority of Rett and non-Rett PDD sera, suggesting that IgG antibodies targeting some non glucosylated epitopes on adhesion proteins of a common human pathogen as *H.influenzae*, were present in human sera and that they were not related to Rett nor to non-Rett PDD diseases. On the other hand higher level of serum IgM recognizing the glucosylated protein HMW1ct were found in Rett patients as compared to the non-Rett PDD group and a certain cross-reactivity of anti-CSF114(Glc) with HMW1ct-Glc emerged from the competitive assay. Considering the overall results of this study we could assume that N-glucosylated moieties are very relevant epitopes targeted by specific antibodies present in Rett patient's sera.

## 6.5 Materials and methods

### 6.5.1 Patients

A total of 164 human sera coming from the Child Neuropsychiatric Unit, University Hospital of Siena (Dr. Hayek) was employed in this study. This population consisted of 3 different groups: 53 Rett patients sub-divided into 41 patients with classical clinical presentation and MeCP2 gene mutation, and 12 with atypical presentation and other gene mutations; 82 pathological controls affected by non-Rett pervasive developmental disorders (non-Rett PDD); 35 age matched healthy controls.

### 6.5.2 SP-ELISA assay

96 well activated polystyrene ELISA plates (NUNC Maxisorp SIGMA) were coated with 1  $\mu\text{g}/100 \mu\text{L}$  of glycopeptide in Coating buffer (12 mM  $\text{Na}_2\text{CO}_3$ , 35 mM  $\text{NaHCO}_3$ , 3 mM  $\text{NaN}_3$ , pH 9.6) or with 1 $\mu\text{g}/100 \mu\text{L}$  of proteins in PBS buffer pH 7.2 and incubated at +4°C overnight. After five washes with Washing Buffer (NaCl 0.9%), nonspecific binding sites were blocked by Fetal Bovine Serum (FBS) 10% in Washing Buffer (120  $\mu\text{L}/\text{well}$ ) at room temperature for 60 min. FBS buffer were manually removed and sera samples were dispensed in duplicate at 3 dilutions (1:100, 1:1000 and 1:10000 in FBS buffer containing Tween 20 0.05%) 100  $\mu\text{L}/\text{well}$ ; incubation was performed at 4°C overnight. Plates were washed 5 times with Washing Buffer containing Tween 20 and 100  $\mu\text{L}$  of alkaline phosphatase conjugated anti-human IgM (Sigma) diluted 1:200 in FBS buffer/Tween 20 or IgG (Sigma) diluted 1:8000 in in FBS buffer/Tween 20 was added to each well. After 3 h at room temperature incubation and five washes, 100 $\mu\text{L}$  of substrate solution consisting of 1mg/mL p-nitrophenyl phosphate (Sigma) in Substrate buffer (1 M diethanolamine, 1 mM  $\text{MgCl}_2$ , 3 mM  $\text{NaN}_3$ , pH 9.8) was applied. After 30min, the reaction was stopped with 1M NaOH (50  $\mu\text{L}/\text{well}$ ), and the absorbance was read in a multichannel ELISA reader (Tecan Sunrise) at 405 nm. Antibody levels were expressed as absorbance in arbitrary units at 405nm (sample dilution 1:100). Differences between groups were evaluated and the efficiency of anti-CSF114(Glc) IgM and anti-HMW1ct-Glc IgM in discriminating Rett from non-RTT PDD patients or healthy control subjects were evaluated using a Receiver Operating Characteristic (ROC) curve analysis.

### 6.5.3 Competitive ELISA

The protocol used for this assay was the same followed for the SP-ELISA; the only difference is about sample application. The selected serum was used at the semi-saturating dilution (corresponding to the dilution giving an absorbance of around 0.5). Serum and inhibitors in FBS buffer were mixed (50:50) and 100  $\mu\text{L}/\text{well}$  were immediately dispensed. Each inhibitor was tested at 6 final concentrations:  $10^{-5}$ ,  $10^{-6}$ ,  $10^{-7}$ ,  $10^{-8}$ ,  $10^{-9}$  and  $10^{-10}$  M, prepared by serial dilution.  $\text{IC}_{50}$  was calculated for each inhibitor as the molar concentration need to obtain half of the maximum absorbance signal.

## 6.6 References

---

- <sup>1</sup> B. Hagberg; Clinical manifestations and stages of Rett syndrome; *Ment. Retard. Dev. Disabil. Res. Rev.* 2002 (8): 61-65.
- <sup>2</sup> M. Chahrour, H.Y. Zoghbi; The story of Rett syndrome: from clinic to neurobiology; *Neuron* 2007 (56): 422-437.
- <sup>3</sup> F.Mari F, Azimonti S, Bertani I, Bolognese F, Colombo E, C.K. Nielsen, N. Landsberger; CDKL5 belongs to the same molecular pathway of MeCP2 and it is responsible for the early-onset seizure variant of Rett syndrome; *Hum. Mol. Genet.* 2005 (14): 1935-1946.
- <sup>4</sup> F. Ariani, G. Hayek, D. Rondinella, R. Artuso, M.A. Mencarelli, A. Spanhol-Rosseto, M. Zappella, A. Renieri; FOXP1 is responsible for the congenital variant of Rett syndrome; *Am. J. Hum. Genet.* 2008 (3): 89-93.
- <sup>5</sup> J.L. Neul, W.E. Kaufmann, D.G. Glaze, J. Christodoulou, A.J. Clarke, P. Huppke, A.K. Percy; Rett syndrome: revised diagnostic criteria and nomenclature; *Ann. Neurol.* 2010 (68): 944-50.
- <sup>6</sup> J. Guy, H. Cheval, J. Selfridge, A. Bird; The role of MeCP2 in the brain; *Annu. Rev. Cell. Dev. Biol.* 2011 (27): 631-652.
- <sup>7</sup> B.B. Zeev, R. Aharoni, A. Nissenkorn, R. Arnon; Glatiramer acetate (GA, Copolymer-1) an hypothetical treatment option for Rett syndrome; *Med. Hypotheses* 2011 (76): 190-193.
- <sup>8</sup> F.Lolli, B.Mulinacci, A. Carotenuto, B. Bonetti, G. Sabatino, B. Mazzanti, A.M. D'Ursi, E. Novellino, M. Pazzagli, L. Lovato, M.C. Alcaro, E. Peroni, M.C. Pozo-Carrero, F. Nuti, L. Battistini, G. Borsellino, M. Chelli, P. Rovero, A.M. Papini; An N-glycosylated peptide detecting disease-specific autoantibodies, biomarkers of multiple sclerosis; *Proc. Natl. Acad. Sci.* 2005 (102): 10273-10278
- <sup>9</sup> N.C. Dereck, E. Privman, J. Kipnis; Rett syndrome and other autism spectrum disorders-brain diseases of immune malfunction; *Mol. Psychiatry* 2010 (15): 355-363.
- <sup>10</sup> Fiumara A, Sciotto A, Barone R, D'Asero G, Munda S, et al.; Peripheral lymphocyte subsets and other immune aspects in Rett syndrome; *Pediatric. Neurol.* 1999 (21): 619-621.
- <sup>11</sup> S.Rath, C.M. Stanley, M.W. Steward; An inhibition enzyme immunoassay for estimating relative antibody affinity and affinity heterogeneity; *J. Immunol. Method* 1988 (106): 245-249.
- <sup>12</sup> **A.M. Papini, F. Nuti, F. Real-Fernández, G. Rossi, C. Tiberi, G. Sabatino, S. Pandey, S. Leoncini, C. Signorini, A. Pecorelli, R. Guerranti, S. Lavielle, L. Ciccoli, P. Rovero, C.De Felice, J. Hayek; Immune dysfunction in Rett syndrome patients revealed by high levels of serum anti-N(Glc) IgM antibody fraction; *J. Immunol. Res.* 2014 (10): 1-6.**

## LIST OF ABBREVIATIONS

### 7 LIST OF ABBREVIATIONS

Anti-Citrullinated Peptide/Protein Antibodies	<b>ACPA</b>
Aquaporin 4	<b>AQ 4</b>
Autism Spectrum Disorders	<b>ASD</b>
Brain Derived Neurotrophic Factor	<b>BDNF</b>
Cyclic Citrullinated Peptides	<b>CCP</b>
Cyclin-Dependent Kinase-Like 5	<b>CDKL5</b>
Central Nervous System	<b>CNS</b>
4',6-diamidino-2-phenylindole	<b>DAPI</b>
Dimethylformamide	<b>DMF</b>
Dimethyl Sulfoxide	<b>DMSO</b>
Dithiothreitol	<b>DTT</b>
Experimental Autoimmune Encephalomyelitis	<b>EAE</b>
Epstein-Barr Virus	<b>EBV</b>
1-ethyl-3-(3-dimethylaminopropyl)-carbodiimide	<b>EDC</b>
Enzyme-Linked Immunosorbent Assay	<b>ELISA</b>
Fetal Bovine Serum	<b>FBS</b>
Fluorescein Isothiocyanate	<b>FITC</b>
Forkhead box protein G1	<b>FOXG1</b>
Flow Through	<b>FT</b>
Glutamic Acid Decarboxylase	<b>GAD</b>
Histone Citrullinated Peptide	<b>HCP</b>
Human Natural Killer-1	<b>HNK-1</b>
Integrated Microfluidic Cartridge	<b>IFC</b>
Multiple Antigen Peptide	<b>MAP</b>
Methyl CpG binding protein 2	<b>MeCP2</b>
Magnetic Resonance Imaging	<b>MRI</b>
Multiple Sclerosis	<b>MS</b>
Normal Blood Donor	<b>NBD</b>
Neutrophil Extracellular Traps	<b>NET</b>
Normal Health Sera	<b>NHS</b>
N-hydroxysuccinimide	<b>NHS</b>
Oligosaccharyl Transferase	<b>OT</b>
Peptidyl-Arginine Deiminase	<b>PAD</b>
Pervasive Developmental Disorder	<b>PDD</b>
2-(2-pyridinyldithio)ethaneamine	<b>PDEA</b>
Post-Translational Modification	<b>PTM</b>
Rheumatoid Arthritis	<b>RA</b>
Rheumatoid Factor	<b>RF</b>
Refractive Index	<b>RI</b>
Receiver Operating Characteristic	<b>ROC</b>
Reactive Oxygen Species	<b>ROS</b>
Resonance Unit	<b>RU</b>
Standard Deviation	<b>SD</b>
Surface Plasmon Resonance	<b>SPR</b>
Tumor Necrosis Factor- $\alpha$	<b>TNF-<math>\alpha</math></b>
Two Partner Secretion	<b>TPS</b>
Viral Citrullinated Peptide	<b>VCP</b>